



LOAN COPY ONLY

MICHU-T-75-002

c. 2

Technical Report No. 43

**CIRCULATING COPY**  
**Sea Grant Depository**

**A FOOD WEB MODEL FOR LAKE MICHIGAN  
PART 2 - MODEL FORMULATION AND  
PRELIMINARY VERIFICATION**

By

RAYMOND P. CANALE,

LEON M. DePALMA

and

ALLAN H. VOGEL

**MICHIGAN SEA GRANT PROGRAM**

March 1975

MICHU-SG-75-201

LOAN COPY ONLY

A FOOD WEB MODEL FOR LAKE MICHIGAN:  
PART 2 - MODEL FORMULATION AND PRELIMINARY VERIFICATION

**CIRCULATING COPY**  
**Sea Grant Depository**

Raymond P. Canale, Ph.D.

Department of Civil Engineering  
University of Michigan

and

Leon M. DePalma  
Allan H. Vogel

Sea Grant Program  
University of Michigan

Technical Report # 43

MICHIGAN SEA GRANT PROGRAM

MICHU-SG-75-201

March 1975

This work is a result of research sponsored by NOAA Office of Sea Grant, Department of Commerce, under Grant #04-5-158-16. The U.S. Government is authorized to produce and distribute reprints for governmental purposes notwithstanding any copyright notation that may appear hereon.

#### ACKNOWLEDGEMENTS

The authors are indebted to the following graduate students who have participated in this study. Janice Boyd of Natural Resources formulated many of the model mechanisms, contributing much to the conceptual framework on which the zooplankton eating mechanisms are based. Richard Bortins of Computer, Information and Control Engineering spent many hours calibrating the model to Grand Traverse Bay data, and assisted in the evolution of the zooplankton life cycle mechanisms and the nutrient regeneration mechanisms. Barry R. Bochner of Bioengineering developed much of the computer software necessary to integrate the differential equations.

## CONTENTS

	page
Acknowledgements	iv
Summary	1
Perspective	3
Model Philosophy	5
A Mechanistic Model	5
The Concept of State	5
Spatial Hypotheses	7
Temporal Hypotheses	9
Statistical Framework	10
Model Mechanisms	11
General	11
Zooplankton	11
Eating rate	11
Assimilation efficiency	23
Preferred diet	25
Predation by other zooplankters and alewives	30
Respiration	31
Life cycles	32
Phytoplankton	35
Production rate	35
Light limitation	36
Nutrient limitation	37
Predation by zooplankters	40
Respiration	40

	page
Sinking . . . . .	41
Seasonal cycles . . . . .	42
<b>Nutrients . . . . .</b>	<b>42</b>
Stoichiometry of phytoplankton and zooplankton	42
Detrital components . . . . .	43
Organic components . . . . .	47
Inorganic components . . . . .	48
Nonaccessible components and turnover . . . . .	49
Loadings . . . . .	49
<b>Model Forcing Functions . . . . .</b>	<b>53</b>
Temperature . . . . .	53
Light Intensity . . . . .	55
Photoperiod . . . . .	55
Extinction Coefficient . . . . .	55
Sinking Rate Multiplier . . . . .	59
Alewife Eating Rates . . . . .	59
Alewife Concentrations . . . . .	61
<b>Computational Topics . . . . .</b>	<b>64</b>
Integration . . . . .	64
Interpolation . . . . .	64
Hatching, maturation and Natural Death . . . . .	65
<b>Results . . . . .</b>	<b>68</b>
Model Calibration . . . . .	68
Model Calculated Energetics . . . . .	92

	page
<b>Analysis</b> . . . . .	111
Calculated Zooplankton vs. Observations .	111
Calculated Phytoplankton vs. Observations .	113
Calculated Nutrients vs. Observations .	114
Model Simulations . . . . .	115
Evaluation of Proposed Food Web . . .	140
<b>References</b> . . . . .	144

## SUMMARY

Previous plankton models for the Great Lakes have considered the interactions among dissolved nutrients, chlorophyll a, and total zooplankton. These models have been developed primarily for the purpose of predicting the gross effects of nutrient input control and urban growth on the phytoplankton standing crop. However, more complex ecological problems, such as the effect of eutrophication on the forage fish and the effect of foreign marine fish species on the plankton composition, require complex food web models. The purpose of this report is to justify, develop, and verify a preliminary lower food web model for Lake Michigan.

Being two-layered and having no horizontal definition, the model has a simple representation of the spatial distribution of species. However, it has a complex representation of the food web interactions and consists of 12 nutrient equations, 4 phytoplankton equations, and 9 zooplankton equations. The nutrients considered in the model are nitrogen, phosphorus, and silicon. Nitrogen and phosphorus can appear in detrital, dissolved organic, or dissolved inorganic form, whereas silicon can be detrital or dissolved. Diatom, green, and blue-green components of the algal community are considered. Furthermore, the diatom population is divided on the basis of size to accommodate feeding preferences of the zooplankton. The zooplankton in the model are divided on the basis of size, feeding mechanism, and taxonomic grouping. A crude representation of age structure within the zooplankton community is included by placing the nauplii in a separate compartment. Alewife predation upon the zooplankton is included through use of time variable forcing functions which represent the feeding rate of the adult and juvenile fish.

The model calculations have been compared with field data from Grand Traverse Bay with encouraging results. The calibrated model has been used to make some preliminary estimates of the effects of eutrophication and higher forage fish levels on the plankton and nutrient distributions in the lake. Simulations have been made where the initial phosphorus levels were increased to the level currently found in Lake Erie. Another set of simulations examines the effect of forage fish levels at high values which approximate the large alewife population explosion that occurred in Lake Michigan in 1966. The results and implications of these simulations are discussed in detail.

It is expected that the model will provide guidance on the requirements of additional scientific research on food

web transfer mechanisms and on the requirements of a comprehensive field monitoring program. Several specific recommendations are made in different parts of this report. Ultimately the model may be useful to decision makers concerned with the control of eutrophication and the management of the Lake Michigan fishery.

## PERSPECTIVE

Part 2 in this series of reports on Lake Michigan food-web modeling will detail the underlying hypotheses, mathematical formulation, and preliminary verification of a lower trophic-level model. Part 1 of the series (Vogel and Canale, 1974) should be consulted for justification of this effort and for a qualitative overview of the biology which the model is to eventually depict.

To summarize Part 1, a taxon-specific food web model of the lower trophic levels of Lake Michigan is required because eutrophication favors the development of certain taxa of algae such as the blue-greens over other types. This in turn reduces the amount of food available for the zooplankton, reducing forage fish food. The blue-greens may sink, die, and decompose, reducing dissolved oxygen in the hypolimnion. This creates an unfavorable environment for fish. A second major reason for requiring this type of model is that the invasion of the Great Lakes by marine species has upset the original food web by the selective removal of certain types of zooplankton and fish which has caused a reduction in the total biomass of fish. Models which fail to include these interactions may result in inaccurate estimates of phytoplankton and fish standing stocks.

Part 1 described alternate spatial and temporal scales which might be considered in a Lake Michigan food web model. The present model and a proposed physical segmentation is described in detail. The taxa used in the present model are defined and justified in Part 1.

The literature abounds in examples where systems-analysis techniques have been applied to ecosystems. Relatively few applications, however, involve as complicated predator-prey interactions as will be detailed in this report. The scope of the work may draw criticism from biologists and mathematicians alike. Anyone who has undertaken the task of modeling an ecosystem has tried to balance reality and tractability: some will argue that this effort strives too much for reality; others will argue that it is too simple. The model described in this report has been developed for the specific purpose of evaluating the combined effects of eutrophication and foreign-species invasion into the Lake Michigan ecosystem. To an extent, the model is a framework about which new experimental investigations can be planned. It is an incentive to accelerate data collection, so that model verification can keep pace with model development.

Part 1 expresses the need for a complex taxon-specific model. This research has shown that development of a large-scale model is feasible, and that sound biological and mathematical reasoning can produce models which agree well with field observations. It is felt that this research provides part of the ground work needed to develop a water quality management tool for Lake Michigan.

## MODEL PHILOSOPHY

A Mechanistic Model

The approach adopted by the University of Michigan Sea Grant Program, as exemplified by the Grand Traverse Bay biological production model (Canale et al., 1974), has been to construct detailed mechanistic models. Such a scheme employs available biological, chemical, and physical theory to describe the interaction of lake variables in a consistent manner. The mass-balance technique has been chosen over bioenergetics techniques primarily because most pioneering research in aquatic modeling has been in this direction (DiToro et al., 1971). Development of mechanistic formulations is essential in ecological modeling because the ecosystem researcher aims not just to construct a predictive device for resource management, but, just as importantly, to obtain additional insight into the response of the system to perturbations. Many questions have been raised during construction of this lower trophic-level model, questions that would not have surfaced during construction of a completely empirical, "blackbox" type model.

The Concept of State

Throughout the report, the collection of lake variables of interest will be referred to as the "state" of the system. Part 1 of this report defines and justifies the zooplankton and phytoplankton groupings of Table 1. Selection of nitrogen, phosphorus, and silicon as essential nutrient variables is discussed by Canale et al. (1974) in the Grand Traverse Bay report. Units have been selected to facilitate development of the equations. The concept of "state" is an important one in systems mathematics. If the state of this system, the 25 variables of Table 1, is known at a particular time  $t_0$ , and if forcing functions of the model are known over an interval of time  $[t_0, t_f]$ , then the state is determinable over  $[t_0, t_f]$ . The following set of ordinary differential equations governs changes of state over  $[t_0, t_f]$ :

$$\begin{aligned}\dot{c}_1(t) &= f_1(c_1(t), \dots, c_{25}(t), t) \\ &\vdots \\ \dot{c}_{25}(t) &= f_{25}(c_1(t), \dots, c_{25}(t), t)\end{aligned}\tag{1}$$

where the dependence of the dynamics upon the forcing functions is indicated by the appearance of time explicitly in the  $f_i$  functions. The functions  $f_i$  portray the mechanisms of mass

State Number	Description	Classification	Units
1	<u>Leptodora</u> & <u>Polypodium</u>	Raptors	
2	<u>Cyclops</u>		
3	<u>Cyclops</u> nauplii		
4	<u>Diaptomus</u> nauplii		
5	<u>Limnocalanus</u> & <u>Epischura</u> nauplii	Selective filterers	$\text{mg C/l}$
6	<u>Diaptomus</u>		
7	<u>Limnocalanus</u> & <u>Epischura</u>		
8	<u>Daphnia</u>	Nonselective filterers	
9	<u>Bosmina</u> & <u>Holopedium</u>		
10	<u>Small diatoms</u>		
11	<u>Large diatoms</u>	Phytoplankton	
12	<u>Blue-greens</u>		
13	<u>Greens</u>		
14	<u>Detrital nitrogen</u>		
15	<u>Dissolved organic nitrogen</u>	Nitrogen	$\text{mg N/l}$
16	<u>Ammonia</u>		
17	<u>Nitrate</u>		
18	<u>Detrital phosphorus</u>		
19	<u>Dissolved organic phosphorus</u>	Phosphorus	$\text{mg P/l}$
20	<u>Dissolved inorganic phosphorus</u>		
21	<u>Detrital silicon</u>		
22	<u>Dissolved silicon</u>	Silicon	$\text{mg Si/l}$
23	<u>Total nonaccessible nitrogen</u>		
24	<u>Total nonaccessible phosphorus</u>	Nutrient mass held in hypolimnion and sediments	$\text{mg N}$
25	<u>Total nonaccessible silicon</u>		$\text{mg P}$
			$\text{mg Si}$

Table 1. The State of the System

interaction and will be expounded upon later. It should be mentioned, for completeness, that some biological phenomena cannot be modeled by such equations. When the reproduction cycle of animals is modeled in detail, there may be a need for delay terms in the equations to handle carrying time, hatching time, etc. Equations of the form,  $c(t) = f(c(t), c(t-t_D), t)$ , may be necessary to adequately describe the dynamics of the state, where  $t_D$  is a delay time. In this case, knowledge of an initial state  $c(t_0)$  is insufficient for integration of the equation over  $[t_0, t_f]$ .

### Spatial Hypotheses

The above equations describe the behavior of the states in a single, completely mixed body of water. Although the ultimate objective of this research is to describe both temporal and spatial variation of the states in Lake Michigan, three factors restrict immediate attention to only temporal variations. (1) Until a large-scale sampling program can be instituted for Lake Michigan proper, models will be verified with Grand Traverse Bay data. Since the open waters of the Bay are predominantly forced by the lake, the data being considered are a reasonable indicator of overall lake temporal variations. These data, however, cannot begin to describe spatial variation within the lake. (2) When spatial detail is added, it may be accomplished using the technique of spatial compartments. This technique assumes that the lake comprises a finite number of completely mixed segments and that the advective-dispersive transfer between segments is linear. The approach avoids partial differential equations, and has been employed by other modelers of aquatic systems because of its simplicity. Temporal variation in state, on the other hand, is described by complex nonlinear mechanisms that require experimental verification. Since the temporal model is the basic block that will describe variation within any given segment of a multi-segment model, it is appropriate to confirm this model first in a single segment. (3) Since every segment of the lake will involve all 25 biological and chemical equations of the model, it is, at present, computationally infeasible to attempt much analysis on a multi-segment model. Without analysis, the value of the construction process is nil.

The lower trophic level model will be verified against the average of data from four stations in the west arm of Grand Traverse Bay. These stations are shown in Figure 1. Zooplankton samples were taken by vertical hauls from the bottom. Phytoplankton was sampled discretely at 2 meters and 20 meters, and average concentrations in the 20 meter column were calculated. Nutrients were sampled discretely at a number of depths between the surface and the bottom.

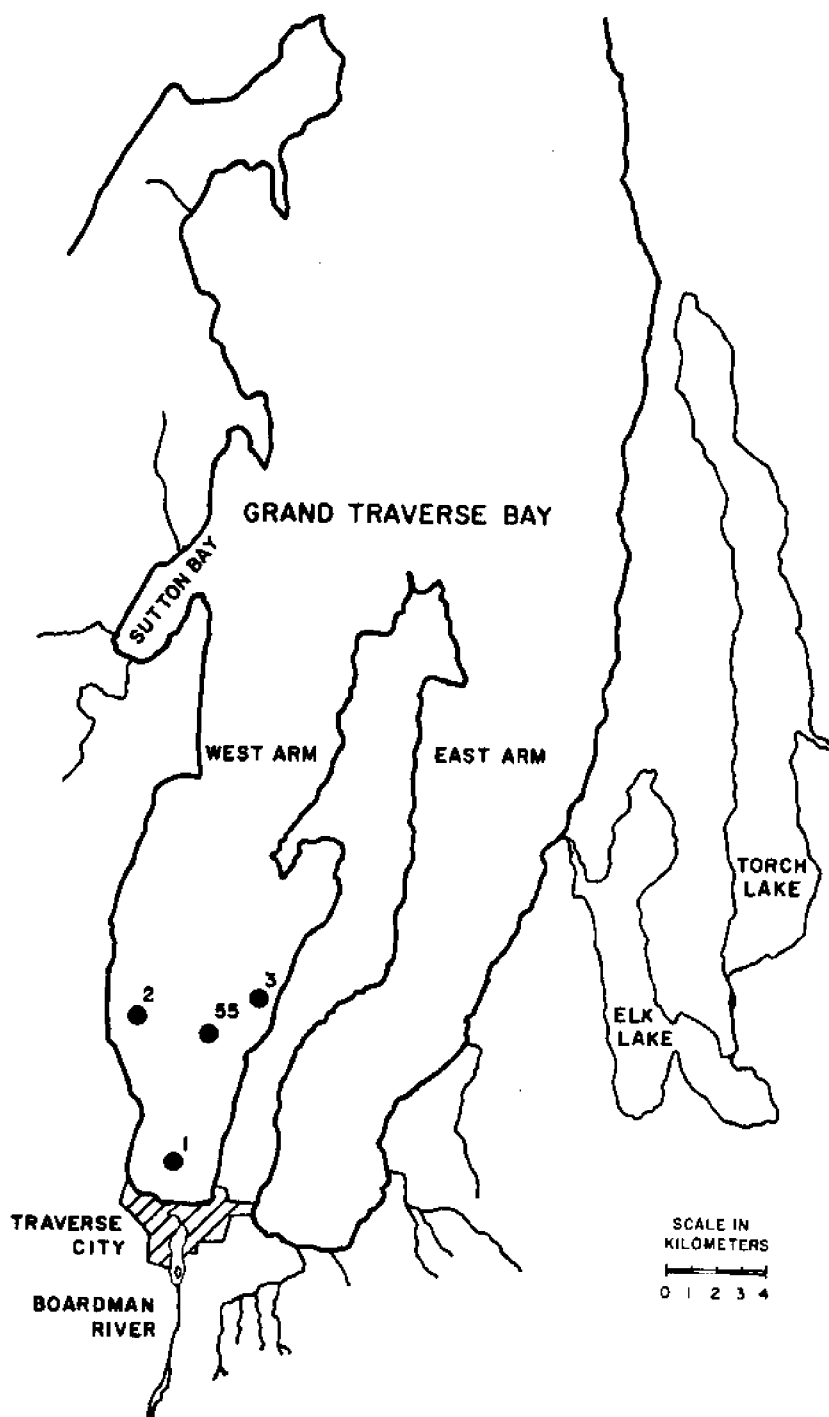


Figure 1. Location of Grand Traverse Bay Sampling Stations

Averages for the epilimnion and the hypolimnion were calculated. Additional details regarding sample collection, handling, storage and analysis are discussed by T.M. Kelly and J.J. Sygo.<sup>1</sup>

### Temporal Hypotheses

The choice of an appropriate time scale for the model deserves considerable attention. Extensive data on the state of the system are available only for the years 1971, 1972, and 1973. With only three years of data, it is difficult to model more than seasonal variations in the state. The interval of interest, then, is a calendar year. No particular year is implied; the objective is to reproduce typical present-day seasonal dynamics assuming the initial state is known. The ultimate objective to this research, as pointed out in Part 1 of this series, is to study long term trends in the lake fish and plankton populations. Extension of this model, and a combined upper and lower trophic level model, to long time intervals will probably involve more than simply integrating the present model beyond 360 days. Just as the present time scale cannot simulate hourly dynamics, it is expected that it cannot simulate year-to-year dynamics. A significant research effort may be required in the future in order to develop a model of long term variation. That task may be simplified by the insights derived during the present study.

Although the time scale chosen cannot be used to predict the fate of animal populations that reproduce once a year, it can be used to predict phytoplankton dynamics. The important distinction is that fish and zooplankton populations observed in one year are dependent on their populations the preceding year, whereas the phytoplankton population, which propagates continuously, is nearly independent of the population the preceding year. The peaks in the phytoplankton concentrations are governed primarily by light and temperature conditions and nutrient availability, and only secondarily by initial conditions and animal grazing. So, application of models to eutrophication studies, as Canale et al. (1974) have done with the Grand Traverse Bay model, is appropriate.

In the Grand Traverse Bay model, the effect of various phosphorus removal programs upon the phytoplankton level of the bay was studied. The annual time-scale model can be applied in this case because the upper food chain, which is supported by the phytoplankton, will adjust its composition to conform to different food levels, but will have little feedback effect on the phytoplankton. Zooplankton and fish populations may take years to reach equilibrium after a

---

<sup>1</sup>Sea Grant report in preparation.

phosphorus removal program has lowered phosphorus levels; however the phytoplankton may adjust rapidly, acquiring a seasonal pattern that would persist if climatic conditions and nutrient loadings did not stray far from normal yearly cycles. Although the lower food web model, with its annual time scale, will have limited long term predictive value, it will help researchers study the interaction of the lower links of the food chain. The time scale chosen is compatible with experimental studies designed to verify the mechanisms of these interactions.

#### Statistical Framework

Attention is seldom given to the statistical framework within which aquatic models are constructed. Temperature, light intensity, light extinction, and other forcing functions needed to integrate the equations for the state must be based on past observation. These functions follow, within some tolerance, average annual cycles. Of course, the degree to which the average cycle depicts a particular yearly cycle depends upon the idiosyncracies of the weather that year. Just as the weather pattern is rather unpredictable, the tolerance associated with model predictions may be rather large. The model should be considered as a simulator of a most-likely state trajectory, that trajectory expected to result if forcing functions were to follow their average cycles. The model should be tested by applying forcing functions constructed from daily monitoring. However the task of monitoring is very complicated, if not infeasible, for such spatially erratic functions as sinking rate and light extinction. Statistical analyses of problems associated with choosing forcing functions, and even with collecting data on the state of the system, are lacking for lake models. The most reasonable test of a model, with the weak statistical framework now available, is to compare its trajectory, using average forcing cycles, with an average trajectory constructed from as many years of data as available.

Stochastic methods have been applied with some success to solve problems that involve uncertainty. Practical techniques have been developed only for linear models so that probes in this direction would first require linearization of the nonlinear model about the "most likely" trajectory. Although there may someday be a place for such techniques in analyzing large-scale lake systems, it appears that at present there is none. The obstacle preventing application of these elegant techniques is the lack of information on the statistics of the uncertainties.

## MODEL MECHANISMS

General

The mechanisms that are thought to contribute to predominant changes in the state of the system have been incorporated into the model. Some of the mechanisms considered are given much coverage in the literature and have been formulated mathematically by other researchers. However, because the model is taxon-specific, some of the mechanisms have not been studied in detail in the literature, and previous mathematical descriptions may not be available. Future experimentation will hopefully focus on these latter mechanisms, filling obvious gaps. It is probable that some of the mechanisms included in the model may have negligible effect and may eventually be eliminated from consideration. However, it is difficult to pinpoint these superfluous areas of the model without further research.

Where a mechanism is known to be important, and where previous research has contributed a sound structural formulation for the mechanism, the difficulty of estimating coefficients for the formulation still persists. The heterogeneity of the biological states makes coefficient estimation a serious problem. Age and size distribution, as well as the spatial distribution of a species in the lake, often suggests a broad range of scientifically acceptable coefficient values. The inherent problem here, of course, is a problem often confronted in population modeling. Model mechanisms must portray the population, not the individual. The following sections will discuss each mechanism in turn, focusing on: (1) the mechanism from a biological viewpoint; (2) the assumptions made in formulating the mechanism mathematically; (3) the formulation; (4) the definitions of coefficients involved in the formulation; and (5) the justification of coefficient values chosen.

zooplankton

Eating Rate. The growth of a zooplankton state,  $z$ , is determined by its present abundance, its rate of grazing, and the efficiency with which it converts food carbon into zooplankton carbon. These factors are assumed to operate independently of one another, in that the positive term determining growth of the population is:

$$[\text{growth}]_z = \frac{[\text{assimilation}]_z * [\text{eating rate}]_z * c_z}{[\text{mg food c}]} \quad (2)$$

$$\frac{\text{mg z c}}{\text{mg food c}} \quad \frac{\text{mg food c}}{\text{mg z c} \cdot \text{day}} \quad \frac{\text{mg z c}}{\ell}$$

In the model, population production is limited only by abundance of food, not by problems associated with over-crowding. This is reasonable for all but extreme eutrophic situations where high concentrations of population wastes may limit growth.

As explained by Vogel and Canale (1974) in Part 1 of this report, the eating mechanism differs greatly enough among species to warrant modeling three types of eating behavior: raptorial, selective filtering, and nonselective filtering. Table 1 lists the feeding category for each zooplankton state. The eating rate attainable by a particular zooplankton state, regardless of classification, is temperature dependent. The temperature dependence is denoted as  $\Phi_z(T)$  for state  $z$ . This function is normalized to a value of unity at 20°C. The maximum snatching rate for raptors, the maximum filtering rate for selective filterers, and simply the filtering rate for nonselective filterers, all at 20°C, are defined as  $A7_z$ .

Raptorial species obtain their food by selecting, snatching, and devouring. This operation is time consuming, and even when food is abundant, the raptor is limited by the rate at which he can consume food. Furthermore, as his food supply dwindles, the rate at which the raptor can find palatable food decreases. Since the eating rate of a raptor increases with food concentration, but reaches a saturation level, a Michaelis-Menton type expression has been utilized in the mathematical formulation of the mechanism. For a raptorial state  $z$ , then:

$$[\text{eating rate}]_z = A7_z * \Phi_z(T) * \left( \frac{\sum_{\text{prey}} c_i}{\sum c_i + KFOOD_z} \right) \quad (3)$$

$\frac{\text{mg food c}}{\text{mg z c} \cdot \text{day}}$

where  $\sum_{\text{prey}} c_i$  = sum of concentrations of all states that can serve as food for raptor state  $z$ .

$KFOOD_z$  = half-saturation food level for state  $z$ .

Two important assumptions have been made in the above formulation and will be made for filter-feeding species also.

(1) There is no lower food threshold below which raptors cannot find their prey. That is, the model does not account for refuge sites which may be available to the prey to protect it from the predator. Gause (1934) has discussed the importance of refuge sites in predator-prey systems. (2) Although preferences must play a role in determining the allocation of the eating rate toward each prey species, they do not affect the rate of intake of food carbon. The animal

is assumed to have a basic food requirement that must be satisfied regardless of the species present. As long as those species are preyed upon by the zooplankton in question, they will be utilized to meet the basic food requirement.

The literature has been consulted for estimates of the temperature multiplier  $\Phi_z(T)$  and the coefficient  $A7_z$  for the two raptorial states of the model. Cummins et al. (1969) have carried out extensive studies on the ecology of Leptodora kindtii in a Pennsylvania reservoir. An analysis of these data has suggested a raptorial rate of  $A7 = 2.14 \frac{\text{mg food c}}{\text{mg z c. day}}$  at 20°C with temperature dependence as indicated in Figure 2. Similar data for Polypheus does not appear to be available. McQueen (1969) studied Cyclops bicuspidatus thomasi in Marion Lake, British Columbia. An estimate of  $A7 = 1.2 \frac{\text{mg food c}}{\text{mg z c. day}}$  has been made from his work, but detailed temperature-dependence data are not available. The curve for Cyclops in Figure 2 has been used pending additional experimental work. Little seems to be known about eating rates for Cyclops, especially during the cold months. The half-saturation food levels,  $KFOOD_z$ , have not been researched by others and can only be speculated upon at present. Summaries of model coefficients and equations appear in Tables 2 and 3.

Selective filterers obtain food by grazing, but have developed an ability to vary their filtering rate. As the concentration of food decreases, a maximum filtering rate is approached, a rate fixed by the physical characteristics of the species. In an environment where food concentration is high, the selective filterer responds by adjusting its particle-size selectivity, and lowering its filtering rate. In this way, the animal is able to make more efficient use of food and its own energy. A proposed formulation of this mechanism becomes:

$$[\text{eating rate}]_z = A7_z * \Phi_z(T) * \frac{\frac{A9 * \sum c_i + A10}{\text{prey}}}{\frac{\sum c_i + A10}{\text{prey}}} * \frac{\sum c_i}{\text{prey}} \frac{\text{mg food c}}{\ell} \quad (4)$$

where  $A9$  = minimum filtering rate multiplier

$A10$  = food level where multiplier is 1/2 ( $1+A9$ )

It has been assumed that, even at high food concentrations, the organism will be filtering at some minimum level. Thus, no provision has been made for extreme eutrophic situations where food concentrations may be so high that the ability

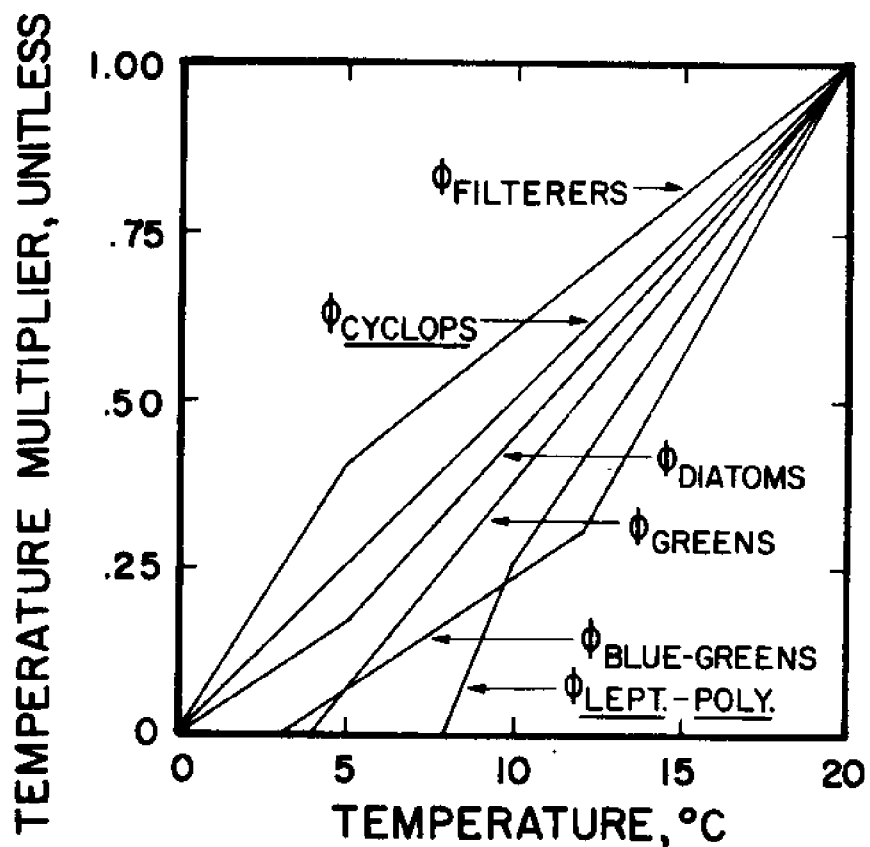


Figure 2. Temperature Dependence of the Growth Rates

### Zooplankton Related Coefficients

Symbol	Definition	Units	Value Used
A7 <sub>Lept.-Poly.</sub>	maximum snatching rates @ 20°	$\frac{\text{mg food c}}{\text{mg z c} \cdot \text{day}}$	0.70
A7 <sub>Cyc.</sub>			0.43
A7 <sub>Cyc. n.</sub>			2.6
A7 <sub>Diap. n.</sub>	maximum filtering rates @ 20°	$\frac{\ell}{\text{mg z c} \cdot \text{day}}$	6.5
A7 <sub>Lim.-Ep. n.</sub>			5.2
A7 <sub>Diap.</sub>			1.0
A7 <sub>Lim.-Ep.</sub>			1.25
A7 <sub>Daph.</sub>	filtering rates @ 20°		4.0
A7 <sub>Bosm.-Holo.</sub>			3.5
KFOOD <sub>Lept.-Poly.</sub>	half-saturation food level for raptors	$\frac{\text{mg food c}}{\ell}$	0.2
KFOOD <sub>Cyc.</sub>			0.2
A9	minimum filtering rate multiplier	unitless	0.1
A10	food level where multiplier is 1/2 (1+A9)	$\frac{\text{mg food c}}{\ell}$	0.2
A11R	assimil. eff. of raptors		0.4
A11S	assimil. eff. of selectives	$\frac{\text{mg z c}}{\text{mg food c}}$	0.7
A11N	max. assimil. eff. of non-selectives		0.8

Table 2. Model Coefficients

## Zooplankton Related Coefficients (continued)

Symbol	Definition	Units	Value Used
A24	half eff. food level for non-selectives	$\frac{\text{mg food c}}{\text{L}}$	0.2
A12 <sub>adults</sub>	respiration rates @ 20°	$\text{day}^{-1}$	0.06
A12 <sub>nauplii</sub>			0.04
A14 <sub>Cyc.</sub>	natural death rates for the copepods	$\text{day}^{-1}$	0.005
A14 <sub>Diap.</sub>			0.005
A14 <sub>Limn.-Ep.</sub>			0.003

Table 2. Model Coefficients (continued)

## Phytoplankton Related Coefficients

Symbol	Definition	Units	Value Used
$A_{1\text{sm}}$ diatoms			2.1
$A_{1\text{lg}}$ diatoms	maximum 20°C growth rate	$\text{day}^{-1}$	2.0
$A_{1\text{blue-greens}}$			1.6
$A_{1\text{greens}}$			1.9
$I_{S\text{sm}}$ diatoms			225.
$I_{S\text{lg}}$ diatoms	optimum light intensities	$\frac{\text{langleys}}{\text{day}}$	225.
$I_{S\text{blue-greens}}$			600.
$I_{S\text{greens}}$			160.
$A_{6\text{sm}}$ diatoms			0.05
$A_{6\text{lg}}$ diatoms	maximum sinking rates	$\text{day}^{-1}$	0.03
$A_{6\text{blue-greens}}$			0
$A_{6\text{greens}}$			0.02
RN	Michaelis constants for phytoplankton growth	$\frac{\text{mg nutrient}}{\text{L}}$	0.015
KP			0.0025
KS			0.030
DEPTH	depth of euphotic zone	m	20.
A3	respiration rate @ 20°C for phytoplankton	$\text{day}^{-1}$	• 08

Table 2. Model Coefficients (continued)

Nutrient Related Coefficients

Symbol	Definition	Units	Value Used
NCR			0.2
PCR			0.02
SCR			0.6
A18	nutrient to carbon ratios	$\frac{\text{mg nutrient}}{\text{mg C}}$	
A20	detrital nitrogen→organic nitrogen organic nitrogen→ammonia ammonia→nitrate	$\frac{\text{day}^{-1}}{\text{°C}}$	0.001 0.0012 0.008
A22	detrital phosphorus+organic phosphorus	$\frac{\text{day}^{-1}}{\text{°C}}$	0.01
A17	organic phosphorus+inorganic phosphorus	$\frac{\text{day}^{-1}}{\text{°C}}$	0.01
A19	detrital silicon+dissolved silicon	$\frac{\text{day}^{-1}}{\text{°C}}$	0.0015
A23	maximum detrital sinking rate	$\text{day}^{-1}$	0.05
A21	fraction of zooplankton resired nitrogen that is organic	unitless	0.7
Q	net flow through Lake Michigan	$\frac{\ell}{\text{day}}$	$1.37 \times 10^{11}$
VOLEP	volume of Lake Michigan epilimnion	$\ell$	$1.218 \times 10^{15}$
VOLHY	volume of the hypolimnion	$\ell$	$3.654 \times 10^{15}$

Table 2. Model Coefficients (continued)

$$\dot{c}_z = [growth]_z - \left[ \begin{array}{l} \text{predation} \\ \text{by other} \\ \text{zooplankton} \end{array} \right]_z - \left[ \begin{array}{l} \text{predation} \\ \text{by} \\ \text{alewife} \end{array} \right]_z - \left[ \begin{array}{l} \text{respiration} \\ \text{loss} \end{array} \right]_z \quad (1)$$

-  $A14_z(t) * c_z$   
natural death  
for copepods

$$\dot{c}_p = [growth]_p - \left[ \begin{array}{l} \text{predation} \\ \text{loss} \end{array} \right]_p - \left[ \begin{array}{l} \text{respiration} \\ \text{loss} \end{array} \right]_p - \left[ \begin{array}{l} \text{sinking} \\ \text{loss} \end{array} \right]_p$$

$$\dot{c}_{14} = NCR * \sum_z \left( 1. - \left[ \begin{array}{l} \text{assimilation} \\ \text{efficiency} \end{array} \right]_z \right) * \left[ \begin{array}{l} \text{eating} \\ \text{rate} \end{array} \right]_z * c_z + NCR * \sum_z \left[ \begin{array}{l} \text{natural} \\ \text{death} \end{array} \right]_z \quad (2)$$

-  $A18 * T * c_{14} - A23 * SINK(t) * c_{14}$

$$\dot{c}_{15} = NCR * \sum_p \left[ \begin{array}{l} \text{respiration} \\ \text{loss} \end{array} \right]_p + NCR * A21 * \sum_z \left[ \begin{array}{l} \text{respiration} \\ \text{loss} \end{array} \right]_z + A18 * T * c_{14}$$

-  $A20 * T * c_{15} + LOAD_{15}$

$$\dot{c}_{16} = NCR * (1. - A21) * \sum_z \left[ \begin{array}{l} \text{respiration} \\ \text{loss} \end{array} \right]_z + A20 * T * c_{15} - A22 * T * c_{16}$$

-  $NCR * \left( \frac{ANH3 * c_{16}}{ANH3 * c_{16} + (1. - ANH3 * c_{17})} \right) * \sum_p [growth]_p + LOAD_{16}$

Table 3. Summary of the Model Equations

(1) Hatch-ing-maturation mechanisms not written into zooplankton equations.  
 (2) Turnover mechanism not written into the nutrient equations.

$$\dot{c}_{17} = A22 * T * c_{16} - NCR * \left( \frac{(1.-ANH3)*c_{17}}{ANH3*c_{16} + (1.-ANH3)*c_{17}} \right) * \sum_p [growth]_p + LOAD_{17}$$

$$\dot{c}_{23} = A23 * SINK(t) * c_{14} + NCR * \sum_p \left[ \begin{matrix} \text{sinking} \\ \text{loss} \end{matrix} \right]_p * VOLEP$$

$$+ [LOAD_{15} + LOAD_{16} + LOAD_{17}] * VOLHY$$

$$\dot{c}_{18} = PCR * \sum_z \left( 1. - \left[ \begin{matrix} \text{assimilation} \\ \text{efficiency} \end{matrix} \right]_z \right) * \left[ \begin{matrix} \text{eating} \\ \text{rate} \end{matrix} \right]_z * c_z + PCR * \sum_z \left[ \begin{matrix} \text{natural} \\ \text{death} \end{matrix} \right]_z$$

$$- A17 * T * c_{18} - A23 * SINK(t) * c_{18}$$

$$\dot{c}_{19} = PCR * \sum_p \left[ \begin{matrix} \text{respiration} \\ \text{loss} \end{matrix} \right]_p + A17 * T * c_{18} - A19 * T * c_{19} + LOAD_{19}$$

$$\dot{c}_{20} = PCR * \sum_z \left[ \begin{matrix} \text{respiration} \\ \text{loss} \end{matrix} \right]_z + A19 * T * c_{19} - PCR * \sum_p [growth]_p + LOAD_{20}$$

$$\dot{c}_{24} = A23 * SINK(t) * c_{18} + PCR * \sum_p \left[ \begin{matrix} \text{sinking} \\ \text{loss} \end{matrix} \right]_p * VOLEP$$

$$+ [LOAD_{19} + LOAD_{20}] * VOLHY$$

$$\dot{c}_{21} = SCR * \sum_p \text{diatoms} \left[ \begin{matrix} \text{respiration} \\ \text{loss} \end{matrix} \right]_p + \left[ \begin{matrix} \text{predation} \\ \text{loss} \end{matrix} \right]_p - A16 * T * c_{21}$$

$$- A23 * SINK(t) * c_{21}$$

Table 3. Summary of the Model Equations (continued)

$$\begin{aligned}
 \dot{c}_{22} &= A16 * T * c_{21} - SCR * \sum_{diatoms} [growth]_p + LOAD_{22} \\
 \dot{c}_{25} &= A23 * SINK(t) * c_{21} + SCR * \sum_{diatoms} \left[ \begin{array}{l} \text{[sinking]} \\ \text{[loss]} \end{array} \right]_p * VOLEP \\
 &\quad + LOAD_{22} * VOLHY
 \end{aligned}$$


---

Table 3. Summary of the Model Equations (continued)

of the organism to filter is hampered. The assumption that the eating rate is determined by the total concentration of edible food in the filtered water may require refinement. The selective filter feeder adjusts its eating rate to supply the minimum edible food required for maintenance. Therefore, it is aware of what it eats, not of the amount of food in the surrounding water. The distinction is important when one considers that, given equal concentrations, some prey species are more likely than others to pass through the filtering parts of the organisms. Instead of basing the above function on  $\sum_{i=1}^n \text{prey}_i$ , it may be necessary to base it on a weighted sum of prey. The natural preference of the filter feeder for some species over others is not neglected in the model since this principle is utilized in allocation of the eating rate to the various edible species.

Filtering rate studies for selective filterers have concentrated on the marine zooplankton genus Calanus. Mullin (1963) has shown that as the concentration of food increases, Calanus increases its intake steadily until a concentration of .56 mg food c/l is reached. Then the intake declines. The maximum filtering rate for Calanus occurred between 0 and .2 mg food c/l. Conover (1966b) and Mullin (1963) suggest that .2 mg food c/l is the incipient saturating food concentration beyond which the selective filterer begins slowing down its eating rate. Therefore a value of A10 of .2 mg food c/l seems to be compatible with their research. A9 has been chosen as .1 rather arbitrarily so that at food concentrations much higher than .2 mg food c/l, the filtering rate will be 10% of the maximum achievable rate at a fixed temperature. Temperature dependence for all filter feeding states has been taken from Burns and Rigler (1967) and appears in Figure 2. Kibby (1971) suggests that this function may be valid only for rapid temperature variation and that it does not include acclimation of the zooplankter to new temperature ranges. Further research is needed to differentiate between these opposing effects. The maximum filtering rates for the five selective filter feeding states have not been investigated thoroughly in the literature. However, using as a guide the maximum filtering rate of 8.34 l/mg z c·day reported by Frost (1972) for Calanus (at 12°C), these five coefficients can be adjusted to yield the amplitude differences observed in the Lake Michigan data.

Nonselective filterers, unlike selective filterers, filter at a uniform rate, and thus operate below maximum efficiency. A formulation of their eating mechanism is:

$$\left[ \begin{array}{c} \text{eating} \\ \text{rate} \end{array} \right]_z = A7_z * \phi_z(T) * \sum_i \text{prey}_i$$

$$\frac{\ell}{\text{mg z c} \cdot \text{day}} \quad \frac{\text{mg food c}}{\ell}$$
(5)

As noted earlier, the dependence on total food concentration may have to be replaced by dependence on a weighted sum of prey concentrations. The literature has been consulted to estimate the filtering rate of Daphnia. The data are summarized in Table 4. Burns (1969) provided a formula for converting Daphnia length into weight. Thus it was possible to convert the literature values into the standard units of the model. Since filtering rate appears to be highly correlated with daphnid length, linear regression was used to determine the filtering rate at 20°C as a function of length:  $A7_{\text{Daph.}} = 1.69 - 1.25(L-2.16)$ , where  $L$  is the animal length in mm. Since Lake Michigan daphnids average 1.05 mm, they can be expected to filter at 3.09  $\ell/\text{mg z c} \cdot \text{day}$ . Bosmina, which has not been studied extensively in the literature, is expected to filter more rapidly than Daphnia because it averages only .5 mm in length.

Assimilation efficiency. The three classes of zooplankton distinguished above convert food carbon into zooplankton carbon at efficiencies primarily determined by their eating behavior. The raptor and selective filterer both have control over the amount of food they ingest, so they may be assumed to operate at some equilibrium efficiency. Data provided by Cummins et al. (1969) suggests an assimilation efficiency of about .40 for the raptor Leptodora. Waterman (1960) reports an apparent assimilation efficiency of about 80% for selective filterers. Conover (1966a) has measured an assimilation efficiency of about .72 for Calanus hyperboreus. The values stated above have been used as a range in selecting reasonable efficiencies for the selective filterers (see Table 2).

Nonselective filterers cannot lower their filtering rate when the plankton content of filtered water increases. Therefore they operate below maximum possible efficiency. A simple but unconfirmed formulation is:

$$\left[ \begin{array}{c} \text{assimilation} \\ \text{efficiency} \end{array} \right]_z = AllN * \left( \frac{A24}{\sum_i c_i + A24} \right)$$

$$\frac{\text{mg z c}}{\text{mg food c}}$$
(6)

where  $AllN^*$  = maximum efficiency possible

$A24$  = half-max. efficiency food level

Species	Length	Reported Filtering Rate at 20°C	Model Units	Reference
<u>D. rosea</u>	1.60 mm	2.0 $\frac{m\ell}{Daphnid\cdot hr}$	2.85 $\frac{m\ell}{mg\ z\ c\cdot day}$	Burns & Rigler (1967)
<u>D. rosea</u>	1.75	1.85 "	2.08 "	Kibby (1971)
<u>D. pulex</u>	2.00	2.0 "	.78 "	Crowley (1973)
<u>D. magna</u>	3.0	2.92 "	.78 "	McMahon & Rigler (1965)
<u>D. magna</u>	2.38	22.1 $m\ell/mg$ dry wt-hr	1.47 "	Burns (1969)

Table 4. Summary of Data Compiled on Daphnia

A formulation similar to this seems justifiable, since non-selective filterers such as Daphnia and Bosmina require more eutrophic waters to flourish than do selective filterers such as Diaptomus and Limnocalanus. The maximum efficiency possible has not been reported in the literature, but may be very close to 100% since it is defined at near-zero food concentrations. It is expected that this efficiency is at least as great as the constant efficiency of selective filterers. Crowley (1973) determined a .52 mg food c/l saturation level for the assimilation efficiency of Daphnia pulex; however, he obtained this value by desiccating his filter samples for 18 hours before weighing. If it is assumed that the samples had not yet half dried, a saturation level of .2 mg food c/l is estimated. If Crowley's saturation level is interpreted as the food level at which efficiency is half of maximum, A24 may be estimated to be .2 mg food c/l. This .2 mg food c/l level seems to be a critical level to the filterers in that selectives have cut their filtering rate approximately in half and the nonselective are assimilating at half maximum efficiency when food levels reach this concentration.

Before considering other mechanisms, it is worthwhile to compare the dependence of growth rate on food concentration for the three classes of zooplankton. In Figure 3, plots of the eating rate and assimilation rate for the three groups are presented (assimilation rate = eating rate \* assimilation efficiency) as functions of food concentration. The curves have been normalized such that the eating rate is unity at .20 mg food c/l. The region between the curves indicates the rate of egestion and rejection of unassimilated matter.

Preferred diet. The mathematical formulations of eating rate discussed earlier involved only total food carbon available. The assumption was made that food intake is controlled by the amount of edible food in the environment, not by the relative abundance of the various species eaten. However, given that a population has a certain food intake rate - determined by the characteristics of the population, the amount of food present, and the temperature - it will prefer certain species over others. The rate at which state  $z$  consumes prey state  $k$  is in general given by:

$$\left[ \begin{matrix} \text{predation of} \\ \text{species } k \text{ by} \\ \text{species } z \end{matrix} \right] = \left[ \begin{matrix} \text{preference of} \\ \text{species } z \text{ for} \\ \text{species } k \end{matrix} \right] * \left[ \begin{matrix} \text{eating} \\ \text{rate} \end{matrix} \right]_z * c_z \quad (7)$$

$$\frac{\text{mg } k \text{ c}}{\text{l} \cdot \text{day}} \quad \frac{\text{mg food c}}{\text{mg } z \text{ c} \cdot \text{day}} \quad \frac{\text{mg } z \text{ c}}{\text{l}}$$

The mathematical formulation of the preference factor involves a simple assumption: the preference of species  $z$

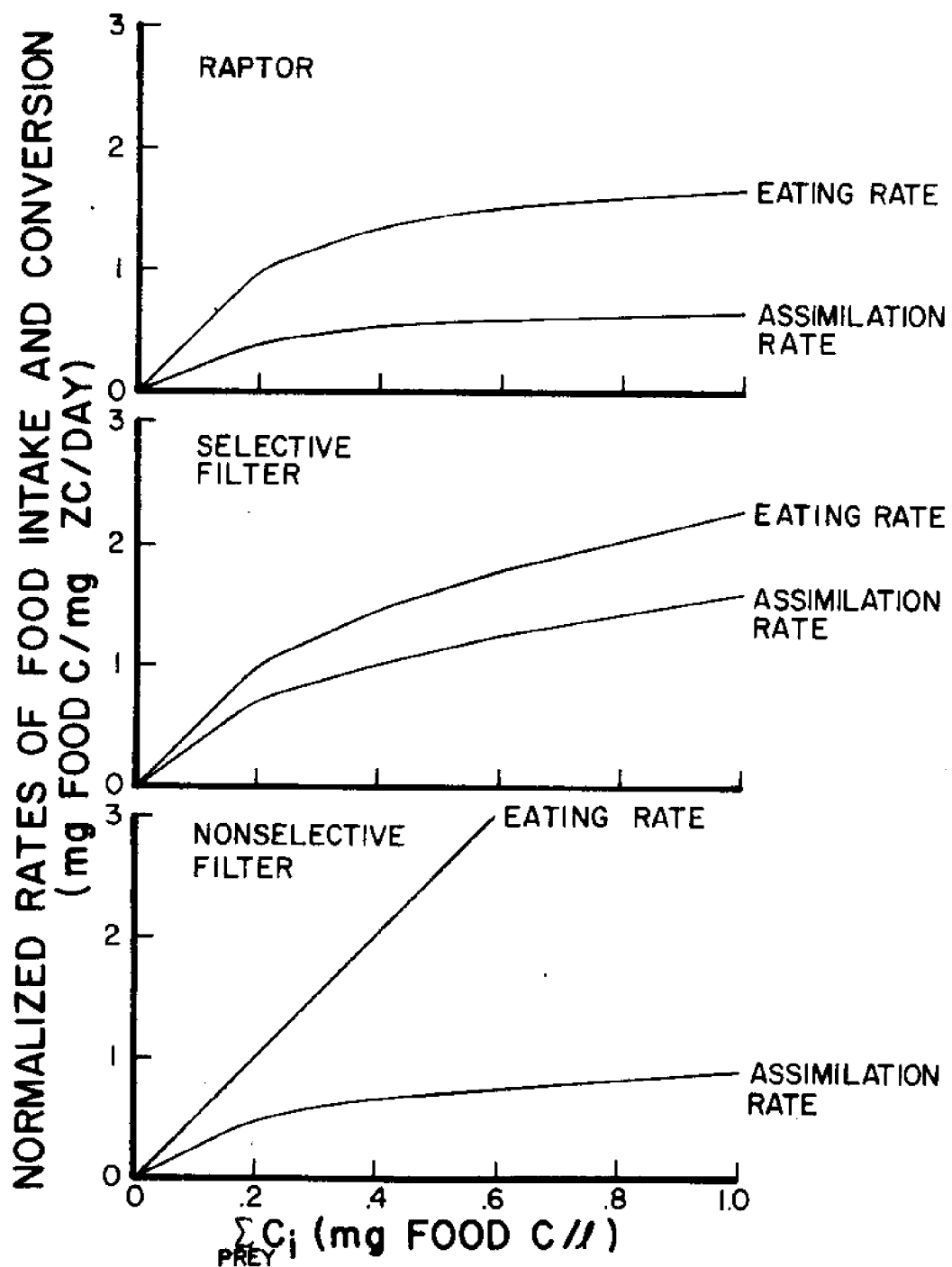


Figure 3. Growth Mechanisms of the Zooplankton Groups

for food species  $k$  is proportional to the product of the electivity of species  $z$  for species  $k$ , and the concentration of species  $k$ . The electivity,  $\alpha_k^z$ , is defined as the fraction of the species  $z$  diet that would be composed of food species  $k$  if all food species were present in equal concentrations. This leads to the formulation:

$$\left[ \begin{array}{l} \text{preference of} \\ \text{species } z \text{ for} \\ \text{species } k \end{array} \right] = \frac{\alpha_k^z * c_k}{\sum_i (\alpha_i^z * c_i)} . \quad (8)$$

When all food concentrations are equal, the above expression reduces to  $\alpha_k^z$ , since  $\sum_i \alpha_i^z = 1$  by definition. The above form

differs somewhat from food preference models proposed by Kitchell et al. (1973) but uses the approach of O'Neill (1969)

Given equal concentrations of prey species, the raptorial zooplankton prefers larger organisms to smaller ones because they provide more food carbon for about the same energy expenditure; similarly, there is a natural preference for slow moving organisms over rapidly moving ones. No studies have been done to establish directly the electivities of the zooplankton states in Lake Michigan. However, Cummins et al. (1969) have indirectly investigated the eating habits of Leptodora kindtii by observing the seasonal variation of it and its prey in a Pennsylvania reservoir. The data indicate a preference for cladocerans over copepods. Although additional direct studies must be done, preliminary estimates of electivities are presented on the food web in Figure 4. Cummins et al. (1969) suggest that the nauplii of Cyclops and Diaptomus contribute to the diet of Leptodora. However, these effects are probably negligible and have been omitted from the present model. A more significant link between rotifers and Leptodora may be important in Lake Michigan, but is not included in this rotifer-free model. Hall (1964) and Wright (1965) have suggested that Daphnia is controlled in mid-summer largely by Leptodora (in Base Line Lake, Michigan and Canyon Ferry Reservoir, Montana, respectively); this link will be scrutinized as additional experimental data become available.

Hutchinson (1967, p. 627) states: "Though the group (Cyclopoida) has been familiar to the amateur naturalist no less than to the professional biologist for more than two centuries, information regarding their [sic] food has been extremely inadequate until recently". A survey of recent literature on the Cyclopoids has revealed the following studies: Anderson (1970a, b); Confer (1971), Fryer (1957a, b),

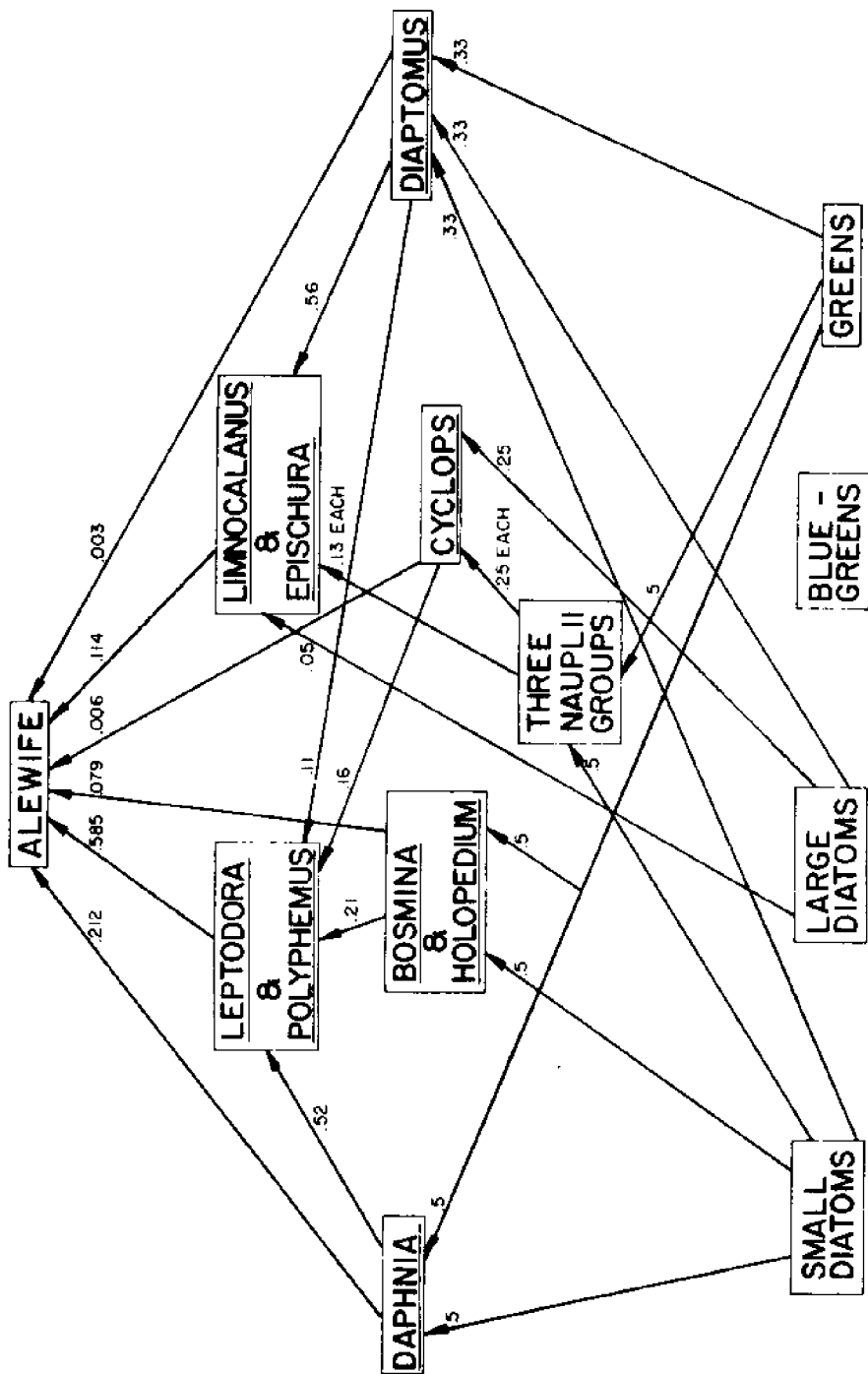


Figure 4. Web of Electivities

Johnson (1972), Lane and McNaught (1970), McQueen (1969), Porter (1973). The following summarizes the views presented in these papers.

Except for Anderson (1970a, b), the evidence indicates that Cyclops bicuspidatus thomasi preys upon the three nauplii groups. Anderson omits cyclopoid nauplii and copepodites from the Cyclops diet. The small size of Cyclops seems to restrict its diet greatly. For example, small adult Diaptomus may be captured only rarely. Fryer (1957a, b), Johnson (1972), and Lane and McNaught (1970) suggest that Cyclops prey upon small cladocerans, immature bosminids, Ceriodaphnia, and similar species, but this view is disputed by Confer (1971). McQueen (1969), Fryer (1957a, b), Lane and McNaught (1970), McComish (personal communication), and Johnson (1972) feel that a rotifer link may also exist. Large diatoms are suggested as part of the Cyclops diet by Fryer (1957a, b), Porter (1973), and Hutchinson (1967). Extensive laboratory studies must be initiated to resolve the nebulous state of knowledge concerning the electivities of Cyclops. At present, the diet of Cyclops is split among the three nauplii states and large diatoms as depicted in Figure 4 above.

The electivities of the filter-feeding species are determined by food size, shape, and palatability. The nauplii, averaging under .5 mm in length, are herbivorous. The diatom groupings have been chosen so that the nauplii are restricted to eating only the small form. Green algae serve as another food source for the nauplii. Equal filterability and equal palatability have been assumed for diatoms and greens. Some blue-greens possess a mucilage coating or have large filaments that make both filtering and digesting of them difficult for most zooplankton species. Diaptomus grazes upon diatoms and greens but, being four to five times the length of a nauplius, is also able to filter some large diatoms.

The omnivorous copepods, Limnocalanus and Epischura, adjust their filtering parts so that larger organisms are ingested when available. Smaller organisms are only taken when larger forms are scarce. Main (1962) has conducted a thorough study of the life history of Epischura. This work suggests that Epischura elects Diaptomus over nauplii and nauplii over large diatoms. These results have been employed for the zooplankton state "Limnocalanus and Epischura".

The nonselective cladocerans, Daphnia, Bosmina, and Holopedium, graze upon small diatoms and green algae. Arnold (1971) contends that Daphnia can filter and digest blue-green algae, but that survival of such Daphnia is very low.

The web of electivities (Figure 4) incorporated into the

lower food web model is subject to modification as researchers collect data and complete experiments on predator-prey relations. With the preference mechanisms formulated as above, the negative predation terms appearing in the zooplankton state equations become obvious.

Predation by other zooplankters and alewives. All the zooplankton states but "Leptodora and Polypheus" and "Limnocalanus and Epischura" are preyed upon by other zooplankters. To be consistent with the formulations of eating rate and preference developed above, the predation of state  $z$  by other zooplankton states must be given by:

$$[\text{predation by other zooplankton}]_z = \sum_{zz} \left( \frac{\alpha_z^{zz} c_z}{\sum_i (\alpha_i^{zz} c_i)} \right) * [\text{eating rate}]_{zz} c_{zz}. \quad (9)$$

The alewife, a major forage fish in Lake Michigan, though not included as a state in this lower food web model, affects the dynamics of the model through forcing functions. The eating rate and concentration of adult and young alewives are applied to the model as known time functions. Allocation of the eating rate to each species taken by the alewife is determined by a preference factor analogous to the preference factor discussed earlier for zooplankton. The uptake of a zooplankton species  $z$  by the alewife population is formulated as:

$$[\text{predation by alewife}]_z = \left( \frac{\delta_z c_z}{\sum_i \delta_i c_i} \right) * \left( [\text{eating rate of young}] * c_{\text{young}} + [\text{eating rate of adults}] * c_{\text{adults}} \right). \quad (10)$$

The electivity of the alewife for state  $z$ ,  $\delta_z$ , denotes the fraction of diet composed of state  $z$  when all zooplankton states are in equal concentration. The simplifying assumption that the alewife does not vary its diet with age can be relaxed later.

Unlike that of zooplankton, alewife-eating behavior has been studied extensively. Brooks (1969) reported that a close relative of the alewife, A. aestivalis, changed the zooplankton composition of a Connecticut lake from one dominated by Diaptomus with Epischura, Mesocyclops, Daphnia, and Leptodora common to one dominated by Bosmina with Tropocyclops, Ceriodaphnia, and Asplanchna common. Experiments performed by Brooks on the alewife suggest that it has similar requirements and preferences to those of A. aestivalis. Wells (1970) showed that nine crustacean zooplankton declined when the alewives increased in Lake Michigan and that six of them recovered after the alewife

crash of 1967. The work of Brooks and Wells suggests that the alewife exhibits strong preferences. The major factors controlling alewife selection seem to be prey size and taxon. The indirect evidence of Brooks and Wells is supported by Hutchinson (1971) and Warshaw (1972), who analyzed the stomach contents of alewives collected from small lakes in New York and Connecticut.

Hutchinson demonstrated that taxon preference may be a significant factor. In this study .27 mm long Bosmina were selected 13 times more frequently than .53 mm cyclopoid copepods. Morsell and Norden (1968) have found that Lake Michigan adult alewives rely upon zooplankton for about only 50% of their diet, with Pontoporeia, ostracods, Mysis, tendipedid larvae, water mites, and fish eggs supplying the other half. Stomach analyses showed that Limnocalanus dominates the diet during winter, while Cyclops, Diaptomus, and Epischura are most common during summer. Daphnia, Bosmina, and Chydorus were the most common cladocerans found. The work of Morsell and Norden (1968) and Norden (1968) has shown that juvenile alewives rely heavily upon zooplankton, including all species eaten by the adults, but in different ratios. The juveniles prefer Leptodora, followed by Daphnia, Limnocalanus, Epischura, Cyclops, Bosmina, and Diaptomus. The work of Hutchinson (1971) and Norden (1968) has been used to establish an electivity of cladocerans over copepods of about 9.7 to 1. This ratio has been weighted by the average volume of each organism in order to establish an electivity of the alewife for each of the six adult zooplankton states of the model. These results are presented in Figure 4 above.

Respiration. Zooplankton respiration research reported in the literature must be analyzed with care. Several factors that should be considered are: (1) Containment increases cladocerans' respiration by 4.5 times, while copepods experience an increase only under very crowded conditions (Burns and Rigler, 1967). (2) Raymont (1959) showed that zooplankton fed before an experiment respire three to five times more rapidly than normally. (3) Halcrow (1963) claims that zooplankton must be allowed four hours to adapt to new temperatures; otherwise, thermal shock causes them to respire twice as fast as they would if acclimated to that temperature. (4) Halcrow (1963) also suggests that copepods are seasonally acclimated, and that respiration varies only within limits in a given season. (5) Conover (1959) has observed that respiration increases independent of temperature when the zooplankton begin heavy grazing. (6) Predators are more sensitive to temperature increases than are grazers of equal weight. (7) The relationship between weight and respiration rate of a zooplankter is negative log-log. Although some of

the above information implies different respiration rates for the zooplankton states of the model, little information is actually available on taxon-specific rates. At this stage, it is reasonable to assume the same temperature dependence for all species and only to differentiate between the respiration rate of adults versus that of nauplii. A linear temperature dependence has been commonly used in plankton production models (Canale et al. 1974). Although some evidence supports an exponential dependence (Warren, 1971), it is thought that a linear approximation for the temperature range of interest is justifiable. Therefore:

$$\left[ \frac{\text{respiration}}{\text{loss}} \right]_z = \text{Al}_2 z \cdot \frac{(\text{T}/20.) \cdot c_z}{\text{day}^{-1}} \quad (11)$$

where  $A12_z$  = rate at 20°C for zooplankton state  $z$  (one rate for adults and one rate for nauplii).

Life cycles. Part 1 of this report (Vogel and Canale, 1974) discussed the life cycles of the zooplankton states. Cladocerans, which are assumed to go directly from egg to mature organism, are simply introduced at appropriate times during the early summer. Egg hatching rates are distributed over time in Gaussian fashion, with a specified mean and standard deviation. Grand Traverse Bay data show that Leptodora and Polypheus hatch over a two-month period centered near mid-June. This is consistent with the observations of Cummins et al. (1969) that Leptodora appear in the spring when water temperatures exceed  $10^{\circ}\text{C}$  and disappear in the fall when temperatures drop below  $10^{\circ}\text{C}$ . Based on the work of Cummins et al. (1969), an estimate of  $100 \text{ eggs/m}^3$  or approximately  $2.2 \mu\text{g c/l}$  has been chosen as the concentration of the Leptodora state introduced by hatching eggs.

Figure 5 contains a summary of the zooplankton life cycles used in the model. The works of Hutchinson (1967) and Hall (1964) have been employed to estimate the number of over-wintering Daphnia eggs available for hatching in late June. Hutchinson (1967) was consulted for similar estimates for Bosmina. Daphnia hatch over a 90-day period, whereas Bosmina complete hatching in less than a month. The initial mass of new Leptodora contributes to over 50% of its peak concentration, whereas that of Daphnia and of Bosmina contributes less than 15% to peak concentration. According to Cummins et al. (1969), the fall decline of Leptodora seems to be caused primarily by predation as the production rate falls off in early fall. Hall (1964) points out that physiological mortality, or natural death, is probably negligible when

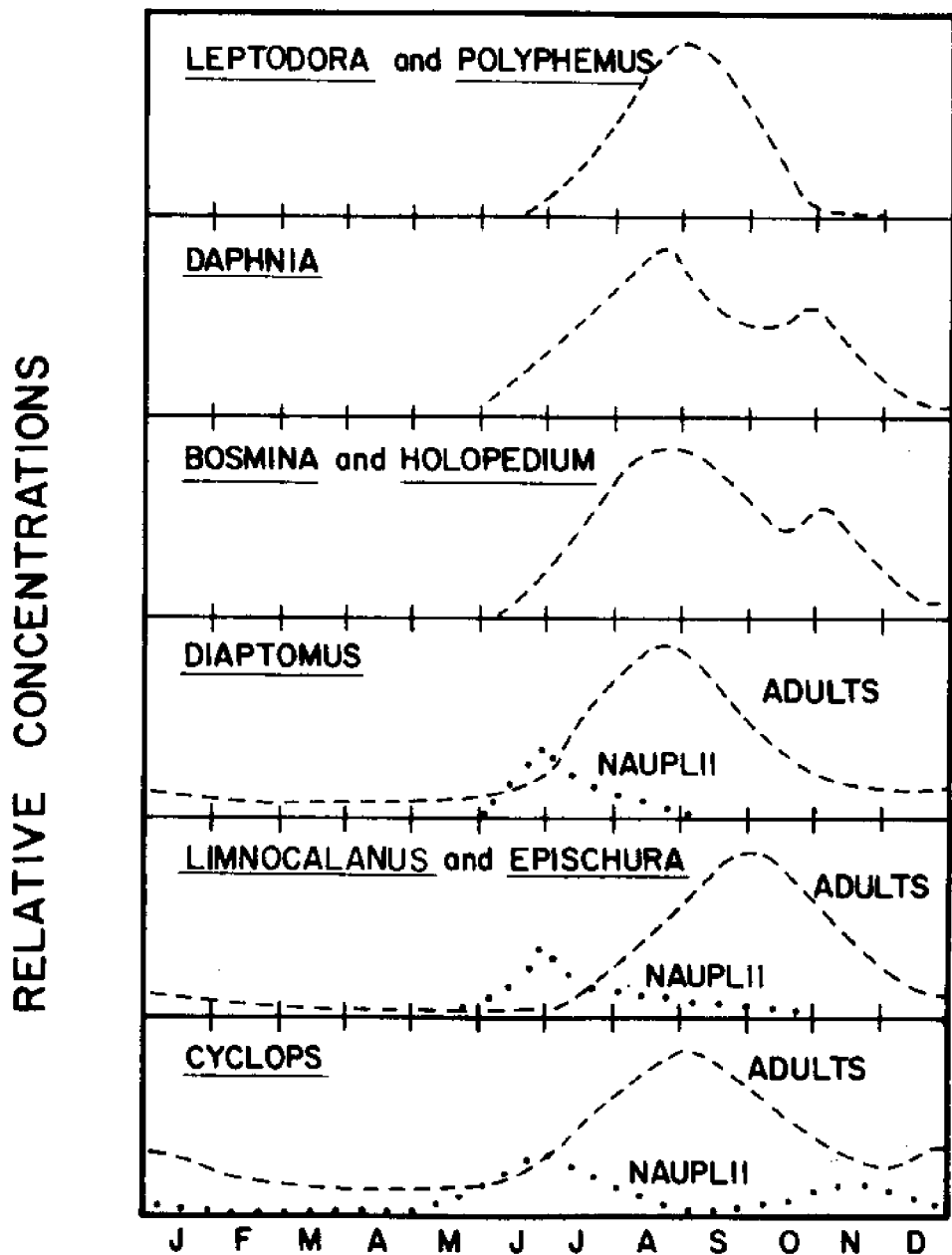


Figure 5. Life Cycles of the Zooplankton

compared to predation as a factor causing the decline of Daphnia in late summer. Although a few daphnids and bosminids are known to survive the winter, because of their small numbers, these individuals are not a factor in winter. Therefore, both states are assumed to have zero concentration between January 1 and hatching.

Unlike the cladocerans, the copepods undergo a more complex chain of transformations from egg to adult. This chain, simplified to egg-nauplius-adult for modeling purposes, is required because of vastly differing eating habits of young and adults. Hutchinson (1967) has been consulted for life-cycle information. Diaptomus undergoes a single cycle each year, holding its eggs until they hatch over a four-month period centered in early May. At that time of the year, approximately  $1200 \text{ adults/m}^3$  are observed in Lake Michigan. 55% of the population is assumed female and each female will lay about 7 eggs. Assuming that the average newborn nauplius comprises about  $.004 \mu\text{g carbon}$ , the total concentration of new nauplii can be estimated as  $.039 \mu\text{g c/l}$ . In mid-July, the Diaptomus nauplii mature into adults. To account for the fact that maturation is not instantaneous and that the division between nauplius and adult is not always distinct, the nauplii are matured through a first order reaction which requires about two months for completion.

The life cycle of Limnocalanus and Epischura has been based upon work of Comita (1956). Limnocalanus drops its eggs to the lake bottom in early fall, where they remain until the water temperature rises in early April. Unlike those of Diaptomus, the eggs all hatch within two months. By late June, the nauplii are maturing into the stages considered adult in the model. In September, when eggs are laid, Limnocalanus number about  $80/\text{m}^3$  in Lake Michigan, of which 25% are egg-producing females. Since each female lays about 6 eggs, and upon hatching the nauplius normally weighs about  $.005 \mu\text{g carbon}$ , the new nauplii population can be estimated at about  $.012 \mu\text{g c/l}$ .

The Cyclops population consists of two overlapping generations. The eggs of one generation hatch in early March over a three to four month span and mature in July; the eggs of a second generation hatch in August over a similar span and mature in January. The adult count at egg-laying times is approximately  $25000/\text{m}^3$  in Lake Michigan, of which 65% lay eggs. A female lays 50 eggs and a new-born nauplius weighs about  $.004 \mu\text{g carbon}$ . Thus spring and summer nauplii populations are estimated at  $.69 \mu\text{g c/l}$ . Since only two states, one each for nauplii and adults, are utilized for Cyclops in the model, it is convenient to require that

the nauplii of one generation completely mature before eggs of the next generation begin to hatch. The generations seem to be isolated from each other enough so that this assumption can be employed.

Simulation runs with the model have indicated that predation and respiration mechanisms may not be sufficient to account for the gradual dieoff of the copepod populations after peaking. Natural death is included as an additional mechanism governing the dieoff. The manner in which the Gaussian egg-hatching and first-order maturation were incorporated into the state equations is discussed in a later section, "Computational Topics".

This completes discussion of the zooplankton mechanisms considered in the model.

### Phytoplankton

Considerable research has been conducted by DiToro and his colleagues at Hydroscience on modeling phytoplankton dynamics (DiToro et al. 1971; Hydroscience Inc. 1973). Canale and others at the University of Michigan (1974) have utilized similar techniques to construct a dynamic model for the natural association of phytoplankton in Grand Traverse Bay. After accounting for taxon-specific behavior, many of the mechanisms utilized in these models can be applied to the present effort.

Production rate. The production of phytoplankton carbon for a particular state "p" is governed predominantly by water temperature, light intensity, and nutrient abundance. Under optimum light conditions and saturating nutrient concentrations, production proceeds at a rate fixed by temperature. Canale and Vogel (1974) have surveyed the wealth of literature on this subject to ascertain the variation of specific growth rate with temperature for diatoms, greens, blue-greens and flagellates. The average maximum water temperature observed in Lake Michigan is about 17°C, which is well below the optimum temperature for the taxa considered in the model. Thus, instead of introducing the maximum saturated growth rate as a coefficient, the model deals with the saturated growth rate at 20°C which is denoted as  $A_{1p}$ . Productivity for phytoplankton state p, then, may be formulated:

$$[\text{growth}]_p = A_{1p} * \Phi_p(T) * \left[ \frac{\text{light}}{\text{reduction}} \right]_p * \left[ \frac{\text{nutrient}}{\text{reduction}} \right]_p * c_p \quad (12)$$

$\text{day}^{-1}$

$\frac{\text{mg c}}{\ell}$

The temperature multiplier  $\Phi_p$  depends on temperature in the manner shown in Figure 2 above.

No reason has been found to differentiate between the temperature response of small and large diatoms. However, because of their greater surface area per unit weight, the small species are expected to grow more rapidly. Spring field data from Grand Traverse Bay seem to confirm this hypothesis. Therefore 20°C growth rates have been chosen within limits to realize the one to two month lag observed between small and large diatom blooms. It is observed that the coefficient values and temperature dependence functions give a strong advantage to the diatom states over the greens and blue-greens, especially at lower temperatures. This advantage is presently manifested in most of Lake Michigan (where silicon levels are high) by the higher percentage of diatoms in phytoplankton samples.

Light limitation. Ryther (1956) has shown that an optimum light intensity exists for phytoplankton photosynthesis. Steele (1965) has formulated a light reduction factor that describes the effect of non-optimum light on the production rate:

$$\left[ \begin{array}{l} \text{light} \\ \text{reduction} \\ \text{at a point} \end{array} \right] = \frac{I}{I_S} e^{\left( -\frac{I}{I_S} + 1 \right)} \quad (13)$$

where  $I$  = light intensity at the point

$I_S$  = optimum light intensity

This reduction factor describes light limitation at a point. However, since the model considers a completely mixed euphotic zone, the reduction factor must be averaged over depth, which accounts for light extinction in the water column. If light attenuation is uniform throughout the column, the light at a depth  $d$  can be expressed by the familiar formula:  $I(d) = I(o) * e^{-KE*d}$  where  $I(o)$  is the surface intensity and  $KE$  the extinction coefficient. DiToro et al. (1971) have integrated the reduction factor over depth with pointwise intensity given by  $I(d)$ . The result expresses the average reduction factor as a function of  $I(o)$  and  $KE$  at an instant of time. The model has not been developed to simulate daily dynamics; thus the cycling of the sun must be accounted for by averaging the reduction factor over 24 hours. If sunlight is assumed to vary as a half cycle of a sinusoid, the light reduction factor cannot be integrated analytically over time. To account for the daily cycling in a tractable manner, surface light intensity is assumed uniform over the daylight hours at a value

IA, equal to the average over the daylight hours. With this simplifying assumption, the average daily reduction factor has been calculated by DiToro et al. (1971):

$$\left[ \begin{array}{l} \text{light reduction} \\ \text{averaged over} \\ \text{depth and time} \end{array} \right] = \frac{e^* \text{PHOTO}}{\text{KE}^* \text{DEPTH}} \left( e^{-\frac{\text{IA}}{\text{IS}} \frac{e^{-\text{KE}^* \text{DEPTH}} - 1}{e}} - 1 \right) \quad (14)$$

P

where  $e = 2.718$ , PHOTO = daylight fraction of day, and DEPTH = depth of euphotic zone.

The taxon-specific nature of the model requires specification of taxon-specific optimum light intensities. Ryther (1956) has explored the effect of light on various groups of marine plankton. However, since lake plankton have evolved under lower light conditions than marine plankton, it is hypothesized that they may exhibit lower optimum intensities than those reported by Ryther. Table 2 lists the coefficients discussed above for the three groups of plankton. The average surface intensity IA, the photoperiod PHOTO, and the extinction coefficient KE follow annual cycles that differ little from year to year. Researchers such as Riley (1956) have investigated the feedback effect of self-shading and have hypothesized formulas for KE expressed as a function of phytoplankton density. KE, in general, varies as a complex function of turbidity and phytoplankton density, and varies considerably with location. For present purposes, such a detailed analysis of this function seems unwarranted, so KE appears in the model simply as a time-varying forcing function. A detailed discussion of KE(t), IA(t), and PHOTO(t) will be given in a later section of the report.

Nutrient limitation. The difference in nutrient utilization between diatoms and the green and blue-green algae groups must be modeled carefully in this effort. Until recently, phytoplankton blooms in Lake Michigan may have been controlled by the availability of inorganic phosphorus. Low phosphorus levels limit the production rate of all three phytoplankton groups in a similar manner. An analysis of the seasonal variation of species in Lake Michigan suggests that diatoms utilize essentially all available inorganic phosphorus by the end of June, and that green and blue-green populations, which are not cold-water adapted, are forced to utilize recycled phosphorus in mid-summer. The low amounts of recycled phosphorus have kept the greens and blue-greens from reaching undesirable concentrations in mid-summer. However, Stoermer and Yang (1969, 1970) have found an interesting phenomenon

developing in southern Lake Michigan, where phosphorus has reached 1930 Lake Erie levels. Diatoms, which require silicon as an essential nutrient, appear to have an excess of phosphorus and are now limited by silicon. However, since greens and blue-greens do not require silicon, they can utilize the inorganic phosphorus left by diatoms to reach higher mid-summer peaks. The above sequence of events may be typical in lakes undergoing eutrophication, making modeling of the underlying causes critical to the development of any control scheme. It is possible to extend the above sequence further by considering the ability of certain blue-green species to fix dissolved nitrogen gas. When phosphorus reaches a critical point, inorganic nitrogen will begin to limit the green algae, whereas certain blue-greens may switch over to nitrogen fixation, thereby surpassing the greens and non-nitrogen-fixing blue-greens in mid-summer.

The mechanisms for nutrient limitation described in the above paragraph have formulated by other workers (Dugdale, 1967; Eppley et al., 1969; DiToro et al., 1971). To date, most useful models have assumed that the productivity of the population follows Michaelis-Menton kinetics as a nutrient becomes limiting. Under this assumption, the nutrient reduction factors for nitrogen, phosphorus, and silicon are respectively:

$$\frac{c_{\text{ammonia}} + c_{\text{nitrate}}}{c_{\text{ammonia}} + c_{\text{nitrate}} + KN} \quad \frac{c_{\text{inorg. P}}}{c_{\text{inorg. P}}} \quad \frac{c_{\text{diss. Si}}}{c_{\text{diss. Si}} + KS}$$

where KN, KP, and KS are the half-saturation levels of the three nutrients, and the state variables are in units of mg basic element/  $\ell$ . As the nitrogen factor indicates, the plankton can utilize both ammonia and nitrate. When ammonia is available in the same concentration as nitrate, ammonia may be preferred over nitrate, a mechanism to be discussed further in the nutrient section of this report. Only the total usable nitrogen determines the reduction due to nitrogen, and the relative amounts of the two inorganic nitrogen states have no bearing on the growth reduction.

Some evidence (e.g. see Herbes, 1974, for an extensive bibliography) indicates that organic phosphorus may be available to phytoplankton. This research, however, indicates that organics provide a small fraction of the phosphorus used by plankton. Until experimental work can confirm the

selectivity for inorganics over organics, organics will be assumed unavailable to the plankton. The calculated growth rate of the diatoms in response to silicon limitation has been modified by correcting for unavailable silicon as suggested by the work of Paasche (1973a, b). The model assumes that  $35 \mu\text{gSi/l}$  is unavailable. The ability of the blue-green state to fix nitrogen gas has been ignored since this mechanism only becomes critical in nitrogen-limiting environments. As the model evolves into a tool for studying eutrophication, this mechanism will be analyzed and included.

The half-saturation constants required for the above formulation have been discussed extensively by Canale et al. (1974). Their literature survey has resulted in the selections tabulated in Table 2. It should be noted that the concentration of nitrogen in the lake is well above saturation levels at present, so that phosphorus and silicon control the dynamics of the spring algal bloom.

The light reduction factor and the nutrient reduction factors have been assumed to operate on the production rate independently. Thus the growth rate expression includes a light factor, a nitrogen factor, and a phosphorus factor for each algal group. The silicon limitation factor only appears in the diatom equations. Experimental data of many researchers have supported the use of the Michaelis-Menton expression when a single nutrient is limiting, but no reports have verified its use for multiple-nutrient limitation. The possibility of coupling the limitation effects other than multiplicatively remains a hypothesis for future research.

Bierman et al. (1973) have recently offered an alternative to the classical Michaelis-Menton approach to modeling nutrient uptake. The approach is based upon the concept of luxury uptake, whereby the algal cell does not use all absorbed nutrients immediately. An intermediate state - an internal nutrient pool - is considered to control cell growth, with transport between water and this state governed by a reversible kinetic mechanism. This refinement in the description of phytoplankton growth, according to Bierman et al. (1973), becomes a necessity when considering the competition between green and blue-green taxa. The transport from water to internal nutrient state occurs more rapidly in blue-greens than in greens, especially at low nutrient levels, affording blue-greens the opportunity to take up more nutrients than they actually need for immediate growth. Although this approach is promising, the mathematics of the mechanism have not yet been verified against extensive data. For this reason and because phosphorus data used to verify the present model cannot be broken into organic and inorganic forms, a complex

growth mechanism beyond the Michaelis-Menton formulation seems premature.

Predation by zooplankton. Once the mechanism of zooplankton predation has been formulated, the loss of phytoplankton mass to the zooplankton is fixed by mass balance. The rate of depletion of phytoplankton state  $p$  due to predation must be:

$$\begin{aligned} \text{[predation loss]}_p &= \sum_z \left( \frac{\alpha_p^z c_p}{\sum_i \alpha_i^z c_i} \right) * \text{[eating rate]}_z * c_z \\ &\quad \frac{\text{mg food c}}{\text{mg z c .day}} \quad \frac{\text{mg z c}}{\ell} \end{aligned} \quad (15)$$

where the  $z$ th term of the summation is the predation on state  $p$  by zooplankton state  $z$ . It has been assumed that no algal cells pass through a filter-feeder without being either assimilated or rendered lifeless. Biomass that cannot be assimilated becomes detrital matter to be regenerated into essential nutrients. The food web has been discussed in an earlier section, but one facet should be reiterated. To emphasize its virtual invulnerability to predation, the blue-green state has been left isolated from the remaining web. Thus, after blue-greens peak, their decline is affected only by respiration, leaving them to die off more slowly than diatoms or green algae. When diatoms are limited by silicon, this slow die off of the blue-greens may result in persistent water quality degradation throughout the summer months.

Respiration. Endogenous respiration acts along with predation to lower phytoplankton carbon during and after a bloom. Most models, including those of DiToro et al. (1971) and Canale et al. (1974), have modeled the effect of temperature on phytoplankton respiration linearly. Riley (1965) has suggested, and many have agreed, that the effect is probably exponential. However, if the proposed exponential dependence is used, with a 20°C rate as reported in most of the literature, the respiration rate below 5°C appears too high to permit persistence of the phytoplankton through the winter months. It is therefore hypothesized that the plankton manifest an exponential dependence at higher temperatures, but that in the lower range of temperatures characteristic of Lake Michigan, a linear approximation may be substituted. The temperature-varying linear kinetics may then be formulated:

$$\left[ \begin{array}{c} \text{respiration} \\ \text{loss} \end{array} \right] = A_3 * (T/20.) * c_p \quad (16)$$

p

$$\text{day}^{-1} \quad \frac{\text{m g c}}{\text{L}}$$

where  $A_3$  is the  $20^{\circ}\text{C}$  respiration rate. DiToro et al. (1971) have tabulated data on the endogenous respiration rate of some plankton species. These data and reports by Hineman (1973) suggest a range of .05 to .1 for the coefficient  $A_3$ .

Sinking. Although sinking is a primary contribution to phytoplankton loss during certain seasons, the mechanism is difficult to model. A myriad of parameters, including temperature, internal nutrient concentrations, internal monovalent-divalent concentration ratios, the presence of gas and/or oil vacuoles, and turbulence affect the net upward or downward velocity of a species. With the present level of sophistication in the area, a reasonable approach is to measure sinking velocities throughout the year and use these data as a forcing function. If the depth-averaged velocity of a species is given by  $VS$ , then the sinking rate is given by  $VS/DEPTH$ , where  $DEPTH$  is the depth of the euphotic zone. If  $A_{6p}$  is the maximum sinking rate of state  $p$ , and the function  $SINK(t)$  exhibits the seasonal variation, then:

$$\left[ \begin{array}{c} \text{sinking} \\ \text{loss} \end{array} \right] = A_{6p} * SINK(t) * c_p \quad (17)$$

Unfortunately, conclusive studies have not been made on the variation of sinking with time in Lake Michigan. Burns and Pashley (1974) have measured sinking velocities in central Lake Ontario at four times of the year. The results indicate that sinking is prevalent in March and September, but that in July and October, plankton are generally rising to the surface. This reverse process cannot be handled in any obvious manner within the confines of the present model hypotheses.

In any event, the sparse data on seasonal variation provided by Burns and Pashley (1974) cannot accurately depict this variation. Their data have been used to estimate only roughly the expected variation. The variation  $SINK(t)$

chosen is plotted and further discussed in the forcing function section of the report. Because the study referenced above dealt with total carbon, it did not yield any taxon-specific information. Because of gas vacuoles, blue-green algae are able to remain suspended throughout their growing season and are thus not affected by sinking. Diatoms, due to their silicon content, are more dense than green algae and probably sink much more rapidly. It is assumed that the experiments discussed earlier were dominated by diatoms, yielding acceptable sinking rates for the diatom state. In theory, small diatoms sink slower than large ones; however, structures on larger cells may retard their sinking rate such that in some cases larger cells sink slower than small cells (Hutchinson, 1967, p. 276).

Seasonal cycles. Division and growth of dominant plankton cells, and therefore the cycles of the plankton population, are largely controlled during much of the year by temperature and light. Since the taxa considered are not equally sensitive to low temperatures and light, the diatom cycle differs greatly from the green and blue-green cycles. Diatoms can be found in measurable concentrations throughout the winter, with their spring bloom controlled by increasing light. However, greens and blue-greens seem unable to reproduce below 5°C. When environmental conditions are adequate, as indicated by a positive derivative in the state equation, the blue-green and green states are introduced into the dynamics. The initial concentration of the population can only be ascertained accurately by sampling the waters in mid-winter in order to determine the low level of dormant cells present then. Model simulations indicate that these initial levels affect subsequent dynamics only slightly. Research must be undertaken to analyze the phenomenon of green and blue-green "appearance" before the model can be used to adequately study taxa shifts brought about by limiting silicon.

### Nutrients

Stoichiometry of phytoplankton and zooplankton. The mass balance equations written for each of the three nutrient cycles under consideration acquire simple forms when one assumes that carbon, nitrogen, and phosphorus occur in the same ratios in all plankton considered. In general, it is known that these ratios can vary among phytoplankton species and are even critically dependent upon relative concentrations of the nutrients in the surrounding water and upon the life history of the cells. DiToro et al. (1971) have summarized the data of Strickland (1965) on the dry weight percentage of carbon, nitrogen, and phosphorus in various taxa of phytoplankton. The great

variability indicated by these data certainly must be accepted as evidence that taxon-specific nutrient ratios must be further investigated. Although the assumption that the ratios do not differ greatly is made with some reservation, the variability within each of the three taxa modeled may be too great to justify the use of taxon-specific ratios. As in the Massdale model of DiToro et al. (1971) and the Lake Erie model contributed by Hydroscience (1973), zooplankton cells are assumed to have the same nitrogen-to-carbon and phosphorus-to-carbon ratios that their phytoplankton counterparts have. Values used in these previous models are consistent with those values adopted in the present study and listed in Table 2 above.

Diatoms, unlike the other phytoplankton groups considered, require the element silicon for continued production. Since green algae, blue-green algae, and zooplankton require only trace amounts of silicon, the silicon cycle involves only the diatoms, detrital (particulate) silicon forms, and dissolved silicon. The silicon-to-carbon ratio for diatoms follows that used by Canale et al. (1974). With the simplified stoichiometry discussed above, the mechanisms that govern each of the three nutrient cycles can be formulated. Figures 6, 7, and 8 are provided as an explanation of these cycles. See Table 3 for a summary of the equations involved.

Detrital components. The undigested matter that passes through zooplankton cannot immediately be utilized in phytoplankton production. The detrital nitrogen and detrital phosphorus components, through partly bacterial and partly physical reactions, decompose into dissolved organic forms. These reactions, like other nutrient reactions to be discussed later, are temperature controlled. Most modeling efforts, including Hydroscience (1973), have incorporated simplified formulations for this breakdown consisting of first-order temperature-dependent kinetics. With no other standard for comparison, the temperature dependence has been assumed linear. Although most nitrogen egested by zooplankton is expected to be in an organic form, evidence indicates (Harris, 1959; Marshall and Orr, 1961) that zooplankton egest inorganic phosphorus along with detrital phosphorus. This mechanism may be unimportant to the phosphorus cycle, however, because subsequent phosphorus reactions are quite rapid.

Unlike nitrogen and phosphorus, silicon is required only by diatoms. The silicon cycle, then, is unique among the three cycles considered. Detrital silicon is generated in the form of particulate silicon through the mechanisms of zooplankton predation and diatom "respiration". Since zooplankton utilize only trace amount of silicon, the silicon frustule of the diatom cell passes undigested from the animal. The "respiration" mechanism does not resemble the

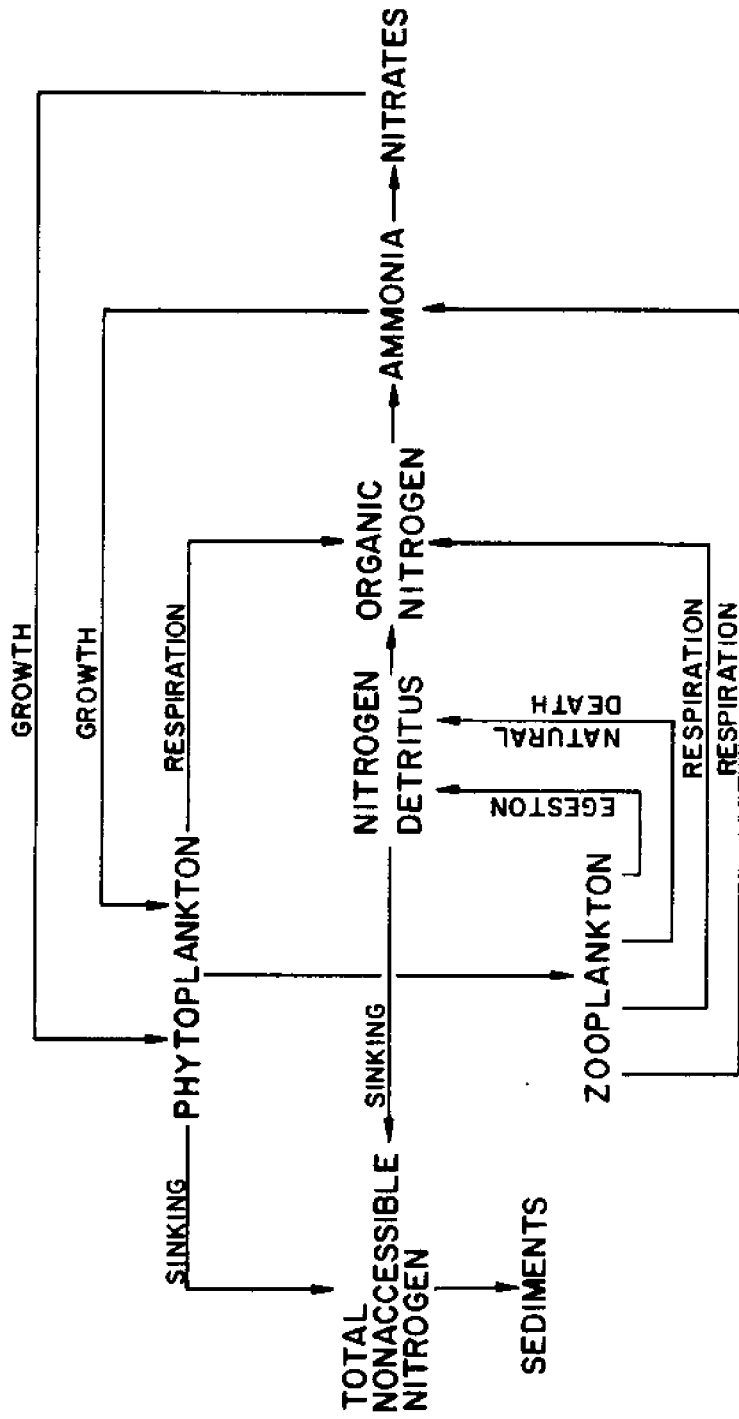


Figure 6. Nitrogen Interactions

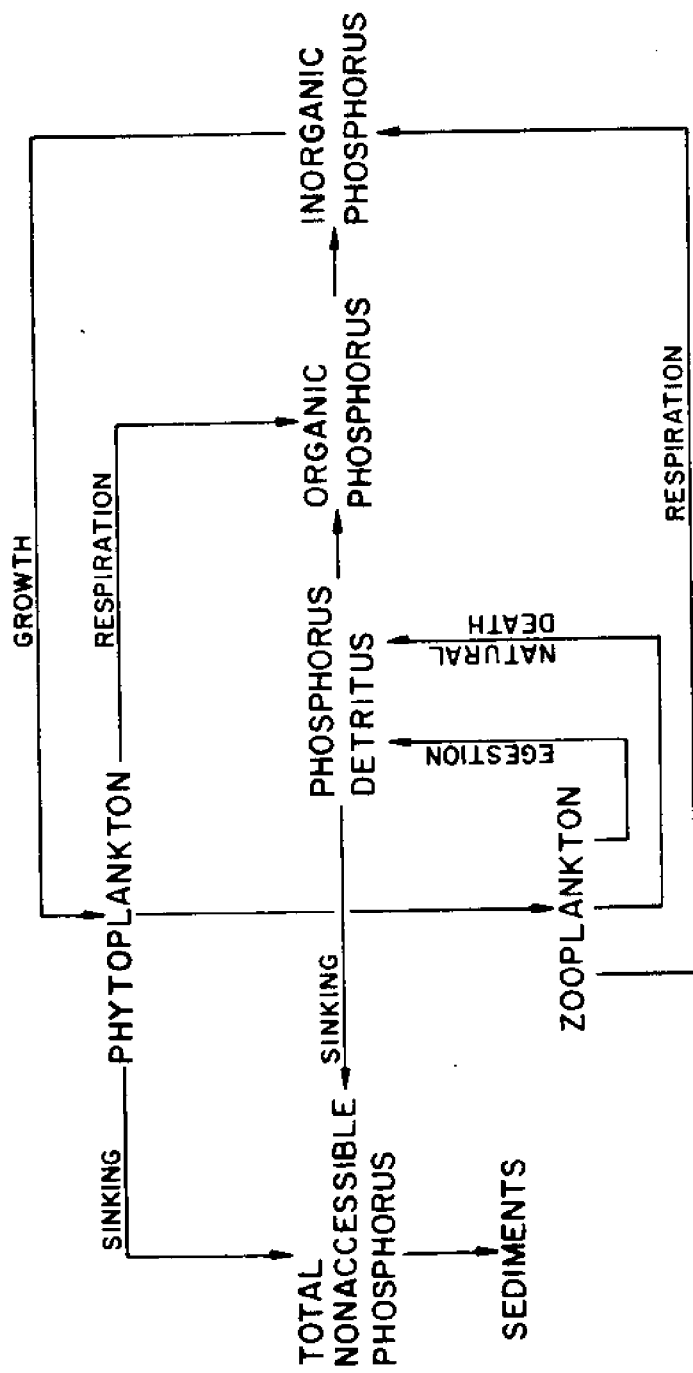


Figure 7. Phosphorus Interactions

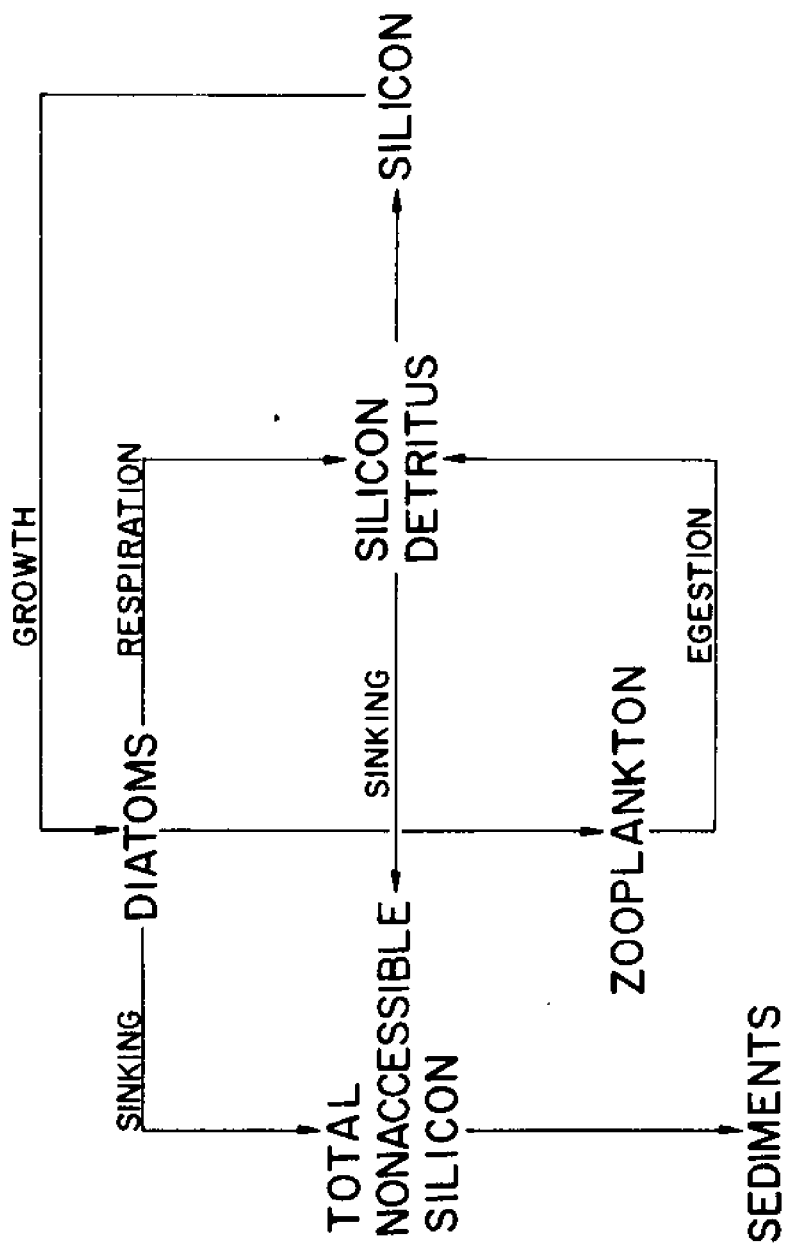


Figure 8. Silicon Interactions

respiration of nitrogen and phosphorus. Diatoms, like other living things, respire only trace amounts of silicon. However, when respiration dominates photosynthesis, the cell eventually collapses, leaving the frustule intact. This silicon shell, like the particulate silicon that passes through a zooplankter, dissolves and is made available once again to the diatom population. In order to account for the silicon being recycled in this manner, one must assume that respiration of a certain mass of carbon can be associated with the isolation of a certain amount of silicon. A similar assumption was made in proposing the amount of silicon taken up when a certain mass of diatom carbon is produced. This relationship between diatom carbon and silicon depends critically upon the average surface-to-volume ratio of the species involved. Since the model considers two size classes of diatoms, the need for detailed analysis of this relationship seems essential to developing an accurate model. At present, the silicon-to-carbon ratio does not differ between the small and large diatom states.

If the breakdown of detrital nitrogen, phosphorus, and silicon proceeds slowly compared with the sinking rate of the detrital matter, then sinking must be considered as an operative mechanism. Although phosphorus reacts more rapidly than the detritus sinks, nitrogen and silicon react more slowly. The detrital sinking rate probably exceeds that of living phytoplankton but confirmed rates are not available in the literature. At present, the maximum sinking rate of the plankton is assumed to apply to detritus also.

Organic components. The bacterial and physical breakdown of detrital nutrients obviously encompasses a myriad of complex reactions, most of which have been investigated very little to date. The chain of reactions proposed in the model hopefully depicts to some degree the mechanisms of recycling observed in lakes. Few models have considered a detailed detrital nutrient system. Hydroscience (1973) partitions the nitrogen component into organics, ammonia, and nitrate. The reaction rates governing the kinetics of this chain are reported by Hydroscience (1973), and at 20°C, are approximately .05 day<sup>-1</sup>. The dynamics of the nitrogen subsystem seem to proceed at rates comparable to the biological rates of the system, so the detail incorporated into modeling this subsystem is justified. The Lake Michigan food web model being discussed considers detrital nitrogen in addition to the three nitrogen forms considered by Hydroscience (1973). The reaction rate for the breakdown of detrital forms into dissolved organic forms has not been found in the literature. Presently for nitrogen, the rate has been set equal to the rate used for the conversion of organic nitrogen to ammonia.

Hydroscience (1973) and Canale et al. (1974) have attempted to partition phosphorus into components. The reaction rates governing detrital-to-organic transfer and organic-to-inorganic transfer, however, appear to lie near  $4 \text{ day}^{-1}$  at  $20^\circ\text{C}$ , a rate far exceeding the fastest biological rate observed in the system. Since the time constant for these phosphorus reactions is less than a week for most of the production season, the phosphorus subsystem might be more conveniently modeled by employing a quasi-equilibrium assumption.

Besides the pathways from nitrogen detritus to organic nitrogen and from phosphorus detritus to organic phosphorus, organic forms are also generated during phytoplankton respiration. Approximately 70% of the nitrogen respired by zooplankton enters the water in organic form, the remainder entering as ammonia. Research indicates that most of the zooplankton-respired phosphorus emerges in an inorganic form (Raymond, 1963). The form of these source terms in the nutrient equations follows directly from mass balance concepts.

Inorganic components. The final products of the recycle reactions, i.e., the inorganic forms, provide the essential nutrients for primary production. Phytoplankton utilize both inorganic nitrogen forms, ammonia and nitrate. Previous models, Hydroscience (1973) and Canle et al. (1974), have distinguished between algal preferences for the two nutrients. Auer (1974), in an extensive literature survey, has reported on nitrogen utilization by algae. The uptake of the inorganic nitrogen forms seems to be controlled by complex environmental and intercellular conditions including trace element availability, light and carbon dioxide levels, internal and external pH, and cell age.

Although some reports of ammonia preference have been found, no consensus has been reached among researchers on the subject. Presently, the uptake mechanism is modeled such that ammonia is preferred 95% to 5% over nitrate when the two forms are in equal abundance. Regardless of what form the algae prefer, the inorganic nitrogen forms may be pooled into a single state with no change in plankton behavior. The ammonification and nitrification rates have been chosen in the range reported by Hydroscience (1973) with temperature variation approximated linearly. The zero degree bias in nitrification rates reported by Hydroscience (1973) has been omitted.

The rate of decay of organic phosphorus compounds into inorganic forms reported by Hydroscience (1973) exceeds all biological rates of the system. There seems to be some discrepancy between these values and those reported by Grill and Richards (1964). At about  $10^\circ\text{C}$ , the former researchers

report  $.20 \text{ day}^{-1}$  and the latter,  $.0381 \text{ day}^{-1}$ . The phosphorus subsystem is so critical to present-day lake dynamics that further laboratory analyses of the phosphorus reactions must be undertaken before an adequate understanding of the system is possible. The mechanisms of silicon recycling also warrant further investigation. If, as some have proposed (Raymont, 1963; Grill and Richards, 1964; Armstrong, 1965), the silicon frustules of diatoms contain a highly soluble and a relatively insoluble component, then multiple pathways must be included for frustule degradation due to diatom respiration and zooplankter egestion.

Nonaccessible components and turnover. Phytoplankton and detritus are subject to sinking during the late-winter ice period and late-summer calm period. Any mass that sinks through the thermocline into the hypolimnion is unlikely to return to the epilimnion before turnover. The model accumulates this mass throughout the year in the total nonaccessible nitrogen, phosphorus, and silicon states. A fraction of the nonaccessible nutrient mass is lost to sediment deposits and can be estimated by sediment core analysis. The remainder will be suspended or dissolved in the hypolimnion waters and available for mixing with epilimnion nutrients at turnover.

For simplicity, the detailed dynamics of hypolimnetic nutrients have not been included in the model. Estimates of the component breakdown of each of the three nonaccessible nutrients can be made (1) by analyzing the epilimnion data just prior to and just after turnover, (2) by accounting for the slow bacterial decompositon that occurs in the low temperature hypolimnion, and (3) by direct measurements of hypolimnion nutrients. Table 5 details the fractions necessary for formulating turnover in this manner. The appropriate fractions of the nonaccessible nutrients are mixed with corresponding epilimnion components during the last two months of the year, the mixing distributed as a Gaussian function centered at day 330. Because productivity is low, there is little change in total nitrogen, phosphorus and silicon concentrations during the winter. Since there is only a small nutrient uptake during the winter, the spring turnover has not been included in the model. In natural systems such as the sea (Raymont, 1963), however, it may be the main route for epilimnetic nutrient resupply. The effect of spring turnover on the lake's temperature is accounted for in the annual temperature cycle.

Loadings. Because the flow of water from Lake Michigan is small in comparison to lake volume, retention time is very large compared to that of Lakes Erie and Ontario. The retention time of 99 years (O'Connor and Mueller, 1970) implies that the lake would take more than three centuries to clean

Component	% of nonaccessible nutrient comprised of this component at turnover	% of total non-accessible nutrient lost to sediments over first 300 days
Detrital nitrogen	0.	
Dissolved organic nitrogen	45.	
Ammonia	0.	10.
Nitrate	45.	
Detrital phosphorus	0.	
Dissolved organic phosphorus	50.	
Dissolved inorganic phosphorus	35.	15.
Detrital silicon	3.	
Dissolved silicon	88.	9.

At day 300, the epilimnion nutrient concentrations and the total nonaccessible nutrient masses are monitored in the simulation routine. The expected breakdown of the non-accessible nutrients, by components, is calculated using the percentages above. The lake is then mixed using the formula:

$$\text{uniform concentration of component after turnover} = \frac{\text{epilimnion concentration before turnover} * \text{VOLEP} + \text{mass before turnover}}{\text{VOLEP} + \text{VOLHY}}$$

The resultant modifications in component concentrations of the epilimnion are implemented over the interval [300, 360] in Gaussian fashion.

Table 5. The Turnover Mechanism

itself if all industrial, municipal, and runoff loads could be shut off. The long retention time implies that initial conditions in the lake have an overwhelming impact when compared with nutrient loadings. The rate of nutrient outflow, the flow divided by volume, lies near  $2.8 \times 10^{-5}$  day $^{-1}$ , negligible when compared with biological and decomposition rates of the system.

The loadings, primarily from agricultural, municipal, and industrial sources, are tabulated by Ayres (1970) and are shown in Table 6. The lake is still relatively unpolluted and near a steady state with respect to nutrient cycling. Since increases of phosphorus and other compounds can be observed over a period of several years in most of the off-shore sections of the lake, it may be hypothesized that loadings more than compensate for settling. Long-term trends in water quality require a detailed examination of inputs and sediment-water interactions. These issues are not addressed in the present model. The proper framework for such considerations may be a model employing simpler kinetics.

State Number	Description	Loading [ $\frac{\text{mg}}{\text{L}\cdot\text{day}}$ ]
1,...,13	The plankton states	Biomass loadings are assumed negligible
14	Detrital nitrogen	Negligible
15	Dissolved organic nitrogen	$8.00 \times 10^{-6}$
16	Ammonia	$1.15 \times 10^{-5}$
17	Nitrate	$9.05 \times 10^{-6}$
18	Detrital phosphorus	Negligible
19	Dissolved organic phosphorus	$3.08 \times 10^{-7}$
20	Dissolved inorganic phosphorus	$9.05 \times 10^{-7}$
21	Detrital silicon	Negligible
22	Dissolved silicon	$5.35 \times 10^{-5}$

The above loads have been calculated based on the entire lake volume as in initial approximation. They are assumed uniform over the 360 day year.

Table 6. Approximate External Loadings to the Lake

## MODEL FORCING FUNCTIONS

Inherent in the equations for the dynamics of the system are certain forcing functions, or exogenous variables, that describe environmental or other conditions assumed to be unaffected by the internal conditions of the system. Four of these variables - temperature, light intensity, photo-period, and extinction coefficient - directly control phytoplankton production. The sinking rate multiplier simulates, as well as is presently possible, the limited data on seasonal variations in phytoplankton and detritus sinking. The alewife-eating rates and concentrations are necessary to approximate the effect of the upper food chain on the lower trophic levels, and would be unnecessary in an expanded version where alewives would be considered as a state (or states) internal to the model. As mentioned earlier in the discussion of model philosophy, these forcing functions must be constructed to represent mean conditions observed in the lake and cannot be expected to duplicate a particular yearly cycle. The amount of deviation from these conditions encountered from year to year dictates the scatter observed in the biological and chemical data from year to year.

Temperature

The University of Michigan Sea Grant Program has sampled water temperature at several stations in Grand Traverse Bay. Depth - and station - averaged temperatures are tabulated by Canale et al. (1974). A spline-interpolated interpretation of these data is used here and plotted in Figure 9. Late winter temperatures fall to a low of about  $1.6^{\circ}\text{C}$  at the end of March. During spring turnover, the temperature recovers to about  $4^{\circ}\text{C}$ , followed by a steady rise to approximately  $17^{\circ}\text{C}$  by the end of August. The near-freezing conditions at the end of March and beginning of April are accompanied by extensive ice cover. The temperature function described here must be an average over the top 20 m so that phytoplankton growth can be averaged analytically over depth. This approximation is well justified during the winter months when the lake is nearly isothermal except for a slight surface gradient. During the summer, however, after the thermocline has been established, temperatures may vary  $10^{\circ}\text{C}$  or more from the surface to the top of the hypolimnion. In order to better approximate phytoplankton production during these months, one would have to either integrate the growth expression over depth, taking into consideration the temperature gradient, or sub-divide the epilimnion.

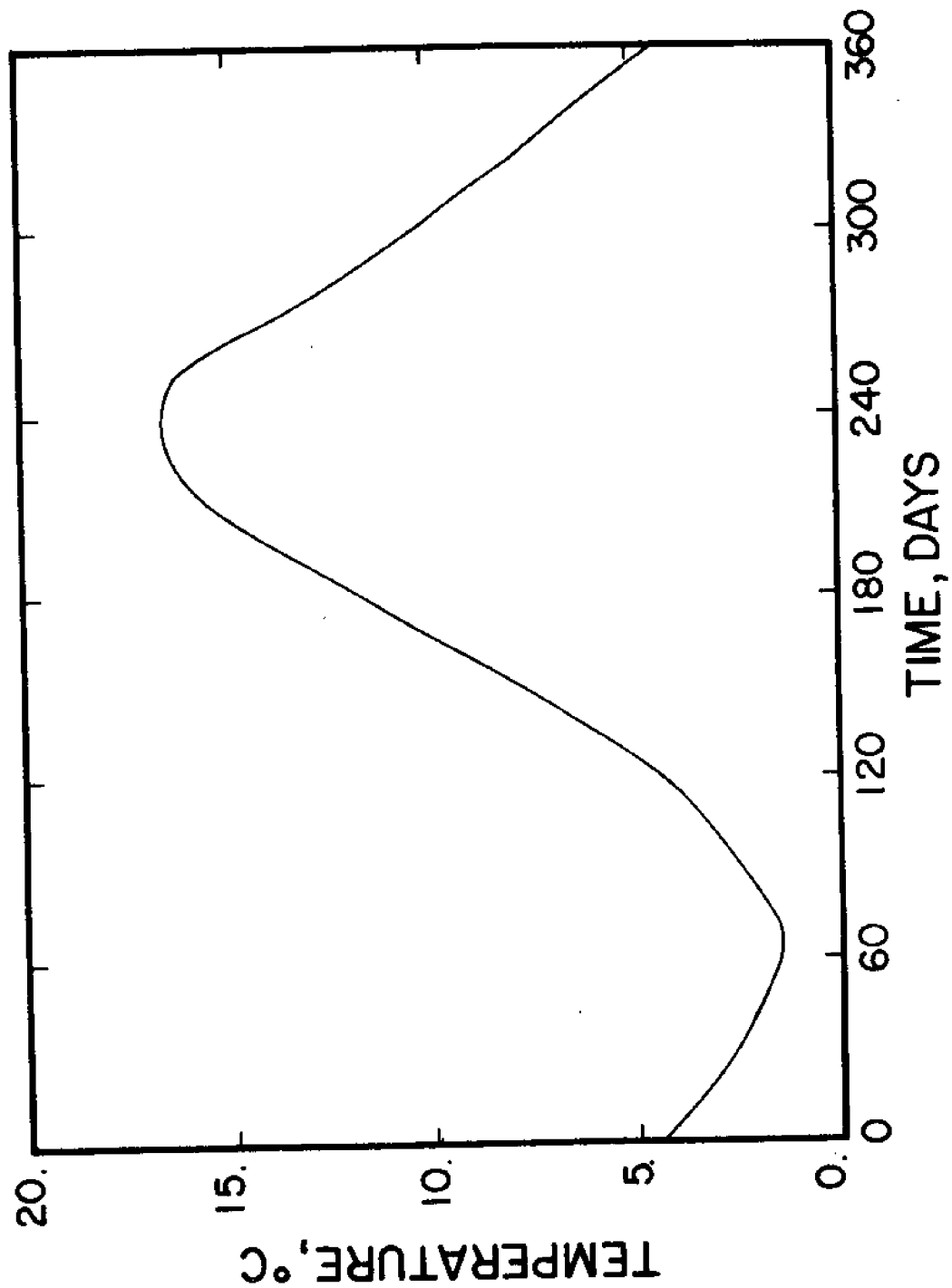


Figure 9. Annual Temperature Cycle

### Light Intensity

Sets of solar radiation measurements for 1962 and 1963 are available in the literature (Great Lakes Institute, 1962 and 1963) for the Lake Erie-Lake Ontario region. Since the location of Lake Michigan and its weather patterns differ little from those of the eastern Great Lakes, these data probably indicate well enough the seasonal variation to be expected. The variation indicated conforms with that used by Hydroscience (1973) and that tabulated for the midwest and northeast United States by Odum (1971). An adjustment must be made in light intensity data during late winter to account for the ice that covers portions of the lake. Ice, especially when covered with snow, acts to lower the solar radiation incident to the water surface. The adjusted light-intensity curve appears in Figure 10. Note that the units of intensity, langleys/day, are a measure of the average irradiance energy over the daylight hours as required by the model.

### Photoperiod

Photoperiod, the daylight fraction of the day, is taken from a report by Hydroscience (1973), which makes use of 1962 Great Lakes Institute data (see Figure 11). The relative proximity of Lake Michigan and the region studied by the Institute suggests that the data are representative of Lake Michigan variation. Photoperiod is the most stable of the forcing functions, accurately predictable years into the future.

### Extinction Coefficient

Canale et al. (1974) have described how light intensity versus depth data from Grand Traverse Bay stations was used to calculate the extinction coefficient KE at various times during the year. The data were fit to the familiar formula:  $I(d) = I(0)e^{-KE \cdot d}$ . Correlation coefficients always exceeded .97, justifying this formulation of extinction. Enough data have been accumulated by the above technique to indicate the likely seasonal trends in extinction, as plotted in Figure 12. The following hypothesis is offered as an explanation of observed trends. As detrital matter from summer plankton populations decomposes, the waters begin to clear in mid-winter. Toward late winter, ice covers reduce turbulence, allowing much of the remaining detritus and silt to settle. The extinction coefficient reaches a relative minimum in early spring. Between day 120 and 160, the lake turns over, followed by a rapid diatom bloom. During this period the extinction coefficient increases to a relative maximum. The

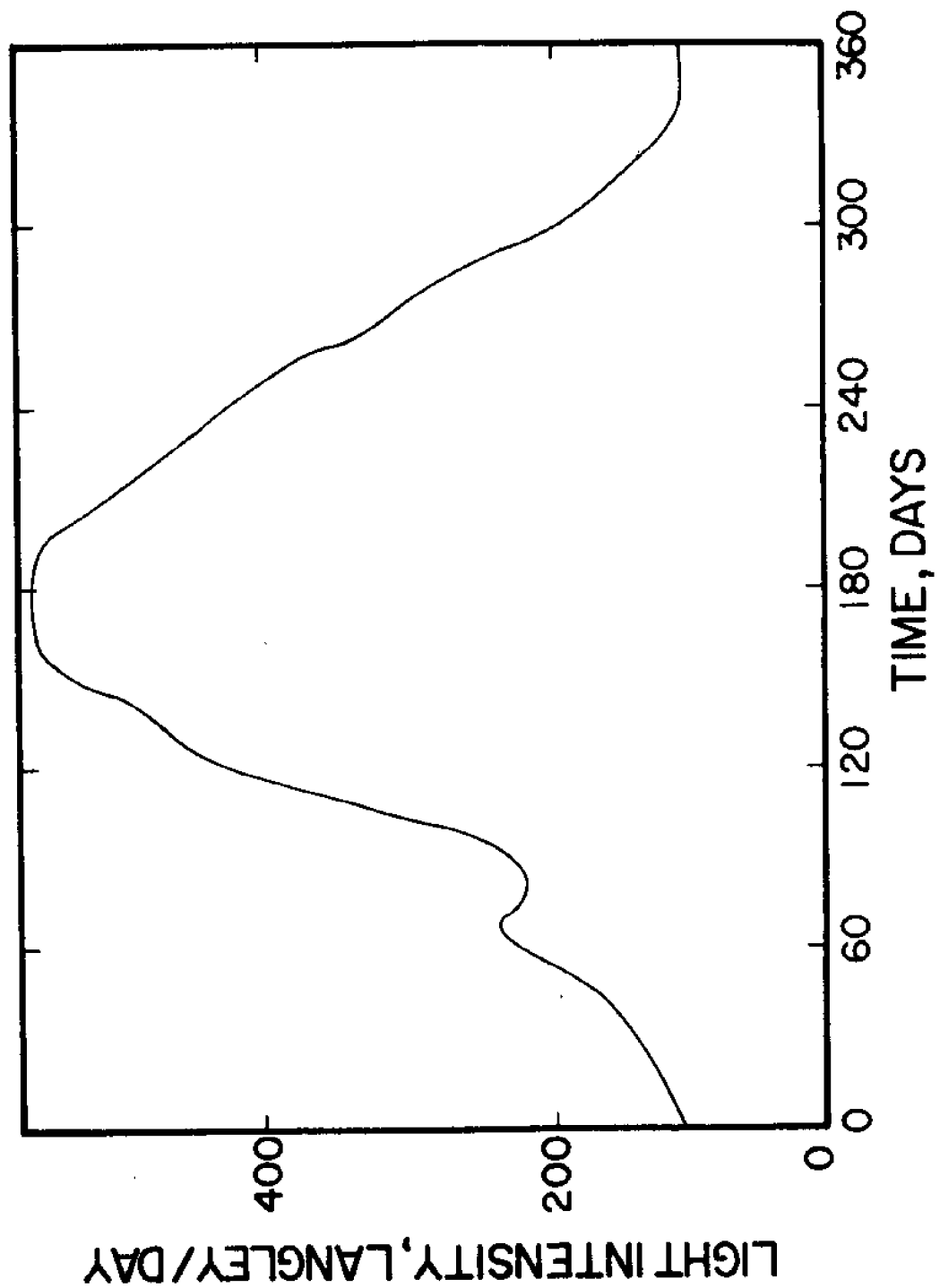


Figure 10. Annual Light Intensity Cycle

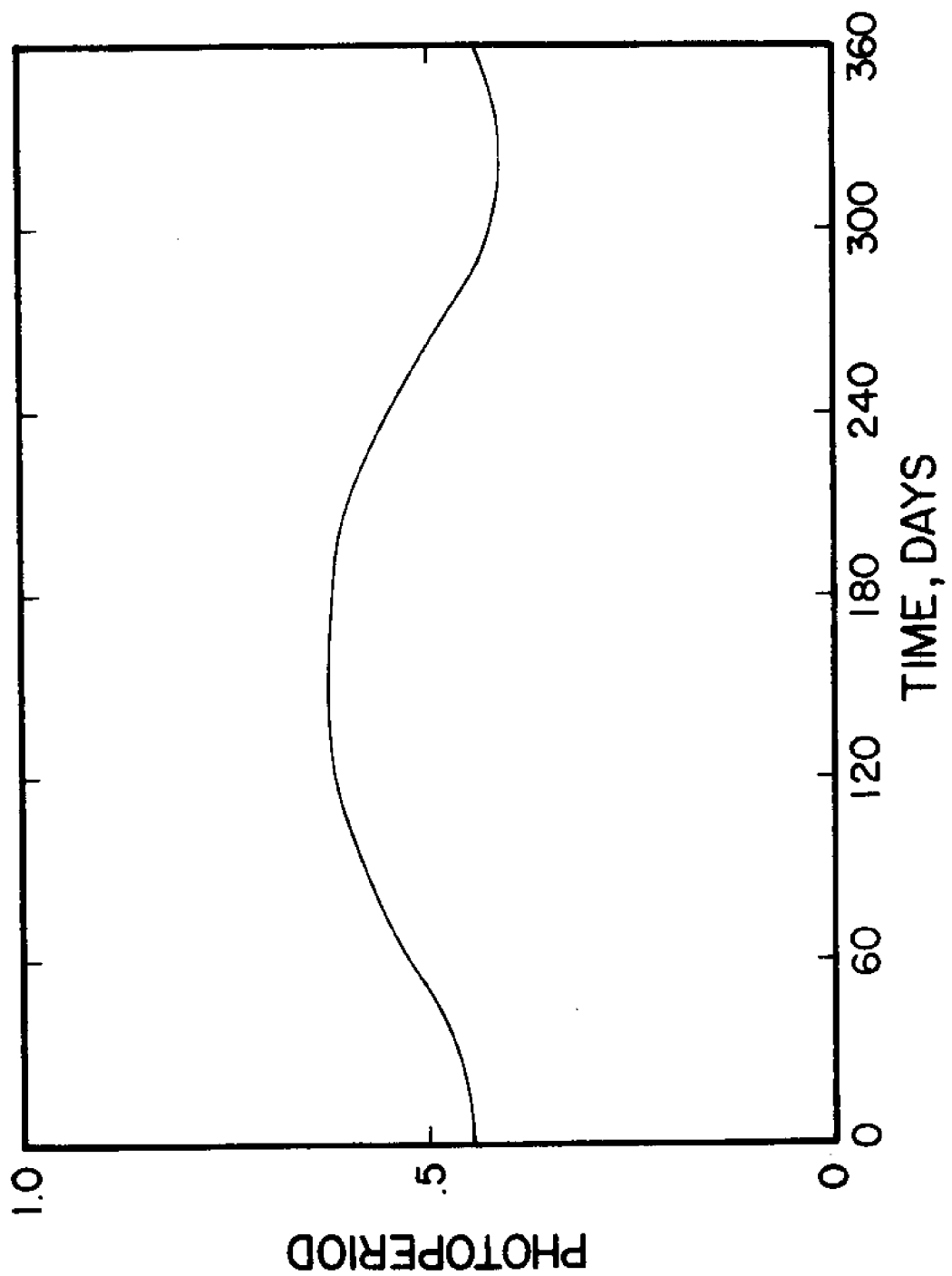


Figure 11. Annual Photoperiod Cycle

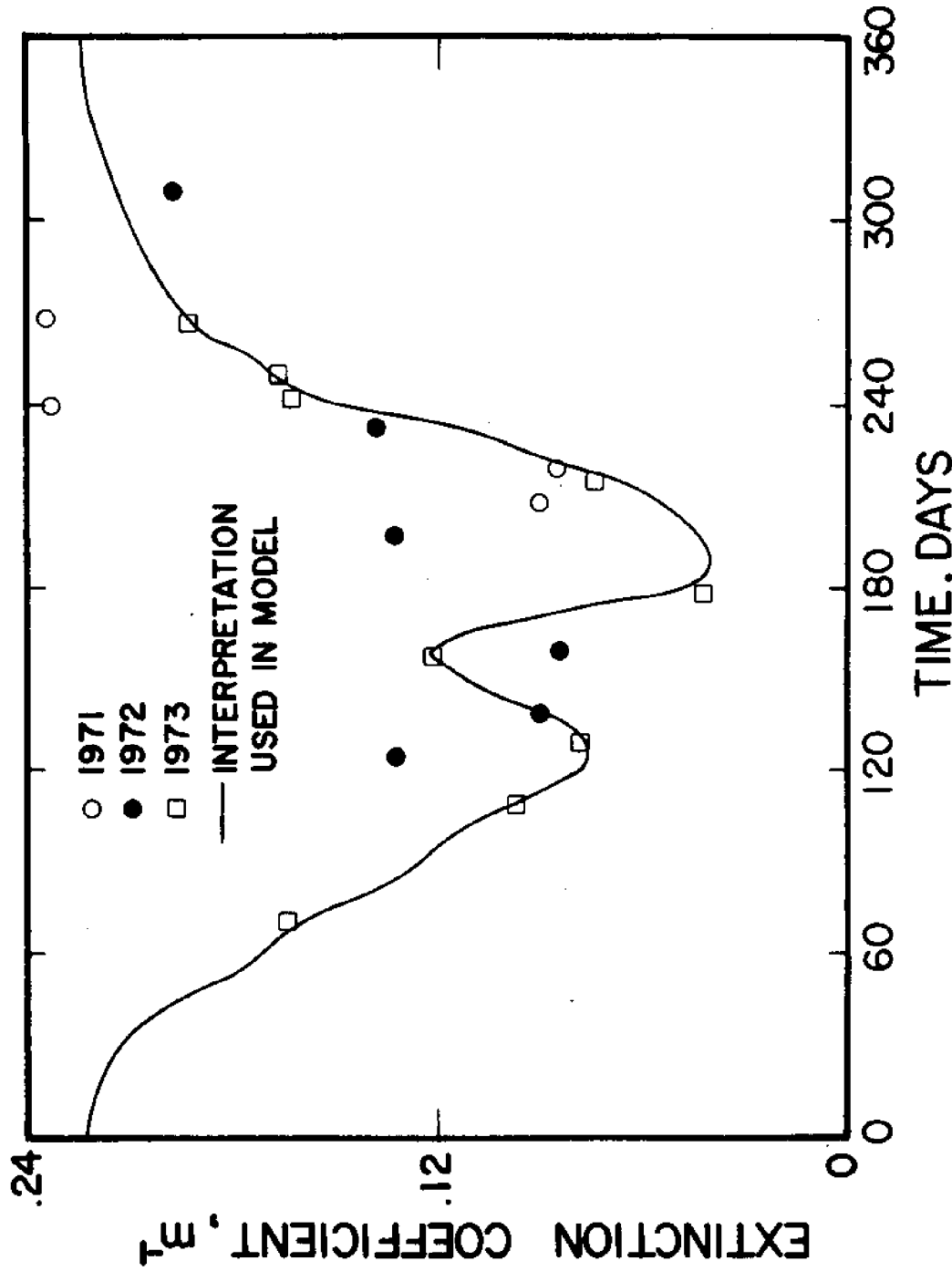


Figure 12. Annual Extinction Coefficient Cycle

diatom bloom is quickly devoured and, as the lake stratifies the lake begins to clear to a yearly low extinction of  $.05\text{ m}^{-1}$  by the end of June. Green and blue-green blooms and subsequent fall turnover cloud the lake throughout the late summer and fall. Since light extinction has been included as a forcing function rather than as a calculated function of the plankton and other dissolved and particulate matter, the predictive value of the model is limited. If standing stocks of detritus or plankton deviate significantly from present conditions, a more appropriate technique for estimation of light extinction must be sought.

#### Sinking Rate Multiplier

Unfortunately, few field studies have concentrated on sinking rates of algae and detritus, and none have investigated the seasonal variation in these rates necessary for an adequate description of the sinking mechanism. Burns and Pashley (1974) have studied Lake Ontario sinking rates, but have concentrated on variation over depth rather than over time. Only four sampling times are reported in their paper, so intuition must be relied upon to complete the picture of seasonal variation. It is expected that sinking can probably be ignored during the turbulent period from November through mid-February, with most particles remaining suspended. However, the ice cover of late February and March prevents wind mixing and allows sinking to prevail.

Diatom data indicate a depression or at least a lull during these 60 days. Subsequently, spring turnover and turbulent waters reduce sinking again, and the establishment of the thermocline retards sinking throughout the summer. In September and October, however, as the thermocline begins to disappear, and before fall turnover occurs, sinking may reach its highest level. Turnover and subsequent turbulence probably reduce the rate in late autumn. These variations are illustrated in Figure 13. This hypothesis is consistent with the data of Burns and Pashley (1974), but obviously needs further support. The sinking rate required here should be an average over the epilimnion, with account made for the impenetrable nature of the thermocline during the summer months.

#### Alewife Eating Rates

The rate at which alewives eat is controlled by two factors, reproductive state and temperature. Between mid-May and early September, the adults do not eat at all since this is during their breeding period (Smith, 1968). Colby (1971) found that alewives can gain 4% of their body weight per day at temperatures above  $15.5^{\circ}\text{C}$ . At  $2.2^{\circ}\text{C}$  alewives cannot eat, and below  $4.0^{\circ}\text{C}$  they eat very slowly and do not attempt to compete aggressively for food with coregonids

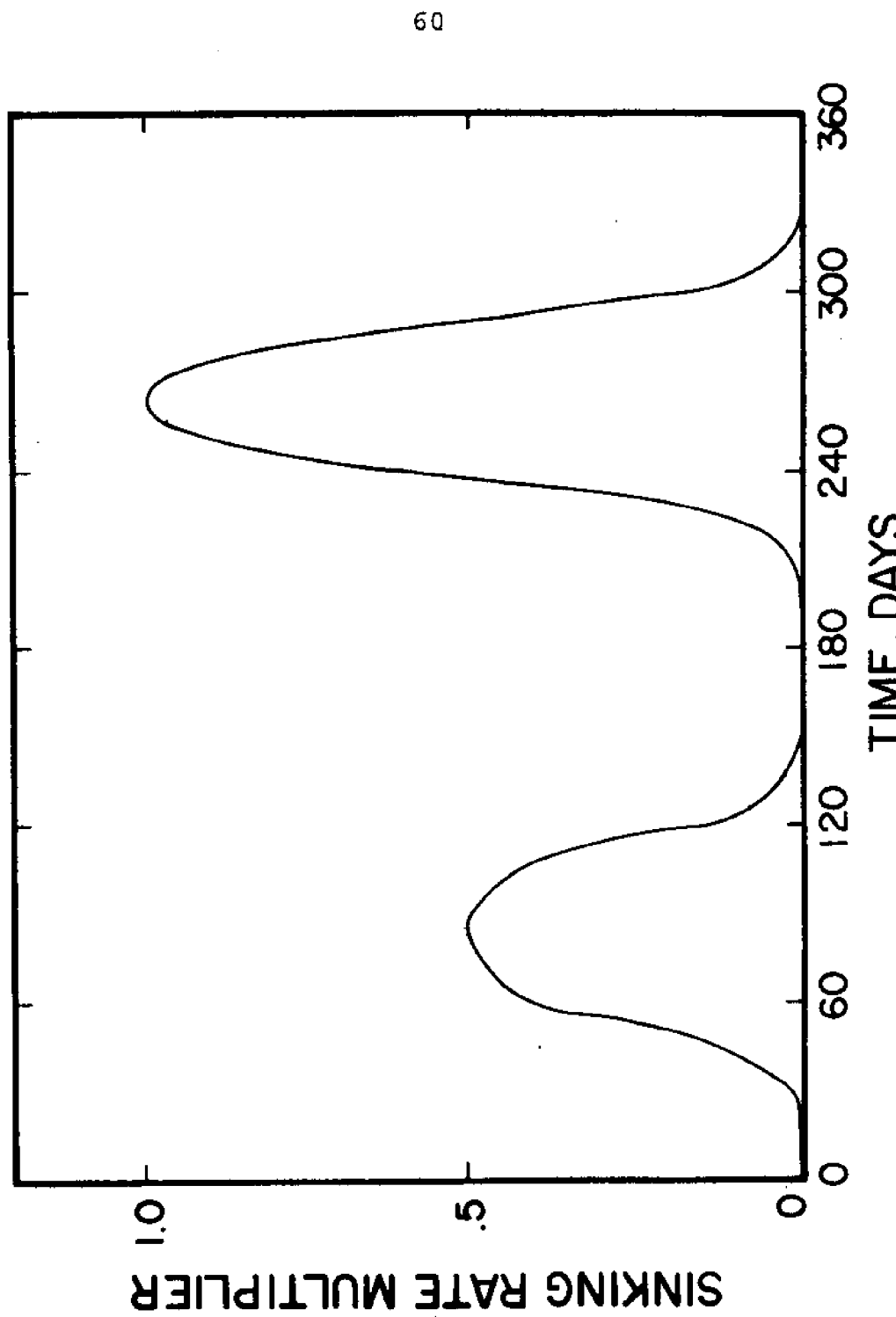


Figure 13. Annual Sinking Rate Multiplier Cycle

native to Lake Michigan. Based upon this information, a temperature-dependent feeding rate in units of mg z c/alewife/day was developed for adult and juvenile alewives and is shown in Figure 14.

#### Alewife Concentrations

In the spring of 1972, the minimum wet weight biomass of alewives in Lake Michigan was  $3.2 \times 10^9$  lbs, or  $1.5 \times 10^9$  Kg (Edsall et al. 1972). The average wet weight per alewife was 42.9 g (derived from Edsall et al. 1972); hence there were approximately  $34.4 \times 10^9$  alewives in Lake Michigan, or about  $7.1 \times 10^{-3}$  alewives/m<sup>3</sup>. Over a one year time period the actual number in the lake varies since the adults leave the lake to reproduce in the tributaries. The adults begin leaving in mid-May and return in the fall. Most alewives mature in their second year (Brown, 1972), so that the juveniles represent 17.5% of the population (Edsall et al. 1972) or about  $6.0 \times 10^9$  fish that do not leave the lake during the summer. The above information has been used to estimate and plot the number of adults and juveniles in Lake Michigan throughout the year and is found in Figure 15.

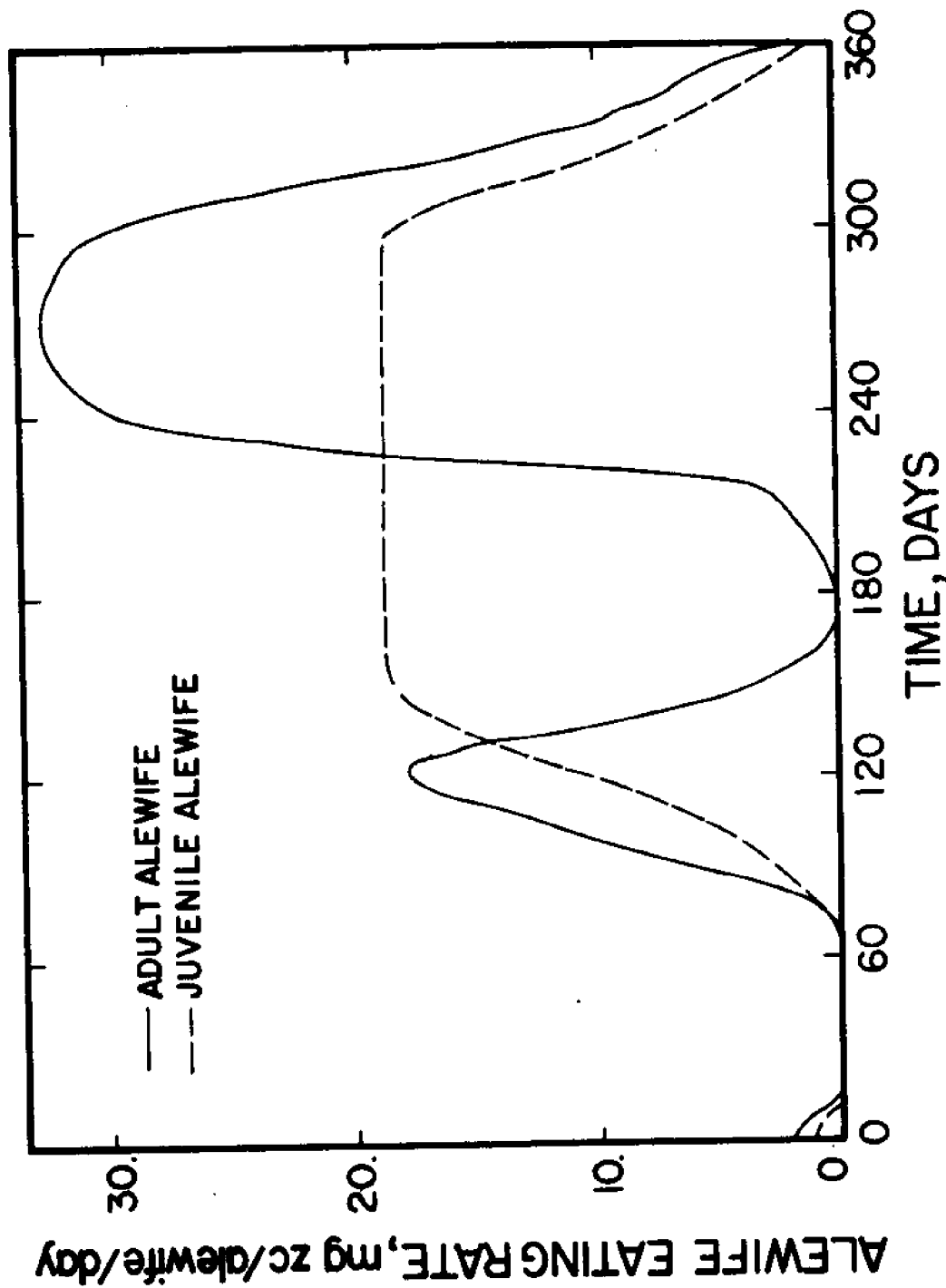


Figure 14. Annual Alewife Eating Rate Cycle

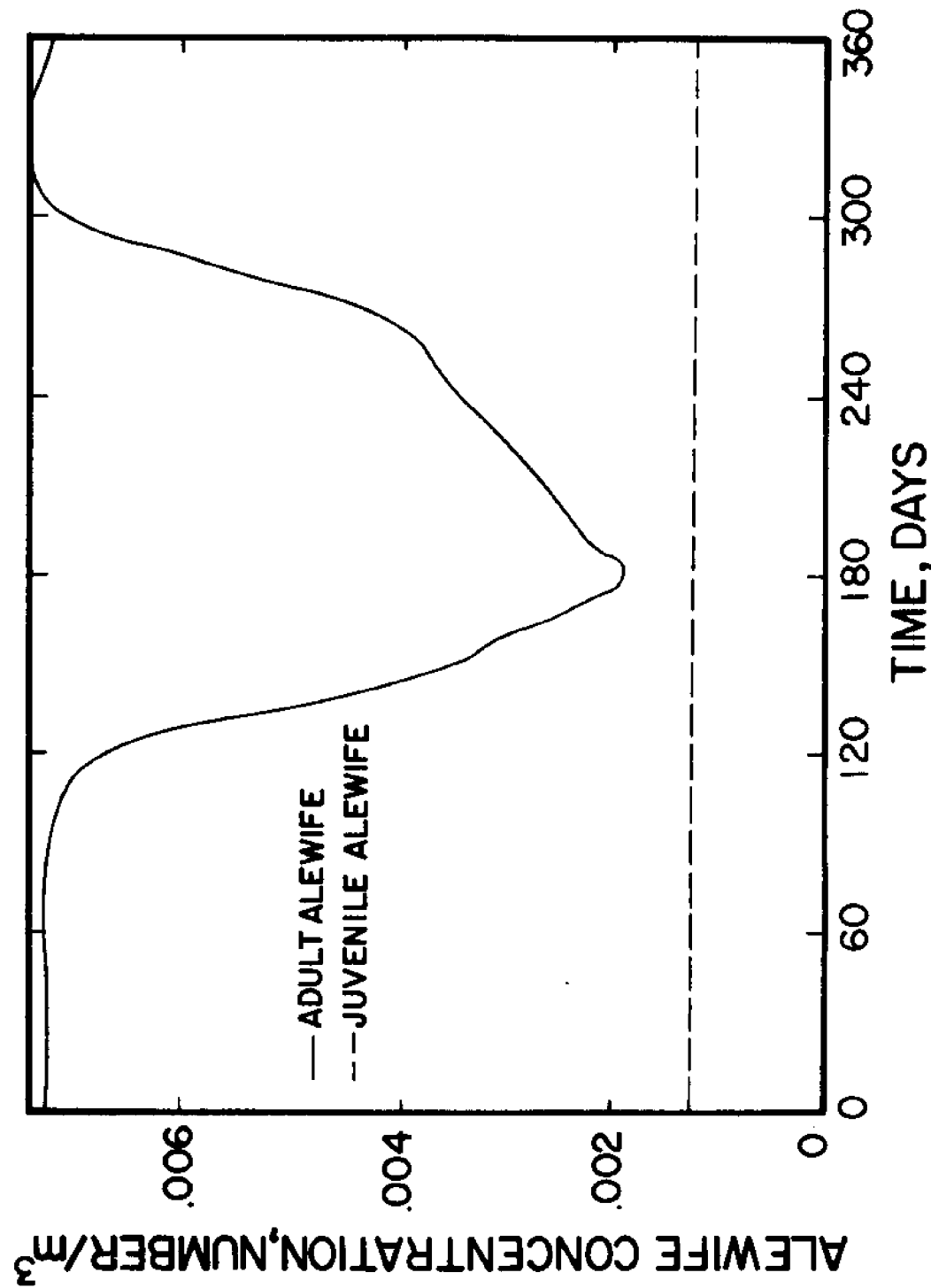


Figure 15. Annual Alewife Concentration Cycles

## COMPUTATIONAL TOPICS

Integration

Due to the highly nonlinear nature of the differential equation system discussed above, it is desirable to choose a numerical integration technique capable of adapting quickly to changing modes of behavior. DVDQ, a variable-order variable-stepsize scheme developed by Krogh (1969), meets the demands of such a complex system. Krogh has built an elaborate routine to adjust stepsize and integration order as rates and error tolerances vary. Also built into the routine are checks for numerical instability and machine error. DVDQ is especially attractive because of its flexibility and the simplicity with which one interacts with the routine. Frazho et al. (1973) discuss further the advantages of DVDQ.

Because the states vary substantially over the year, computer time can be saved by employing a relative error tolerance. A 4% global error tolerance is used for those states for which field data exists and a 5% tolerance for those states without data. When the absolute tolerance calculated by this technique falls to 1% of the maximum value of the state, in order to avoid requiring unreasonably low tolerance at relatively unimportant times of the year, the tolerance is not further reduced. Simulations run with gradually decreasing relative tolerance have shown that the tolerance chosen is well below those levels at which problems might arise.

Interpolation

Because the model forcing functions must be developed and stored using a finite number of time points, interpolation must be used. It has been observed that the variable stepsize integrator DVDQ can be sensitive to the interpolation scheme chosen. Some investigations have focused on a comparison of simple linear interpolation with the piecewise cubic spline technique. The latter approach interpolates between data points with a cubic polynomial, with continuity in the interpolation function and its first and second derivatives enforced at the data points. If one is seeking minimum curvature, this technique yields the smoothest interpolation possible. When linear interpolation is applied to the forcing functions of the model, discontinuities are introduced into the derivative of  $\dot{x}(t)$  at the discrete times where the forcing functions are defined. These discontinuities in  $\ddot{x}(t)$  provide no insurmountable numerical difficulties for DVDQ, but require a reduction in stepsize and a corresponding increase in computation time. It has

been found that the spline interpolation scheme can cut computation time by a factor of two to three. A disadvantage of the splines procedure, however, appears to be that it exhibits unusual behavior between data points when the partitioning of the time axis is coarse in comparison to the variation in the data. This enigma may be circumvented by avoiding large gaps between the points which define the forcing functions. The functions plotted in Figures 9 to 16 have been defined at twelve-day increments and spline-interpolated elsewhere.

Although the eight forcing functions have been smoothed using spline interpolation, the functions defining the temperature dependence of zooplankton and phytoplankton growth (Figure 2) have been allowed to contain the corners that accompany linear interpolation. Due to the uncertainty in these functions, it has been essential that modification be made easily and cheaply, a characteristic of linear interpolation.

#### Hatching, Maturation, and Natural Death

The timing of these three mechanisms governs the behavior of the zooplankton states and is partially outlined in the "Life Cycles" subsection of this report. The hatching distributions for the cladoceran states (Leptodora & Polypheus, Daphnia, and Bosmina & Holopedium) are modified Gaussian curves which have been truncated beyond three standard deviations from the mean, biased down to eliminate the discontinuities at the truncation points, and readjusted to unit area. The mean and standard deviation for each distribution appears in Table 7.

The need for tractability dominated the choice of the copepod timing described below and detailed in Table 7. The copepods (Cyclops, Diaptomus, and Limnocalanus & Epischura) are characterized by two stages, termed "nauplius" (including all growth stages except the final two subadult copepodites) and "adult". The nauplius stage emerges over a few months, since all eggs do not hatch simultaneously. The expected hatching distributions described in the "Life Cycles" subsection, although representative of reality, are difficult to work with in an initial verification attempt. With some loss in reality, the eggs are hatched through an impulse at the mean of these distributions. The impulse is simulated by halting integration, introducing appropriate discontinuities into the nauplii states and restarting integration. Upon hatching, the nauplii enter a growth period during which the mechanisms of growth, respiration, and predation influence their dynamics. When appropriate, as indicated in the earlier subsection, the nauplii enter a maturation period where growth

## Gaussian hatching distribution

	mean (days)	standard deviation (days)	area (mg/l)
<u>Leptodora &amp; Polyphemus</u>	200.	10.	.00220
<u>Daphnia</u>	172.	8.	.00291
<u>Bosmina &amp; Holopedium</u>	172.	4.	.00278

	hatching time (days)	hatching concentration (mg/l)	growth period (days)	maturity period (days)	maturity rate - 1 (days - 1)	adult death period (days)
<u>Cyclops</u>	64.	$6.9 \times 10^{-4}$	$64 \leq t \leq 170.$	$170 \leq t \leq 244.$	.04	$64 \leq t \leq 170.$
	244.	$6.9 \times 10^{-4}$	$244 \leq t \leq 320.$	$320 \leq t \leq 360.$	.04	
<u>Diaptomus</u>		$3.9 \times 10^{-5}$	$128 \leq t \leq 170.$	$170 \leq t \leq 360.$	.04	$0 \leq t \leq 170.$
	128.					
<u>Limnocalanus &amp; Epischura</u>	128.	$1.2 \times 10^{-5}$	$128 \leq t \leq 170.$	$170 \leq t \leq 360.$	.015	$0 \leq t \leq 170.$

Table 7. Timing of hatching, maturation and natural death

and respiration are no longer present, but where predation and maturation govern the dynamics. Adult copepods die a natural death, governed by the first order rate coefficients of Table 2, at the beginning of the year, but never during a nauplii maturation period. This chain of events has been adopted for its tractability, with the premise that increased understanding of the mechanisms involved will lead to refinements.

## Results

### Model Calibration

Data collected from Grand Traverse Bay during 1971, 1972, and 1973 have been compared with model calculations. The station locations are shown in Figure 1. The water quality at these stations is similar to that in northern Lake Michigan and is superior to that in lower Lake Michigan and Green Bay. Biological data are available as species counts for both the phytoplankton and the zooplankton. These data have been converted to model units using the carbon content conversion factors listed in Table 8. With the exception of a few inconsistencies, these years indicate patterns of variation that are generally reproducible by the model. The results are presented in Figures 16 through 37.

The following procedure has been adhered to throughout this work. When prior investigations reported in the literature persistently restrict the value of a coefficient to a narrow range, this range has not been violated. However, when the reported range of a coefficient indicates substantial scientific uncertainty, the coefficient has been freely manipulated to achieve desired results. In a sense, then, the coefficient values listed in Table 2, especially those associated with zooplankton production rates, are a hypothesis requiring substantial experimental validation. Without this validation the model can be considered calibrated but cannot be considered completely verified.

Although most coefficients were adjusted by repeated simulation, a numerical routine has been developed to take advantage of parameter identification techniques. The routine seeks to minimize the sum of the squares of the deviations between model and data for any number of states by adjusting any number of coefficients within stipulated bounds. Optimization is accomplished using the Davidon-Fletcher-Powell variable-metric scheme described in Fletcher and Powell (1963), with gradients calculated by finite difference. The routine has proven valuable in tuning less complex models encountered in the study of bacterial growth, estuaries, and predator-prey interactions. Due to the complex nature of the dynamics in the Lake Michigan food web model, the routine was not successfully employed. Repeated simulation, requiring 15 seconds of computer time and an average of \$2.00 for a 360 day integration, proves more economical and efficient. Furthermore, considerable insight into complex mechanisms can be obtained when repeated simulations are made. This insight is lost when coefficients are adjusted by an optimization routine.

Taxon	Conversion Factor
<u>Leptodora</u> & <u>Polyphemus</u>	24.8 $\mu\text{g}$ c/individual
<u>Cyclops</u>	1.3
<u>Diaptomus</u>	1.4
<u>Limnocalanus</u> & <u>Epischura</u>	22.1
<u>Daphnia</u>	4.9
<u>Bosmina</u> & <u>Holopedium</u>	1.9
<hr/>	
Nauplii	
<u>Cyclops</u>	.2 $\mu\text{g}$ c/individual
<u>Diaptomus</u>	.2
<u>Limnocalanus</u>	.6
<hr/>	
Small Diatoms	.00006 $\mu\text{g}$ c/cell
Large Diatoms	.00025
Greens	.00011
Flagellates	.00008
Blue-Greens	.00003

Table 8. Carbon Content of Individual Model Taxon

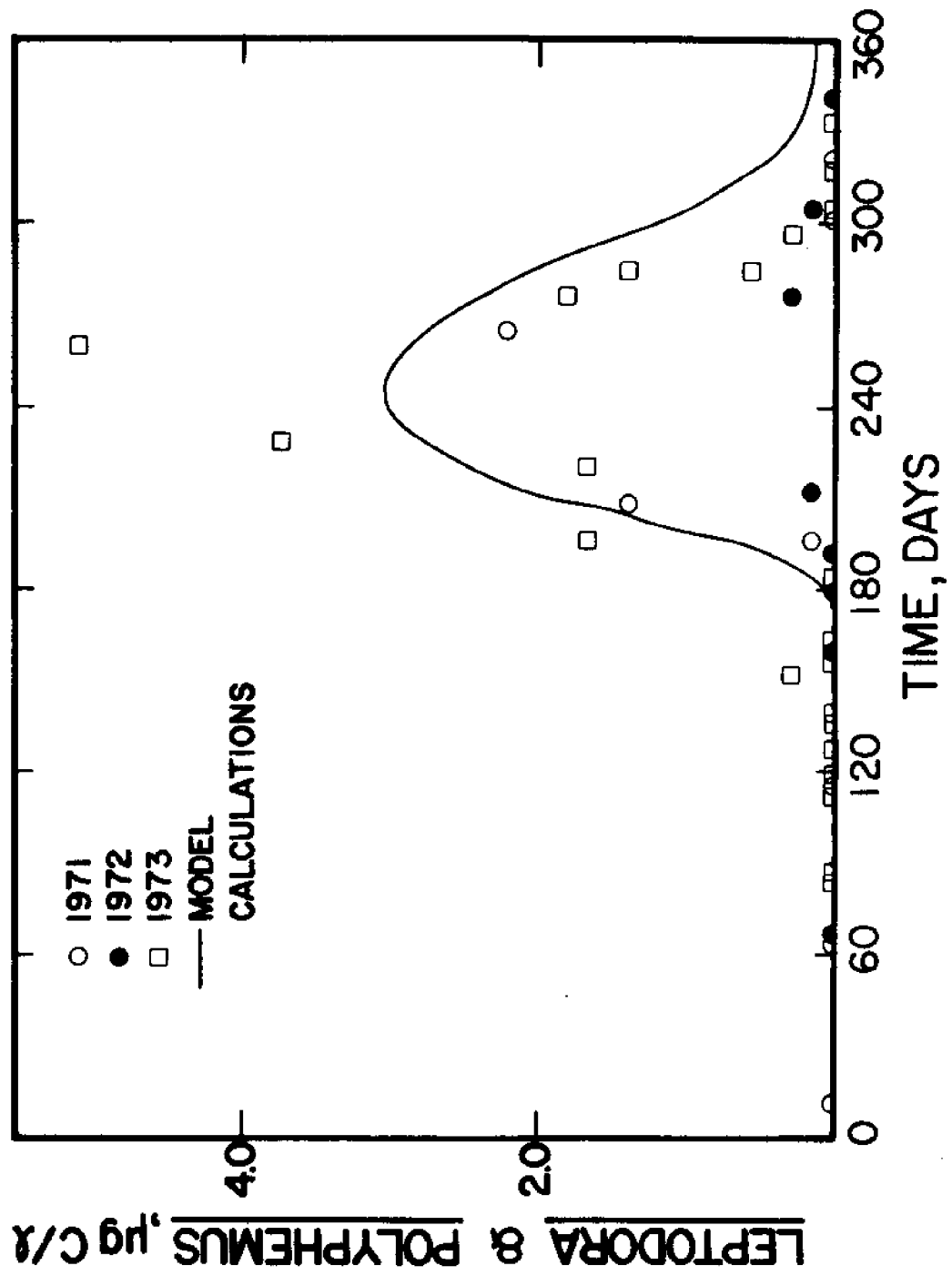


Figure 16. Model calibration

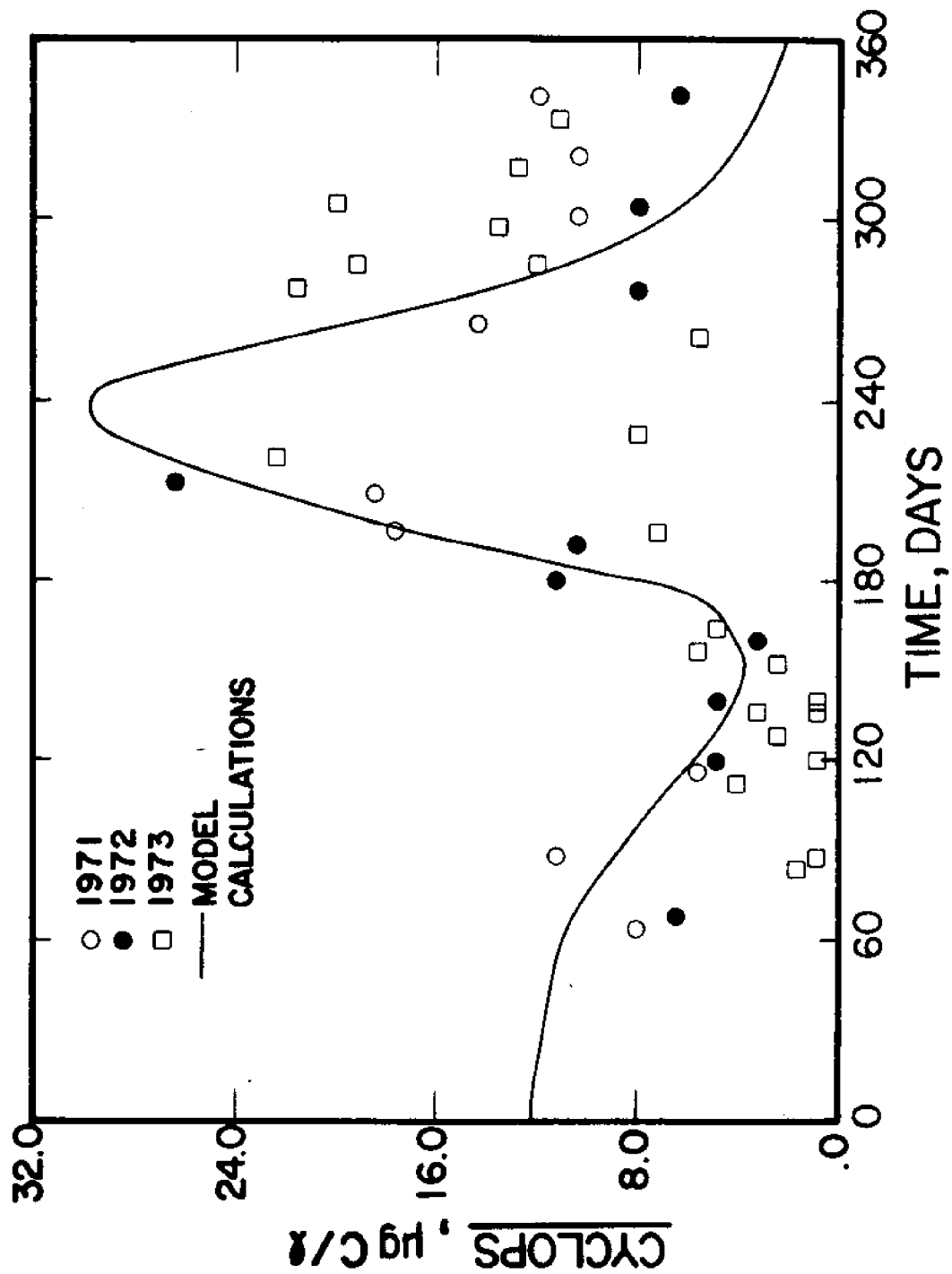


Figure 17. Model Calibration

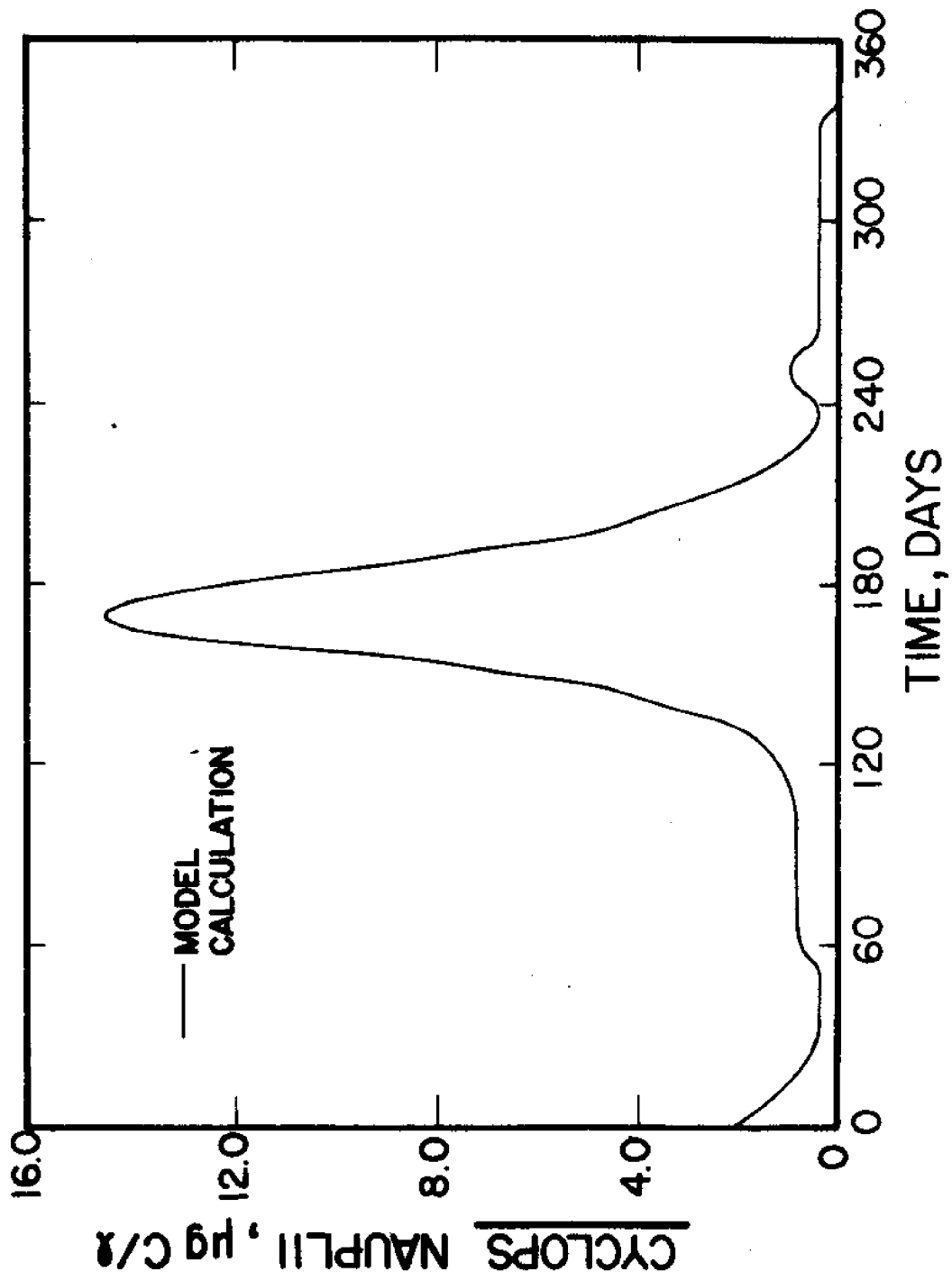


Figure 18. Model Calibration

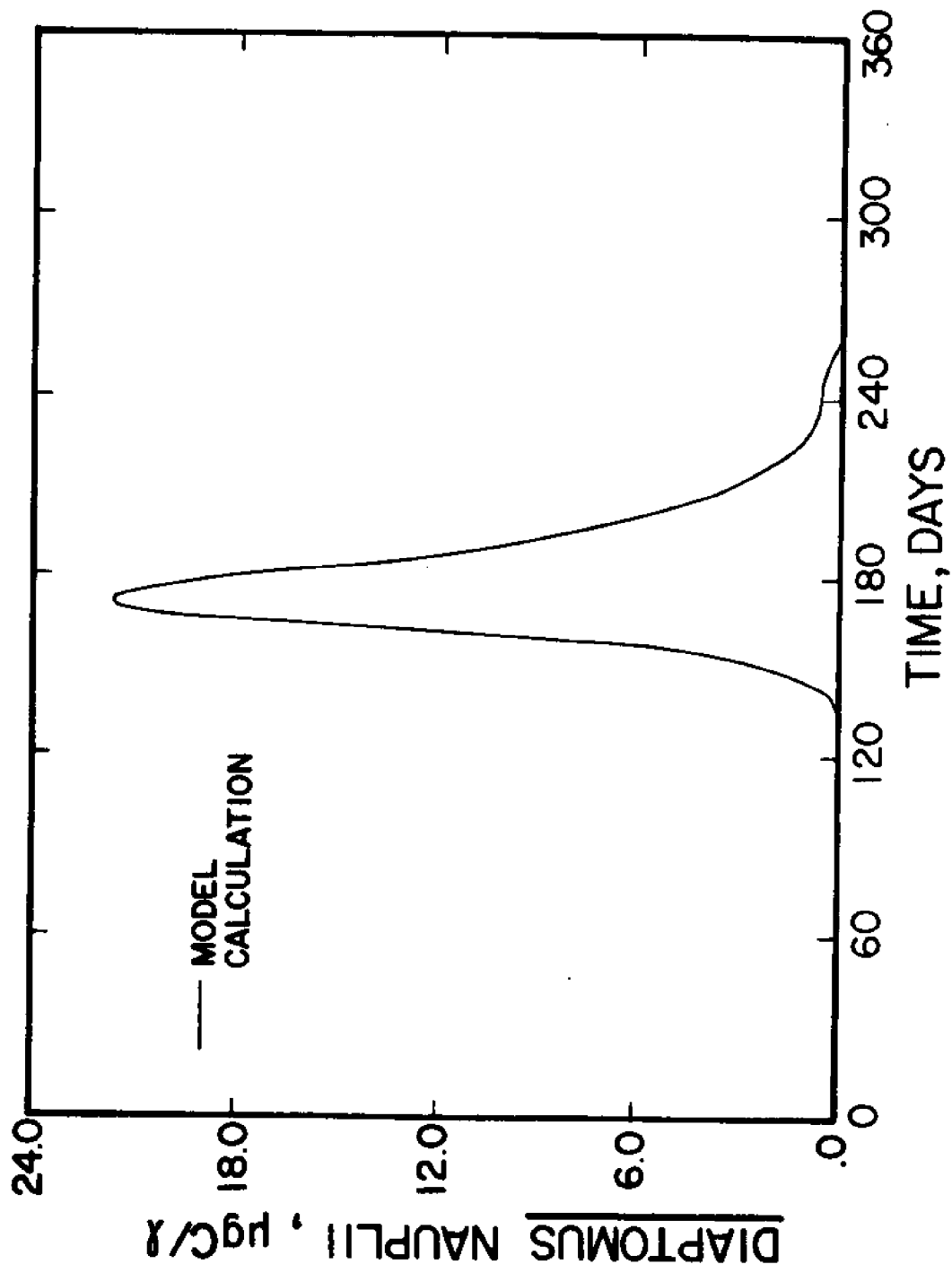


Figure 19. Model Calibration

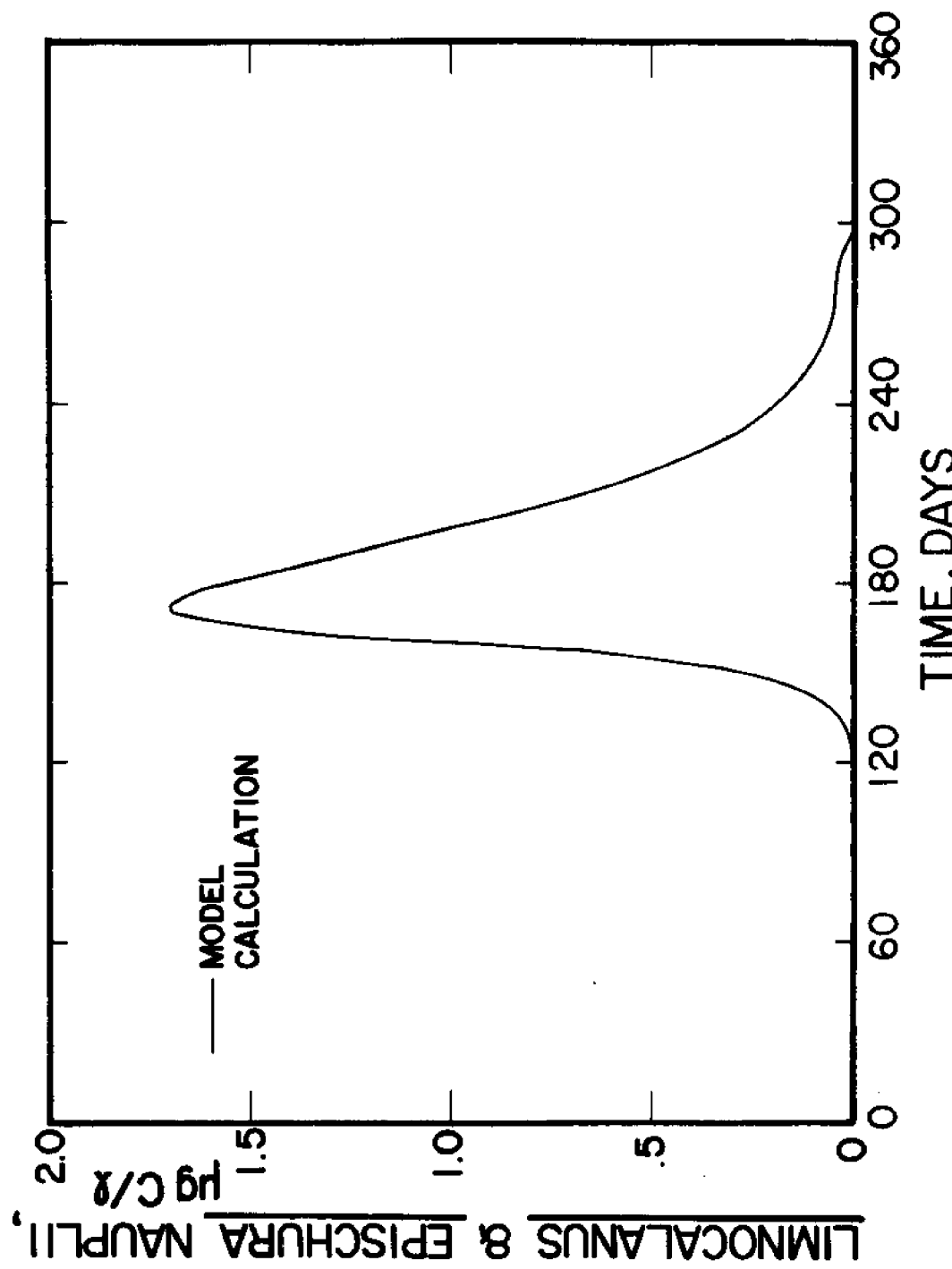


Figure 20. Model Calibration

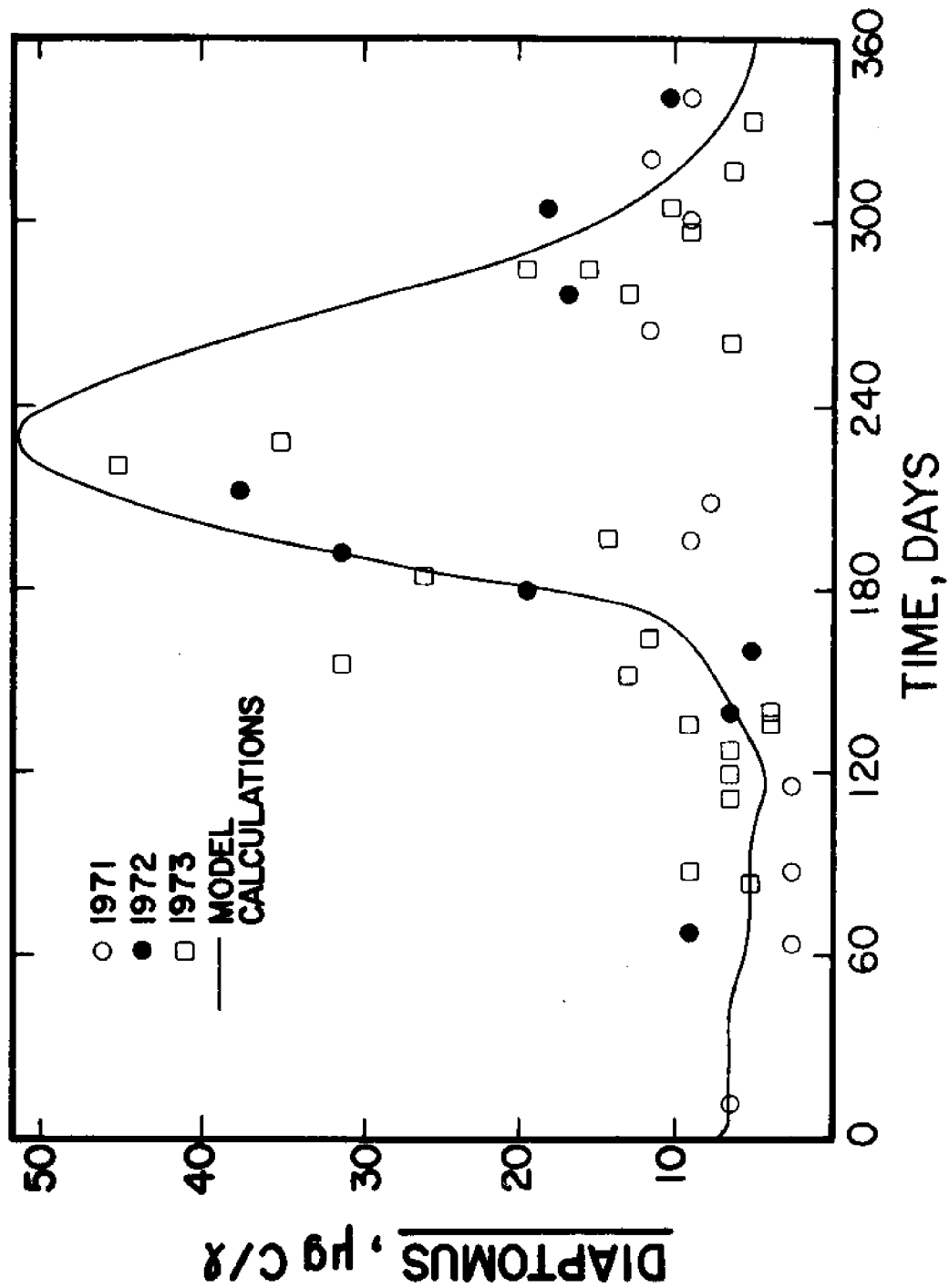


Figure 21. Model Calibration

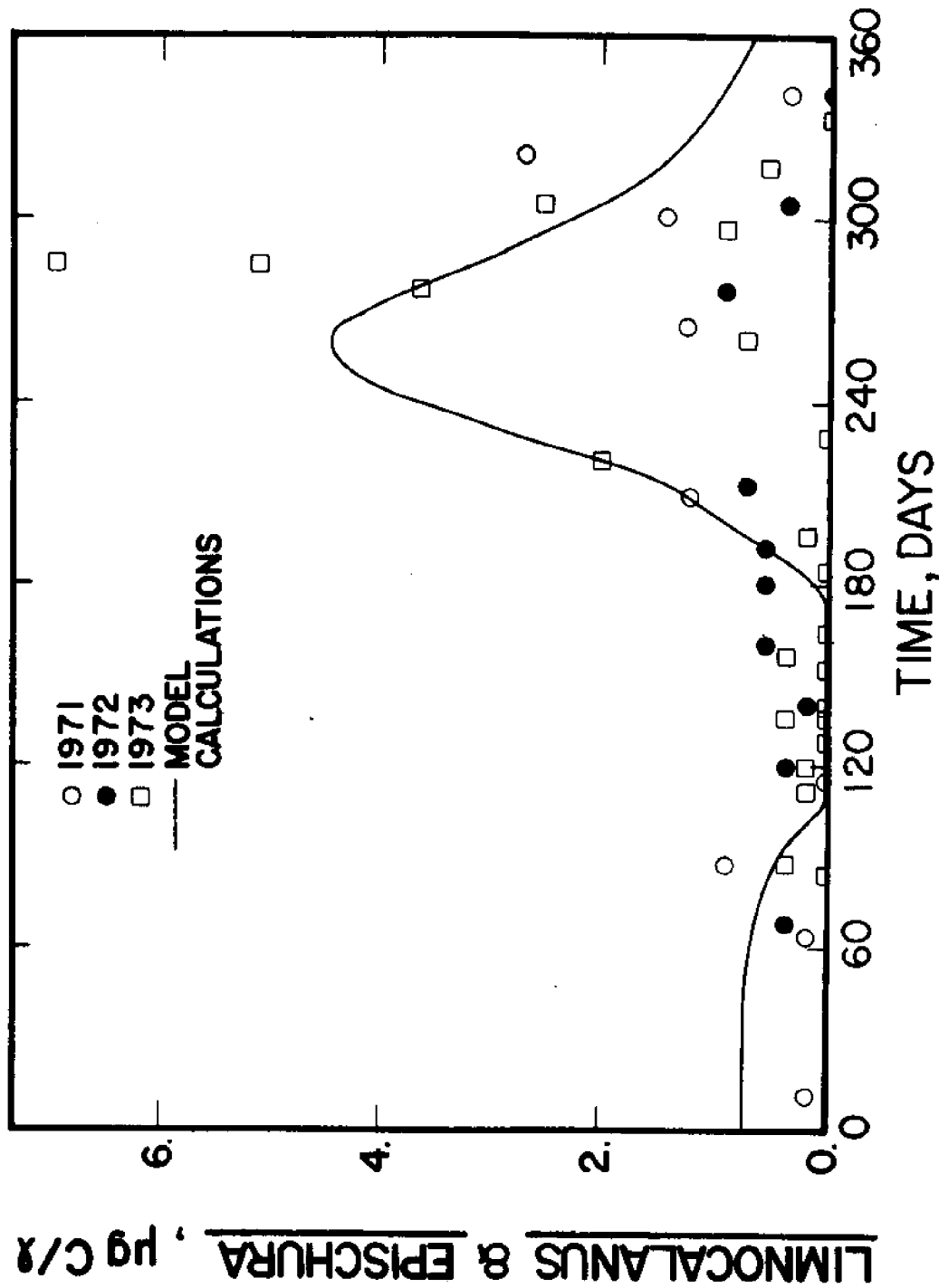


Figure 22. Model Calibration

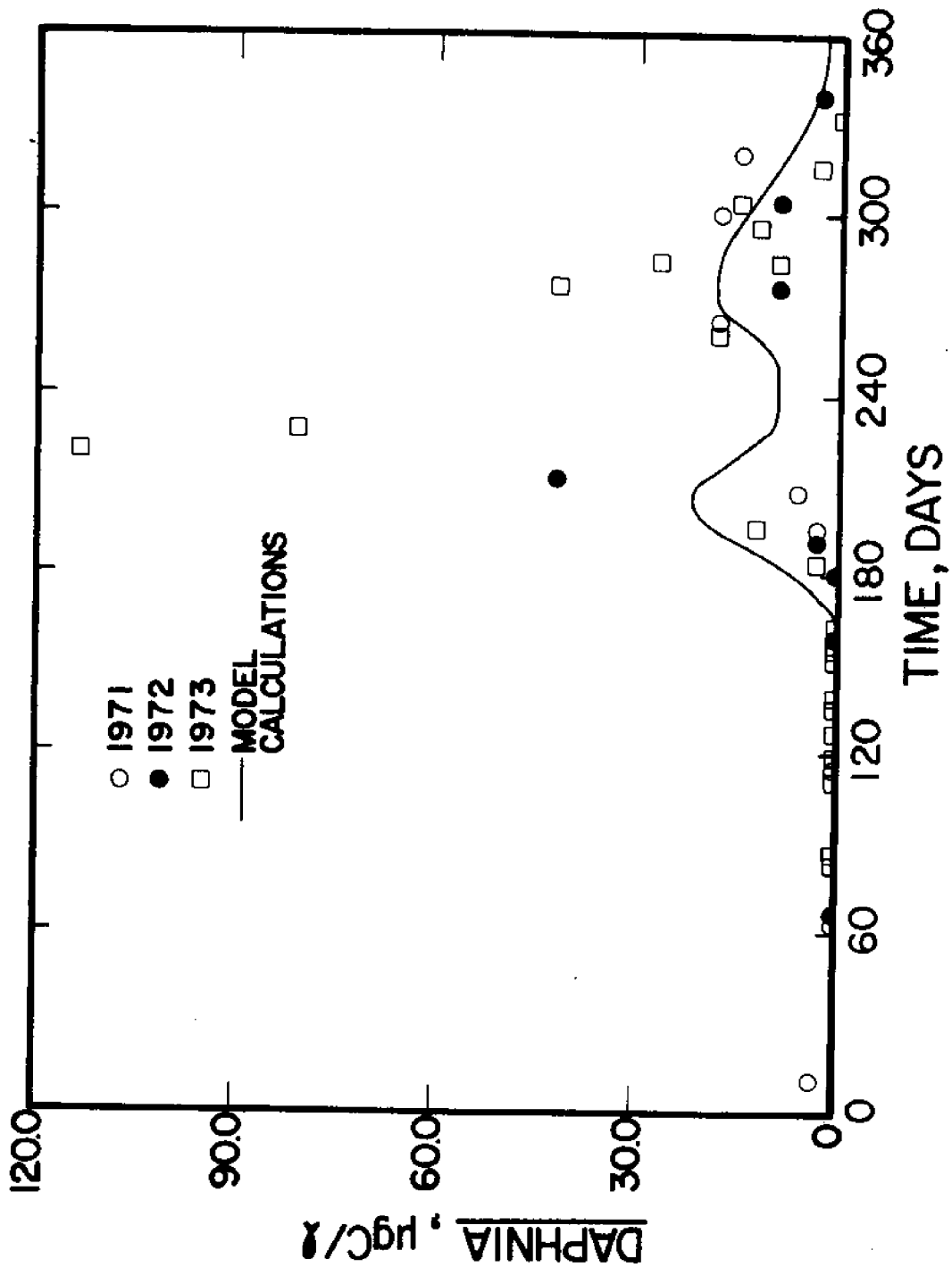


Figure 23. Model Calibration

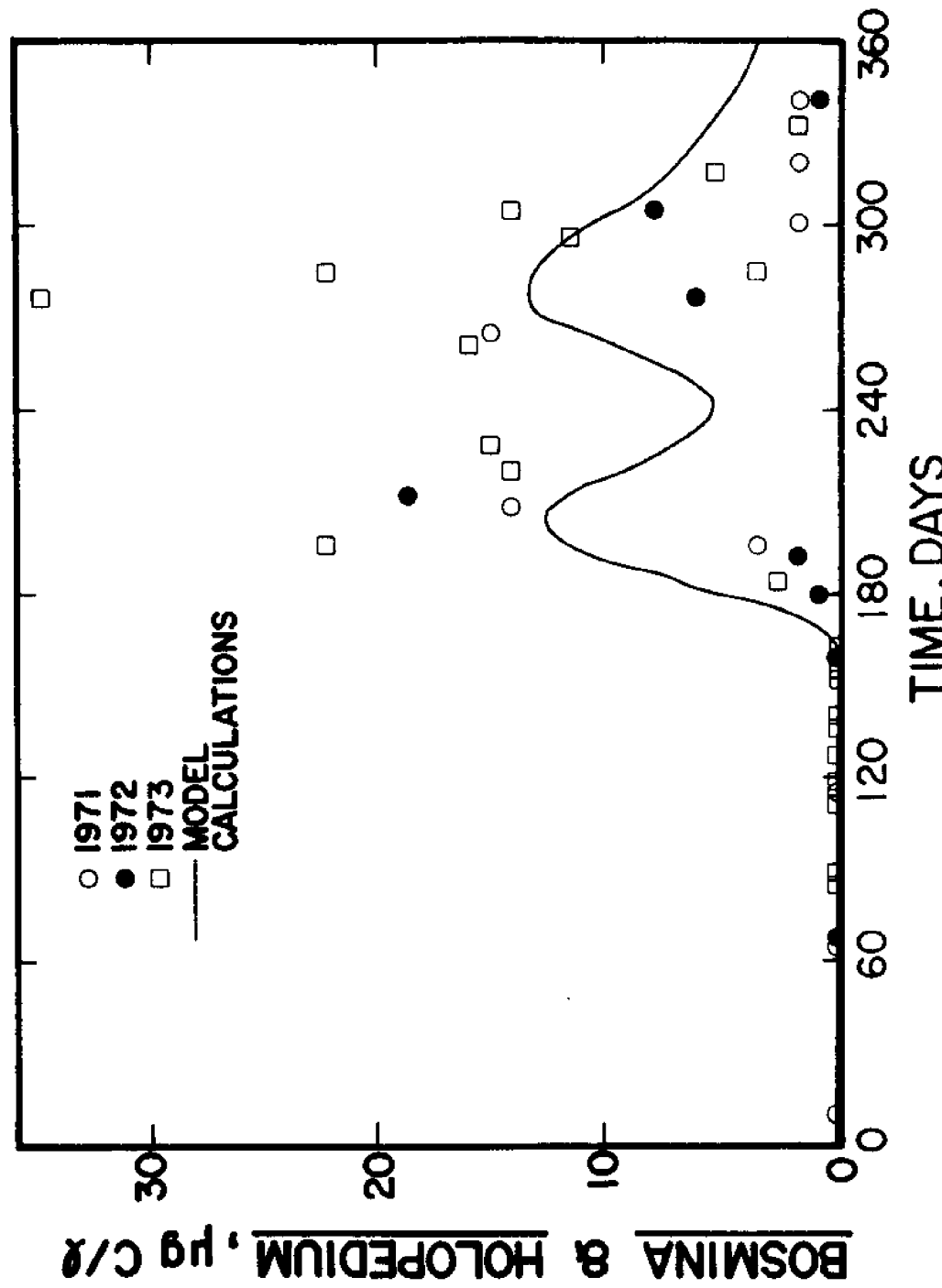


Figure 24. Model Calibration

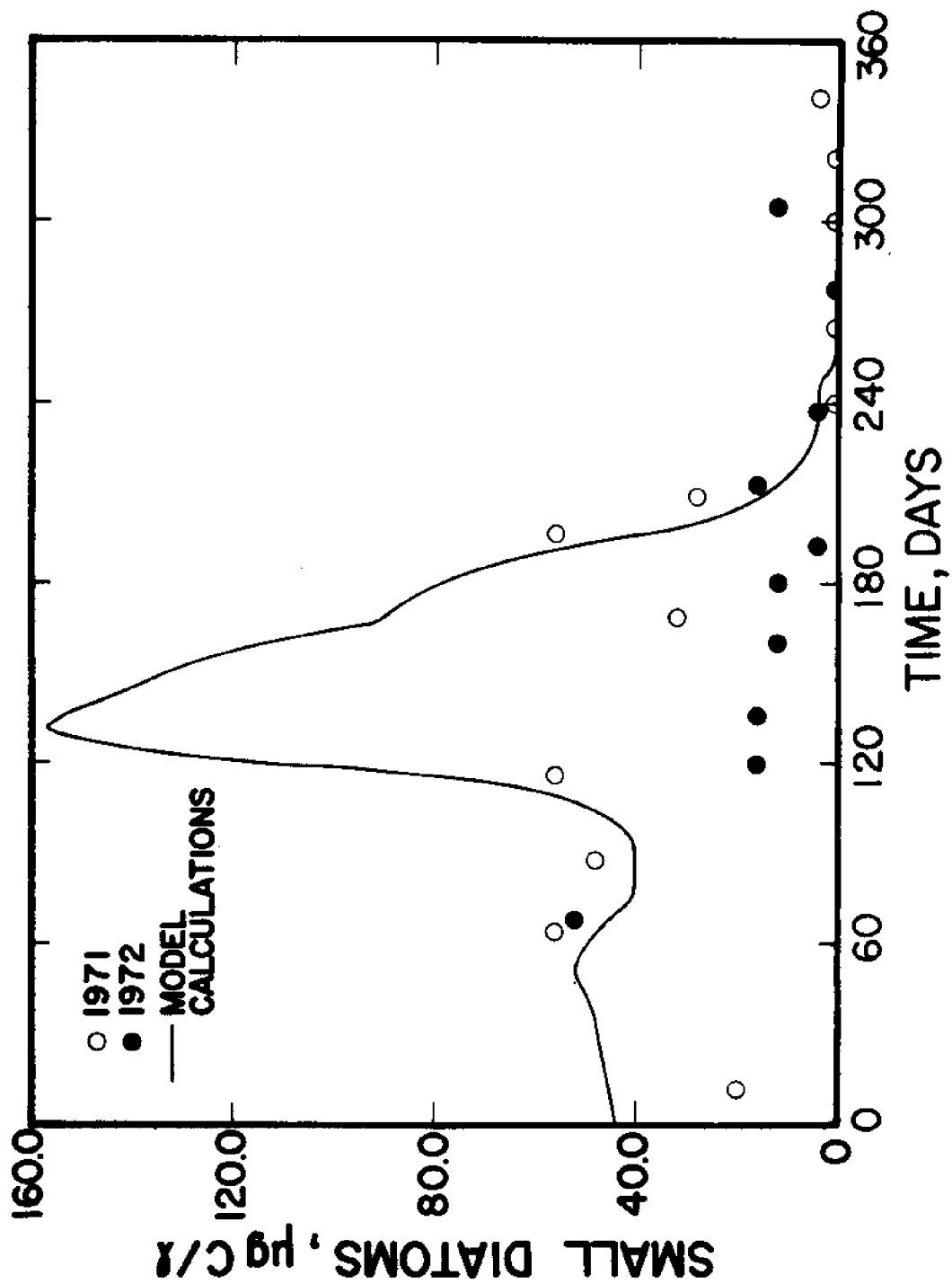


Figure 25. Model Calibration

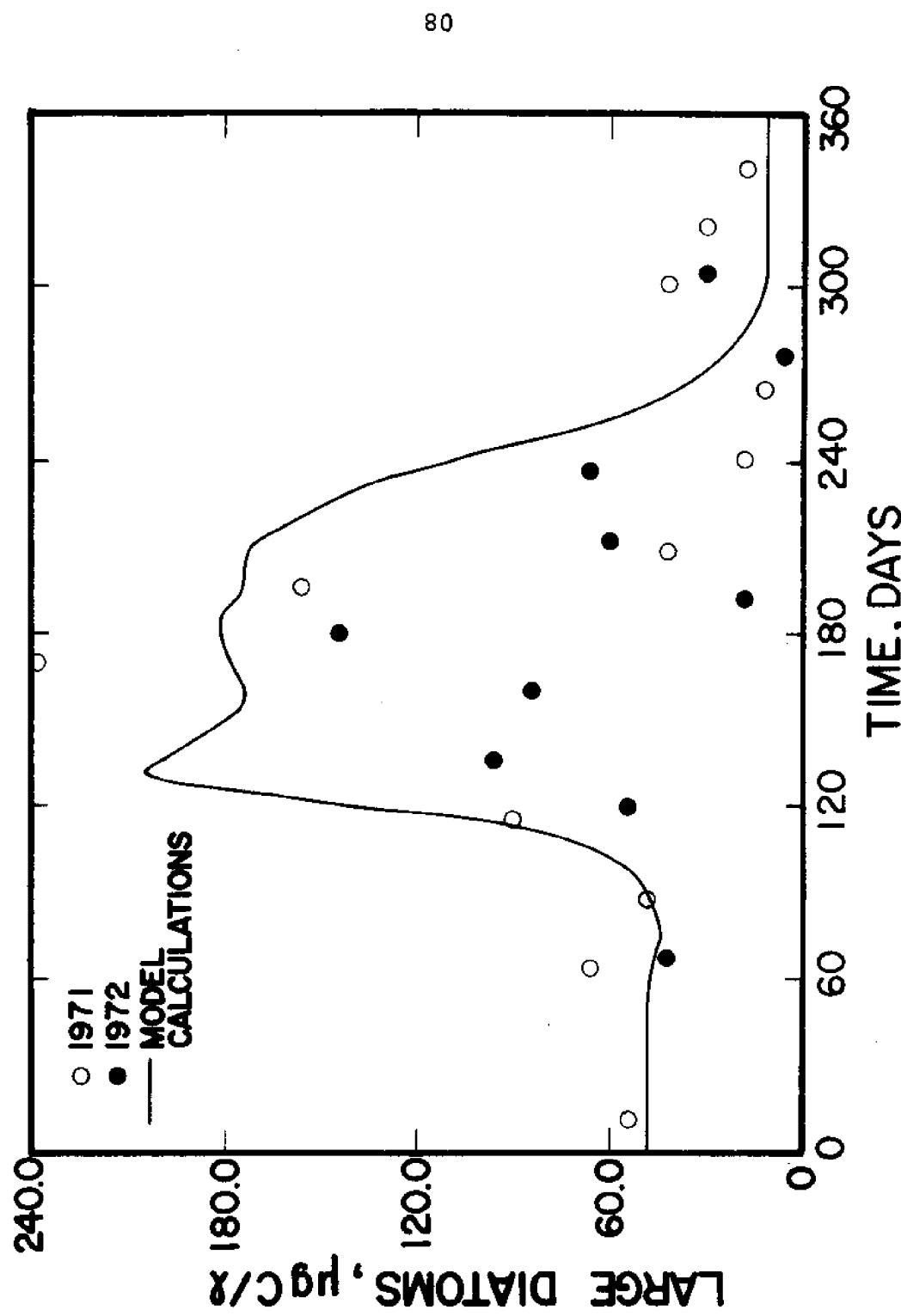


Figure 26. Model Calibration

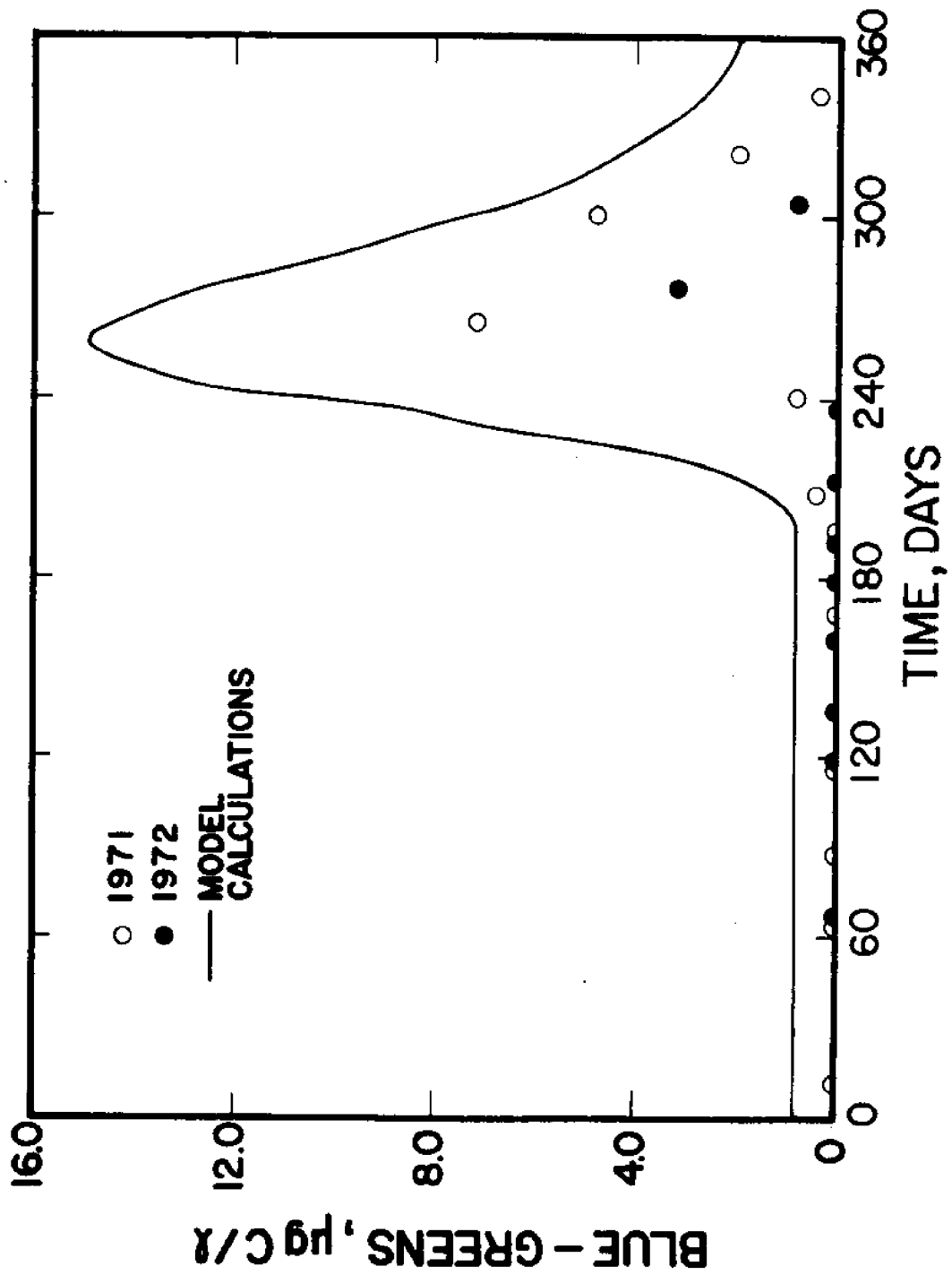


Figure 27. Model Calibration

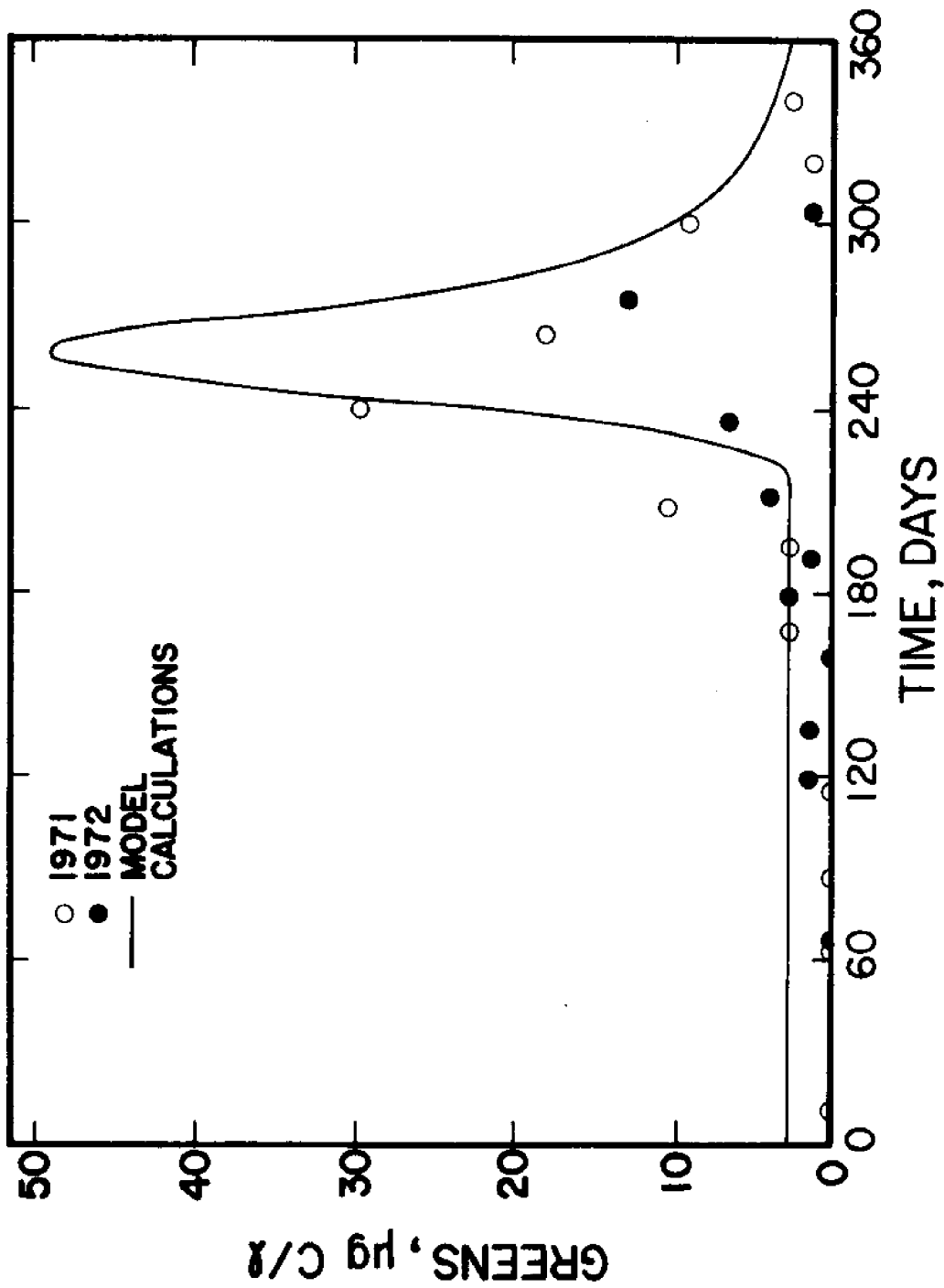


Figure 28. Model Calibration

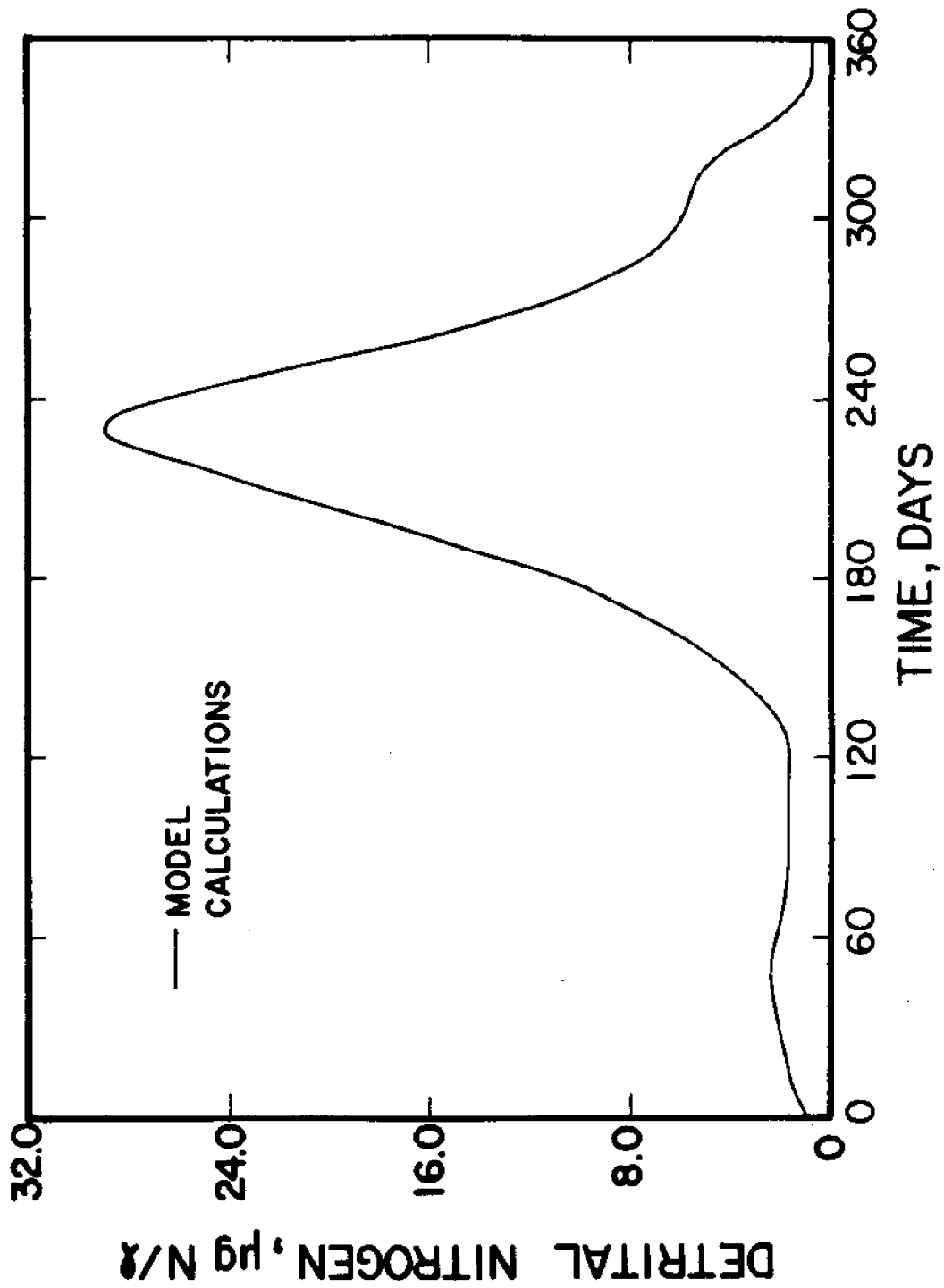


Figure 29. Model Calibration

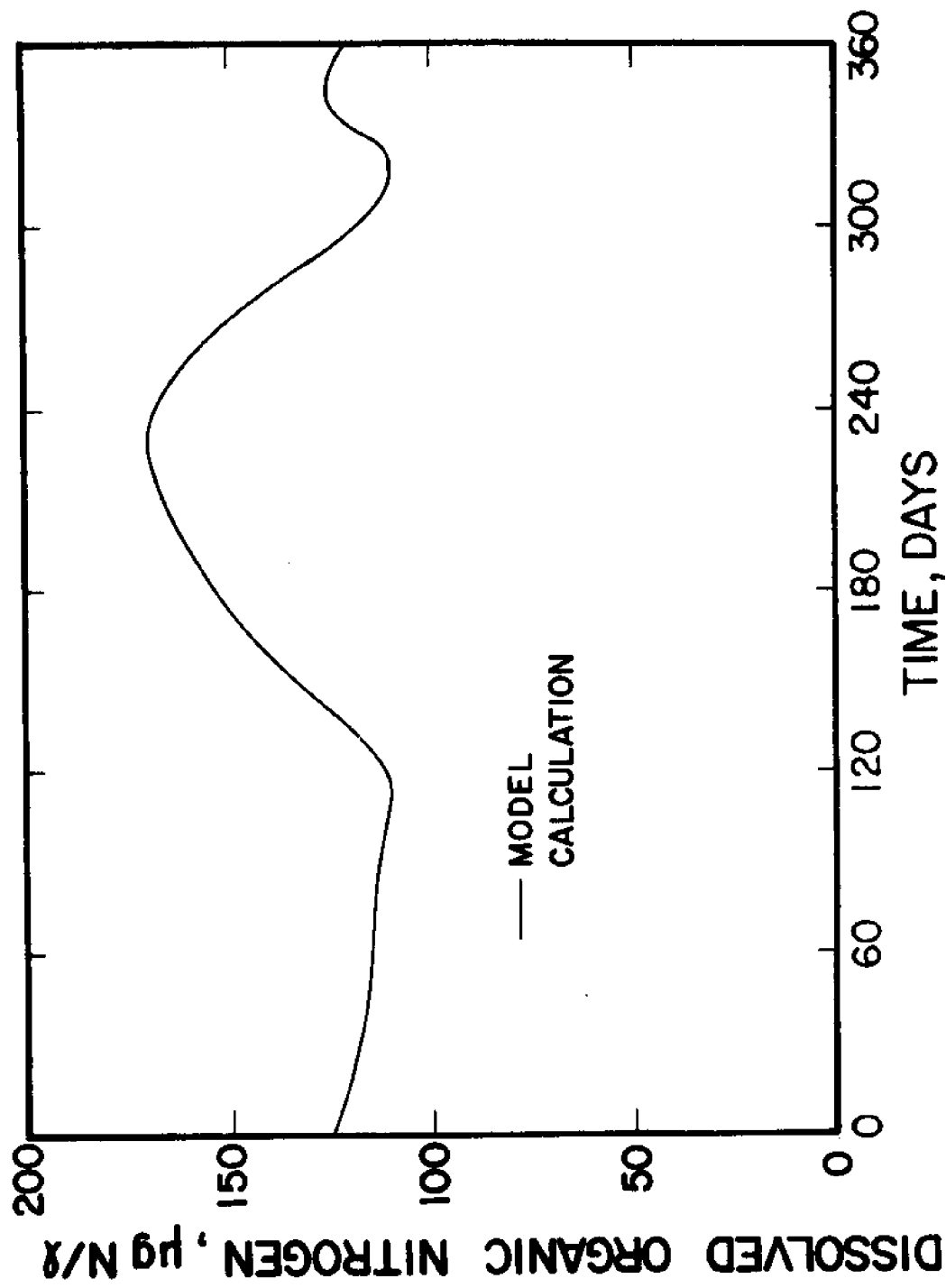


Figure 30. Model Calibration

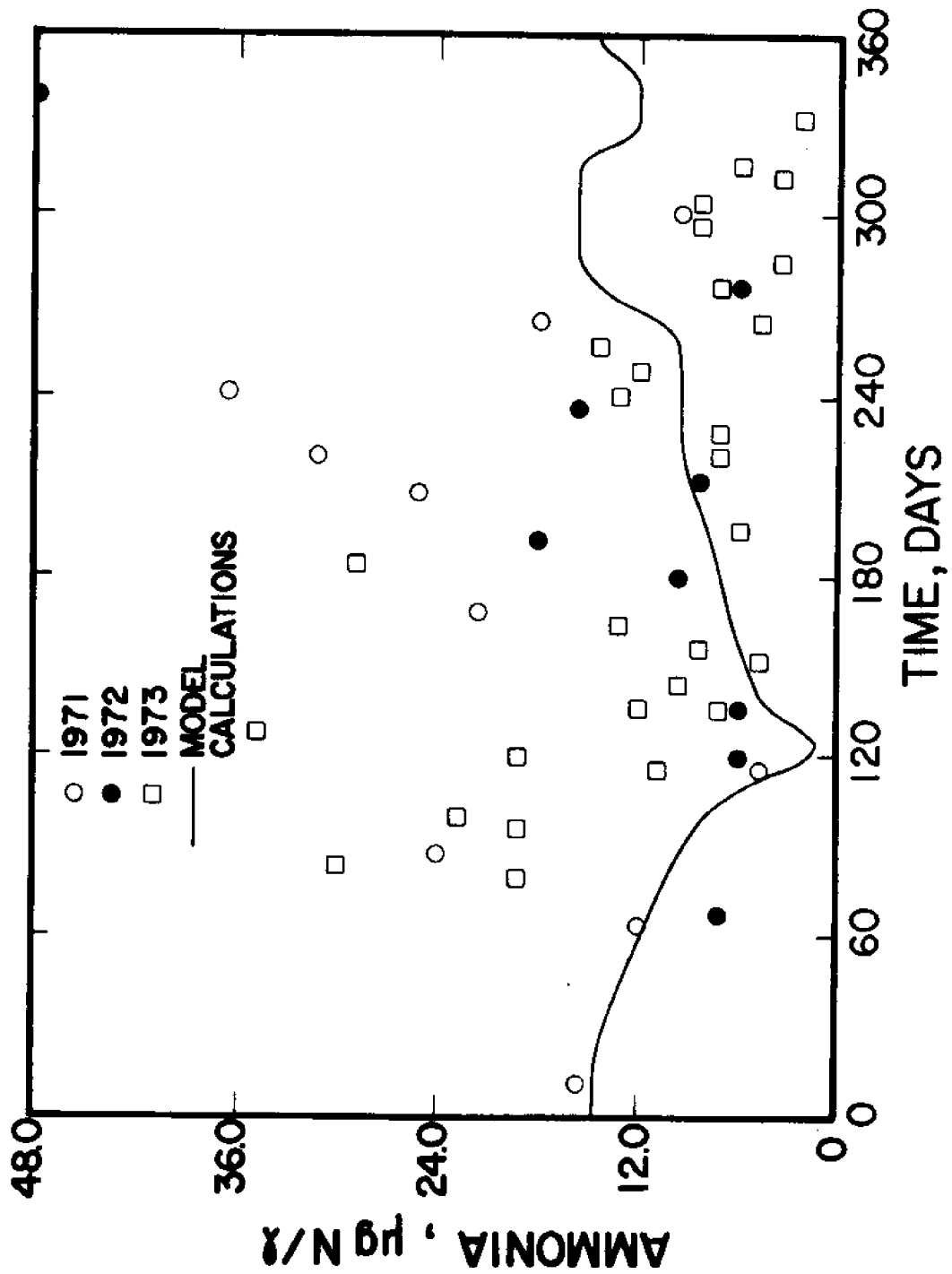


Figure 31. Model Calibration

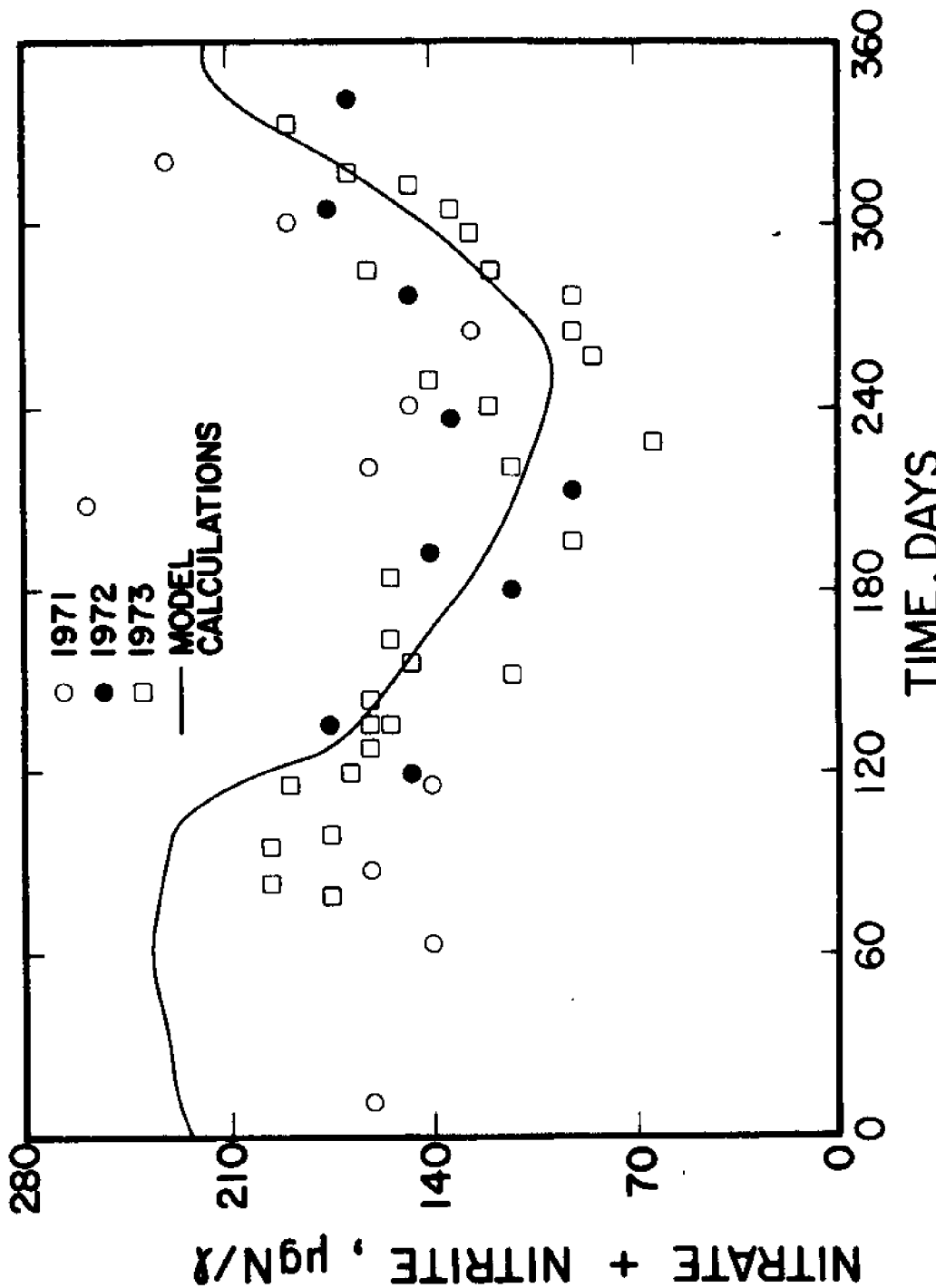


Figure 32. Model Calibration

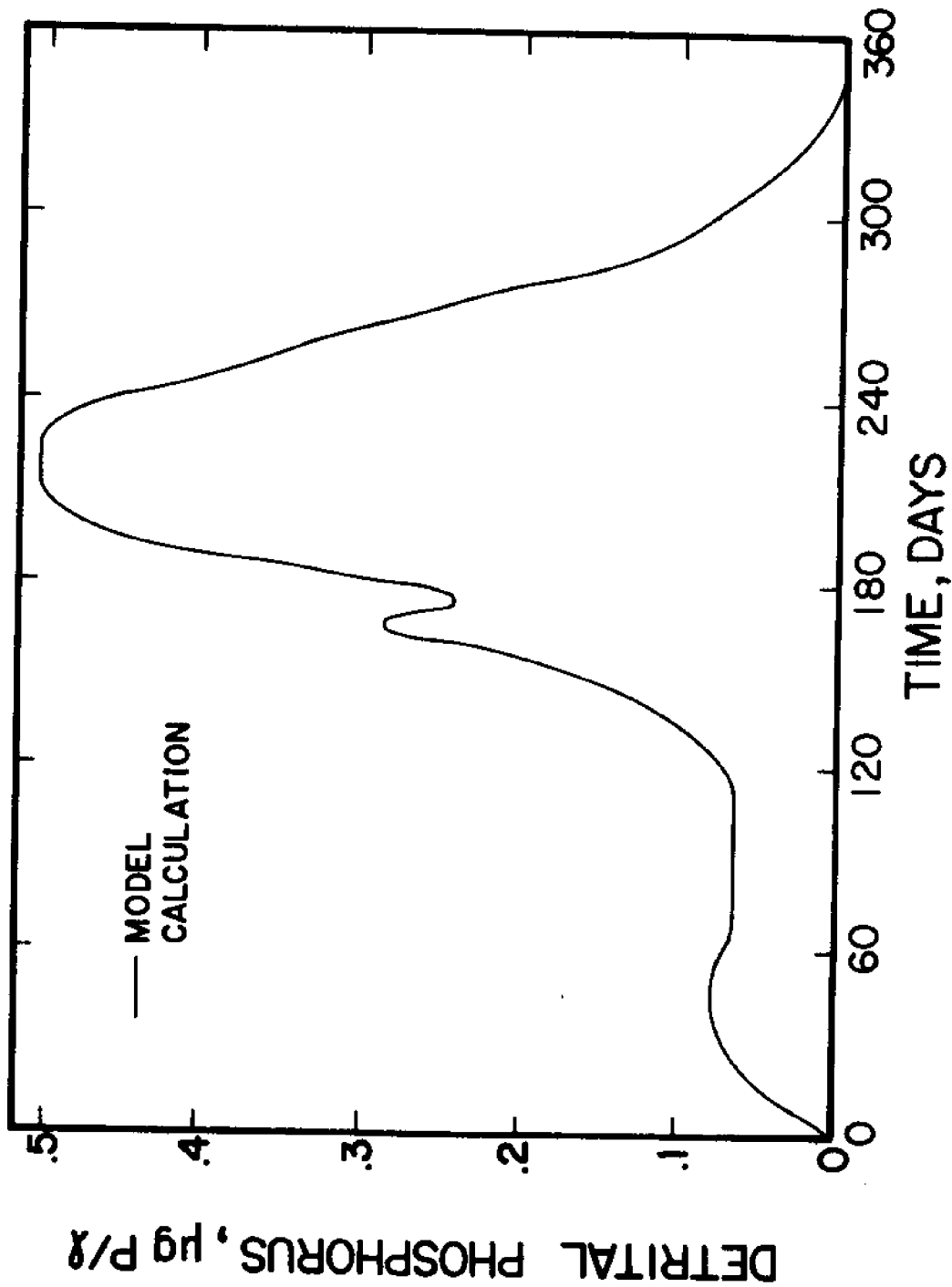


Figure 33. Model Calibration

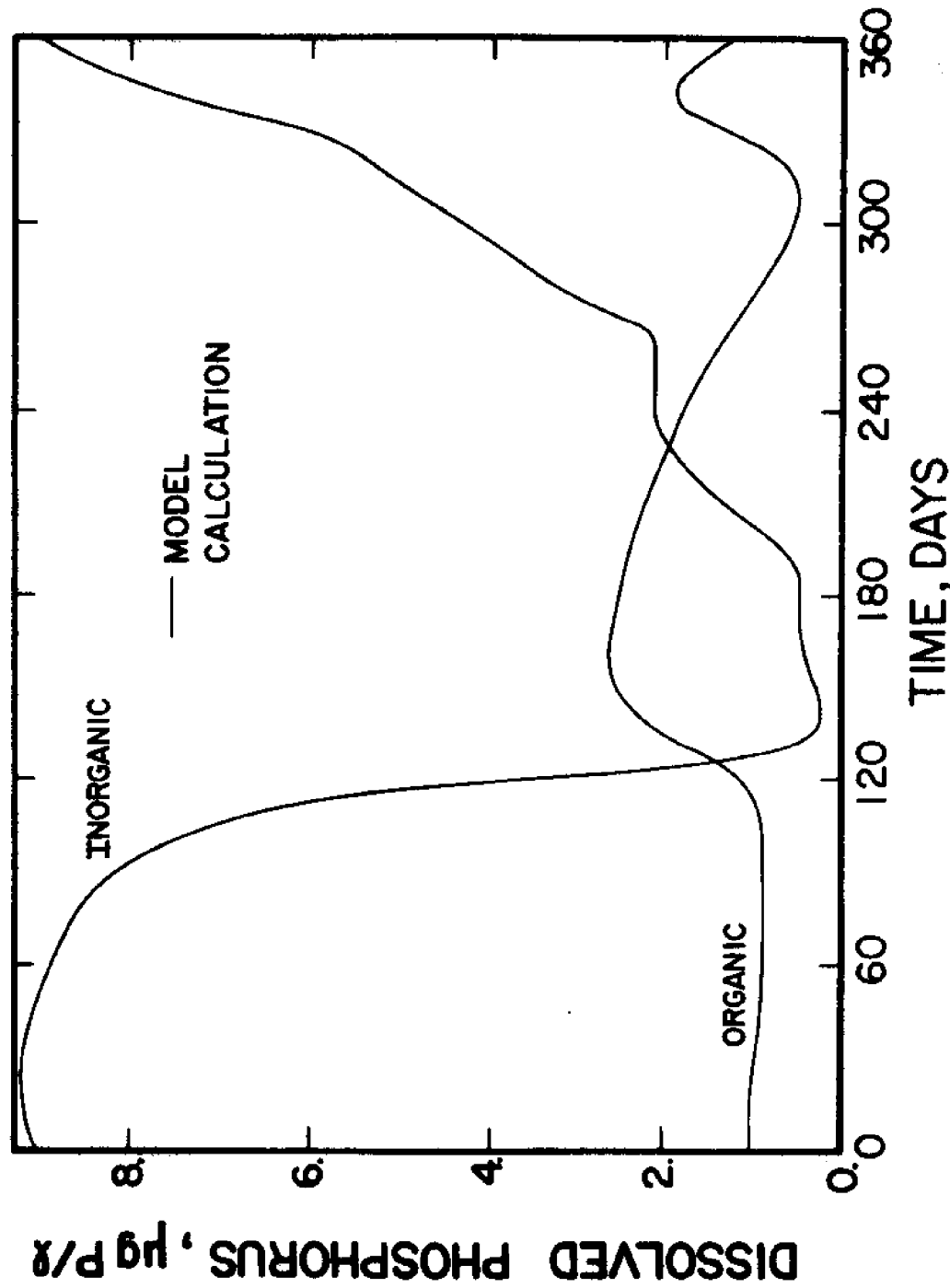


Figure 34. Model Calibration

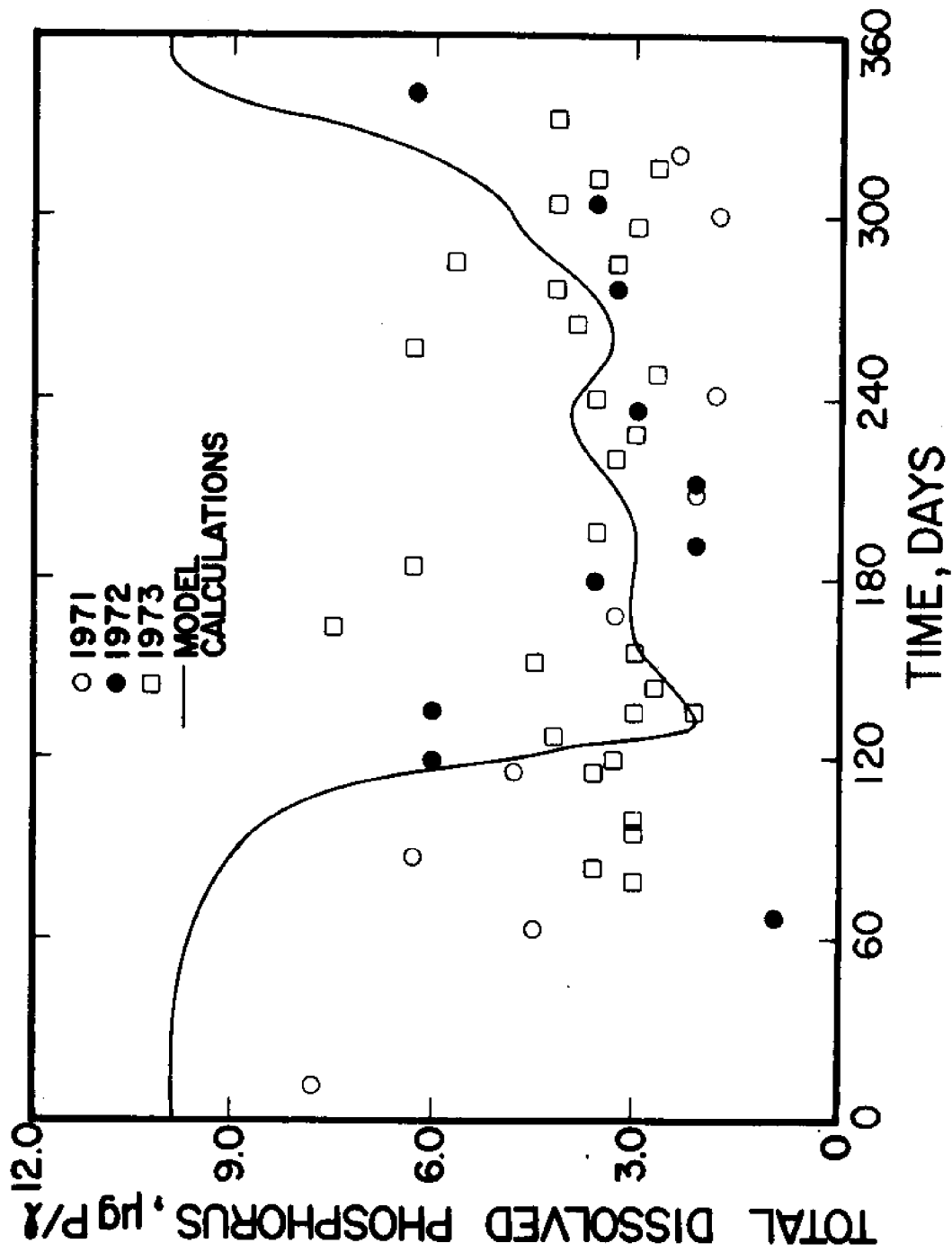


Figure 35. Model Calibration

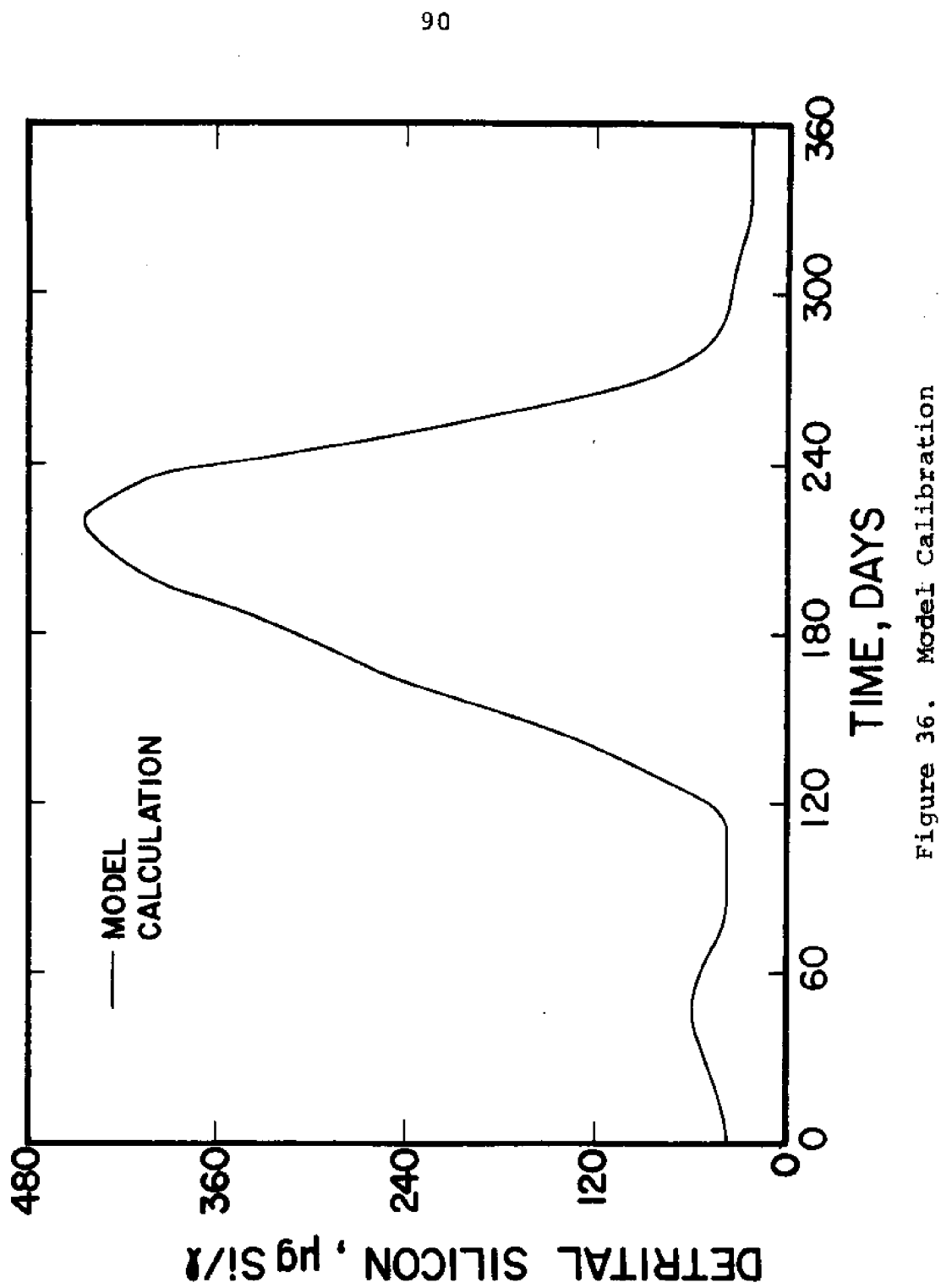


Figure 36. Model Calibration

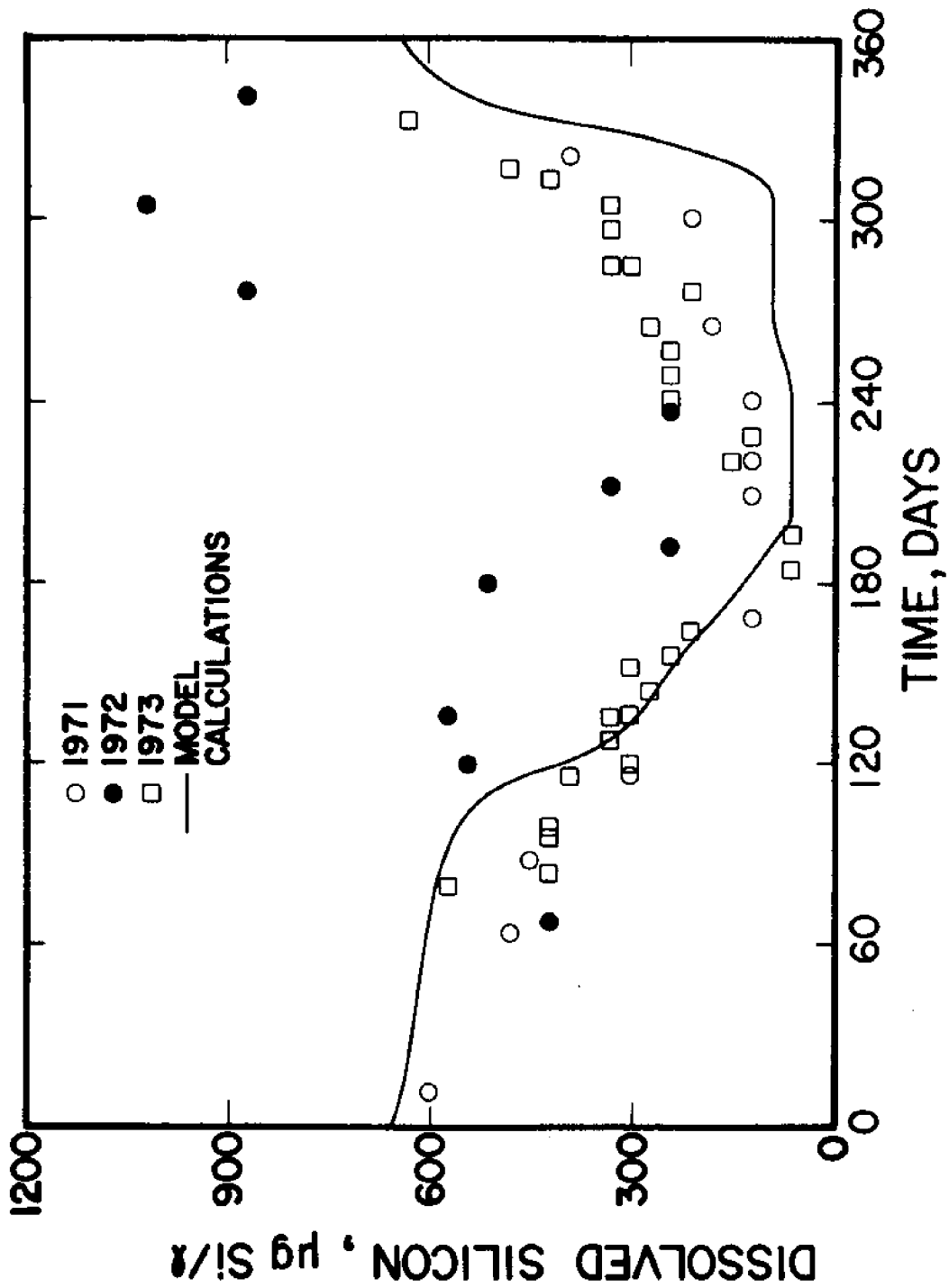


Figure 37. Model Calibration

### Model Calculated Energetics

In order to track the flow of mass through such a complex system model as the Lake Michigan food web model, information beyond the integrated state responses is essential. The dynamic behavior of the states only suggests some of the pathways critical to the behavior of the model, such as the relationship between the sharp rise in phytoplankton and the decline of phosphorus. Other interactions can be disguised. Phytoplankton loss due to a zooplankter might be disguised by excessive zooplankton respiration or predation on the zooplankter from the higher levels of the food chain. One way to study the interactions is to plot the various contributions to the derivative of each state as a function of time. However, it is difficult to extract useful quantitative information from such plots. One would find it very laborious to compare the consumption of various food sources for a zooplankter.

What is needed is the integral of these derivative contributions. It is known that  $X_i(t) - X_i(0) = \int_0^t \dot{X}_i d\tau = \sum_j \int_0^t f_{ij}(\bar{X}, \tau) d\tau$ , where the summation is over the various mechanisms in the  $i$ th differential equation. Since the equations are coupled ( $f_{ij}$  may depend on  $X$ , not just  $\bar{X}$ ), the system must first be integrated using a numerical integrator as discussed in the section, "Computation Topics". However, the integrals of the individual components of the derivative,  $\int_0^t f_{ij}(\bar{X}, \tau) d\tau$ , can be evaluated using any simple quadrature technique. Since there are no problems with instability in evaluating such integrals, the trapezoidal rule has been chosen, where discrete values of the state vector  $\bar{X}$  have been stored every 4 days during the DVDQ integration.

Plots have been generated for the breakdown of the phytoplankton and adult zooplankton states and for the alewife (see Figures 38 to 48). For ease of comparison, the cumulative contributions  $\int_0^t f_{ij}(\bar{X}, \tau) d\tau$  are stacked one upon another. Therefore, the uppermost curve is generated by integrating the positive (growth) term of the equation from the initial condition. The curve just below this is attained by subtracting off the first negative contribution, and so on, until the lowermost curve represents the total of all contributions and coincides with the state trajectory. It is observed that the width of a band is nondecreasing from day 0 to day 360 since by construction  $f_{ij} < 0$  or  $f_{ij} \geq 0$  holds for all time. It should be noted that the procedure used to generate these plots is not equivalent to that of integrating the system without a mechanism to determine the con-

tribution of all other mechanisms. Thus, for example, the contribution of respiration to phytoplankton biomass loss is not that which occurs without other phytoplankton effects in the system.

Other plots have been generated to help in the interpretation of phytoplankton behavior. Figures 49 to 53 exhibit the factors governing the seasonal variation of growth rate for each of the four taxa. The plots respectively display temperature reduction, light reduction, nitrogen limitation, phosphorus limitation and silicon limitation. The cumulative effect of these factors is illustrated in the total growth rate plots of Figure 54.

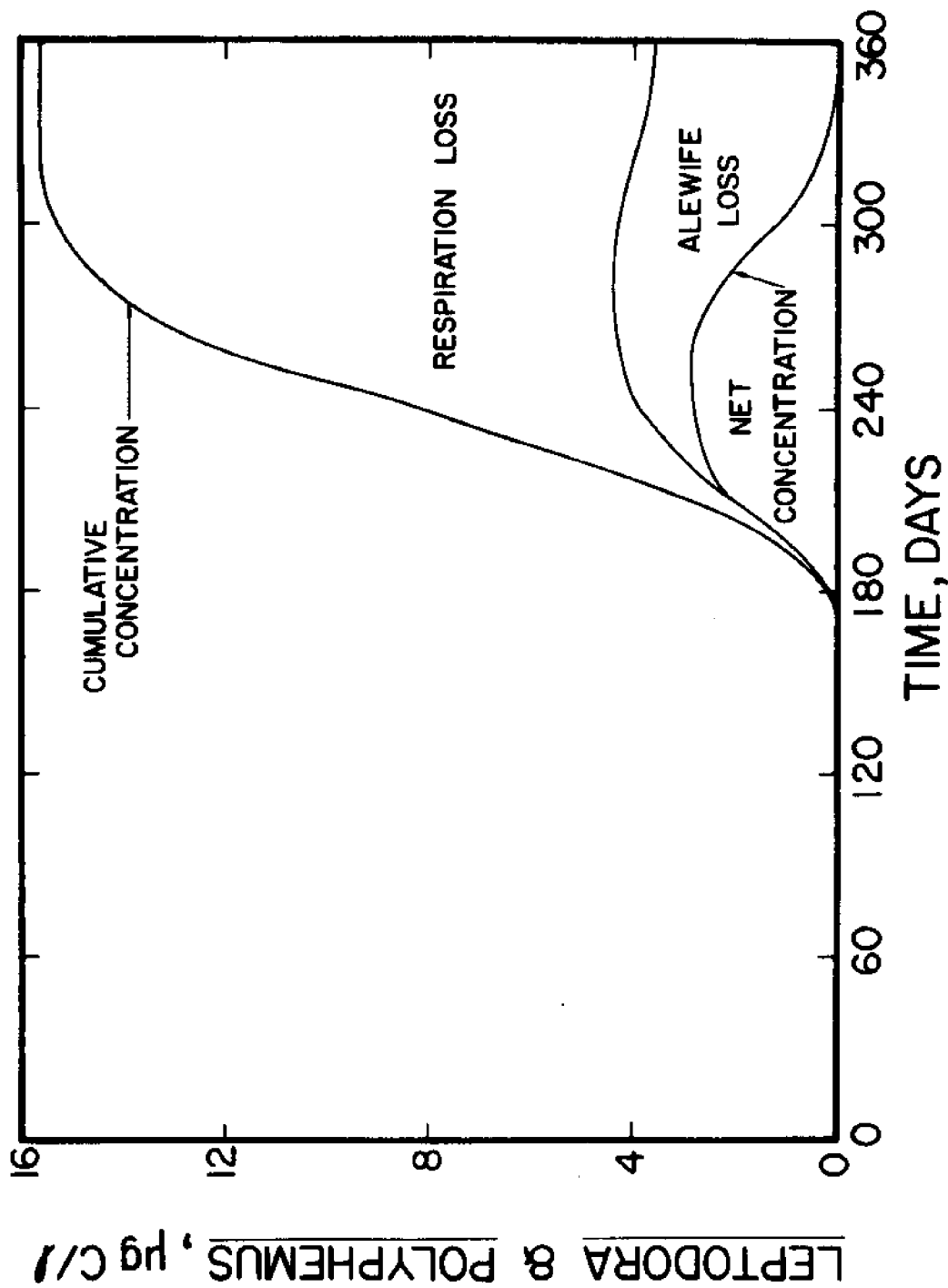


Figure 38. Calculated Energetics for Calibration Run

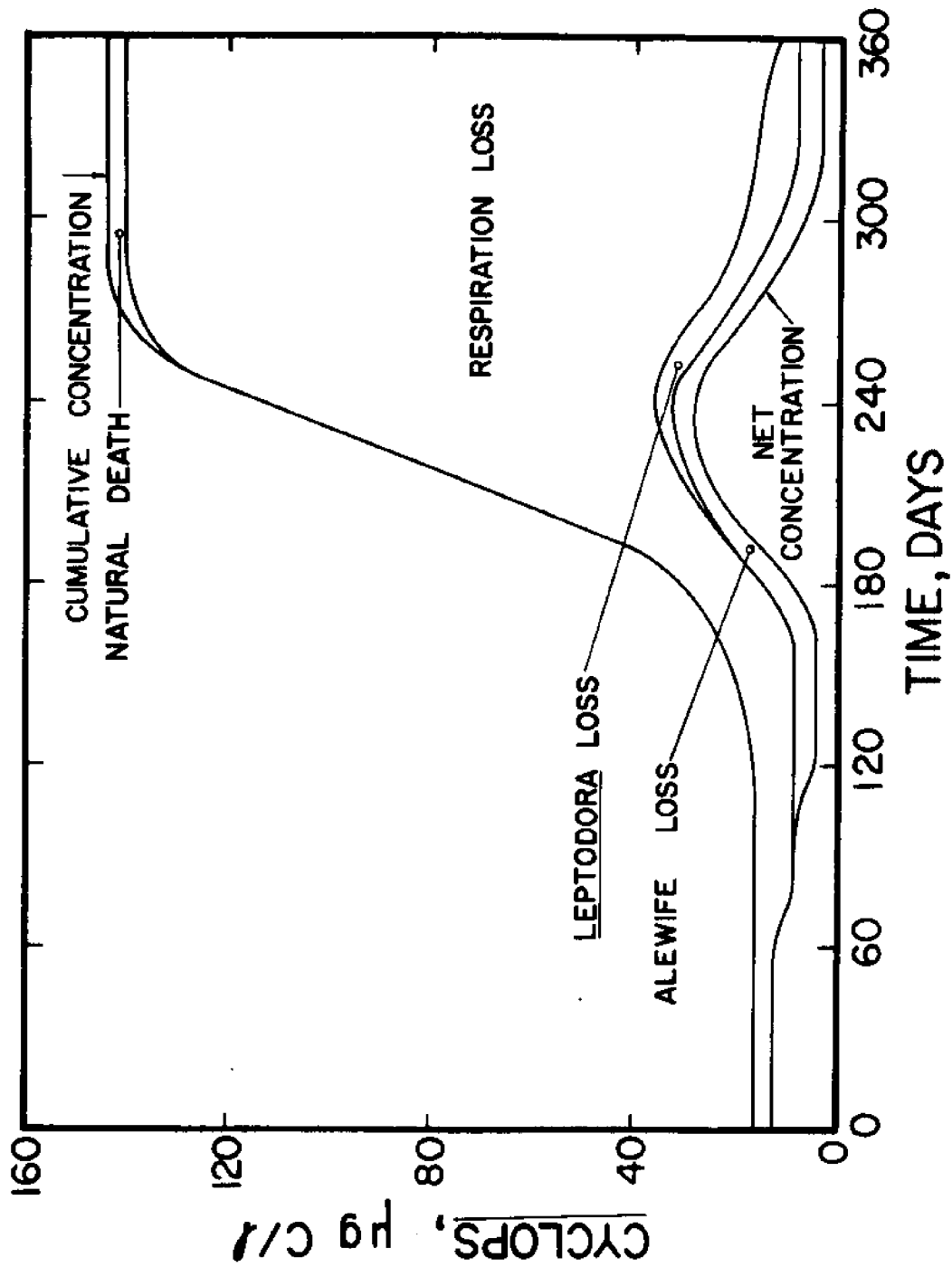


Figure 39. Calculated Energetics for Calibration Run

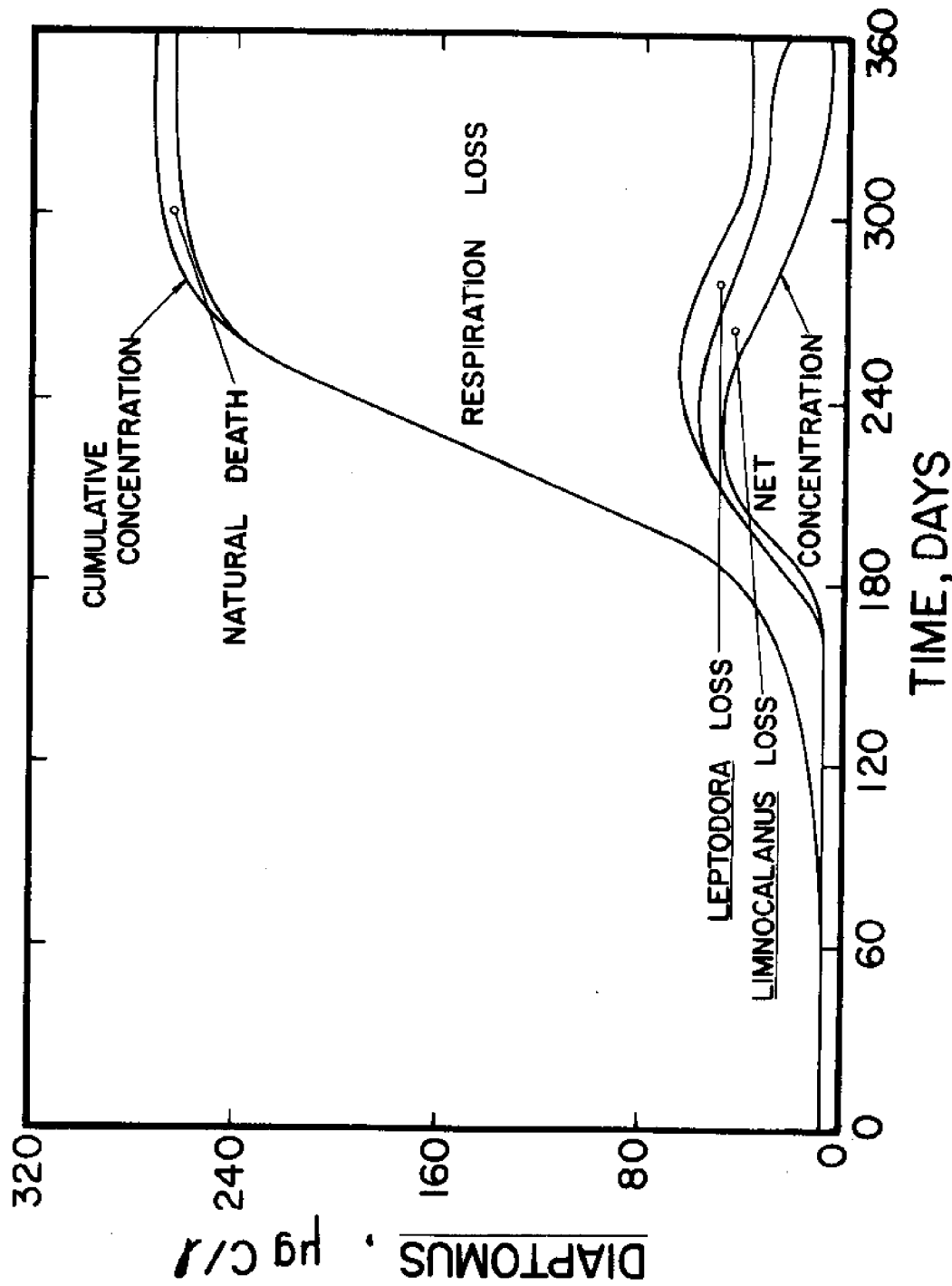


Figure 40. Calculated Energetics for Calibration Run

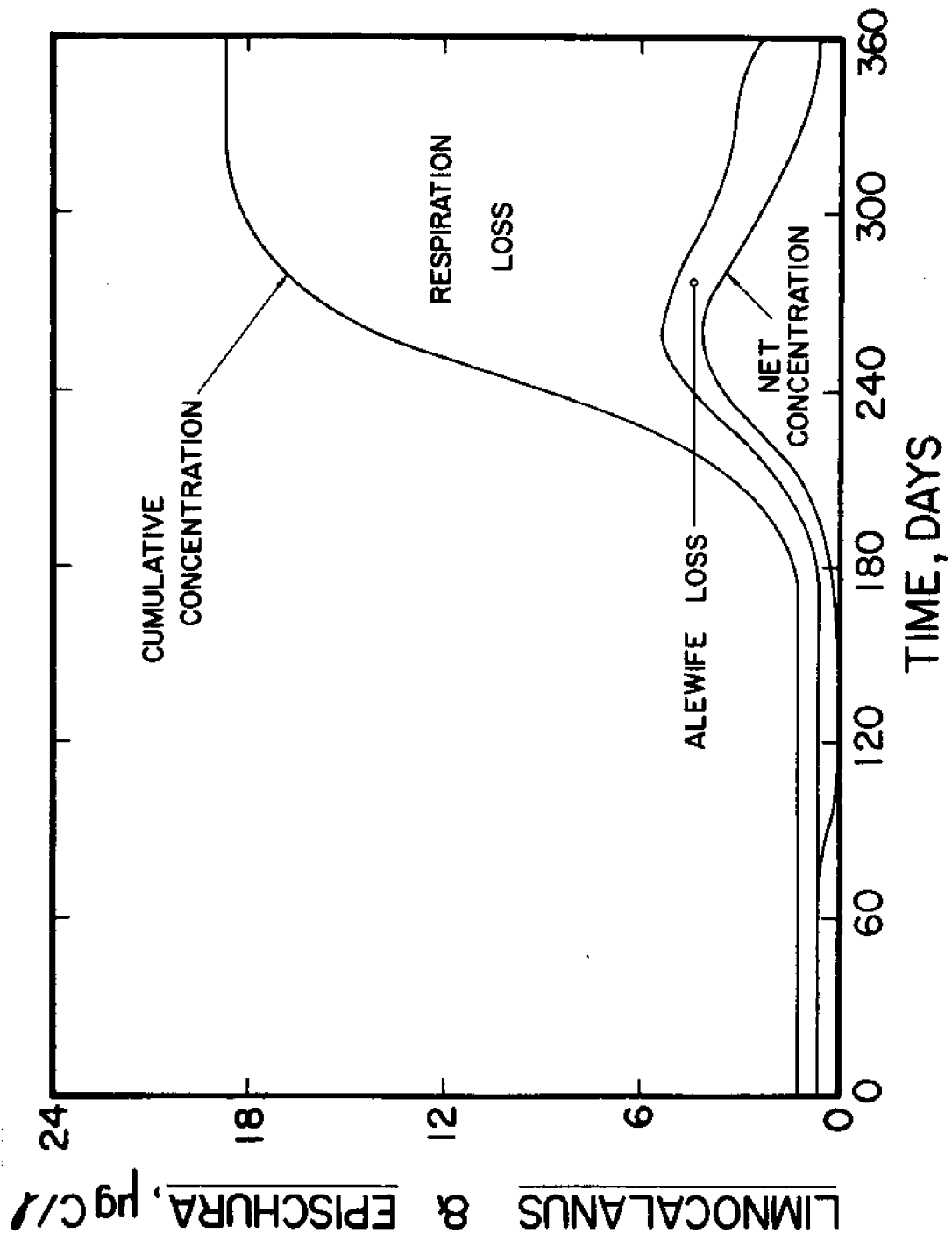


Figure 41. Calculated Energetics for Calibration Run

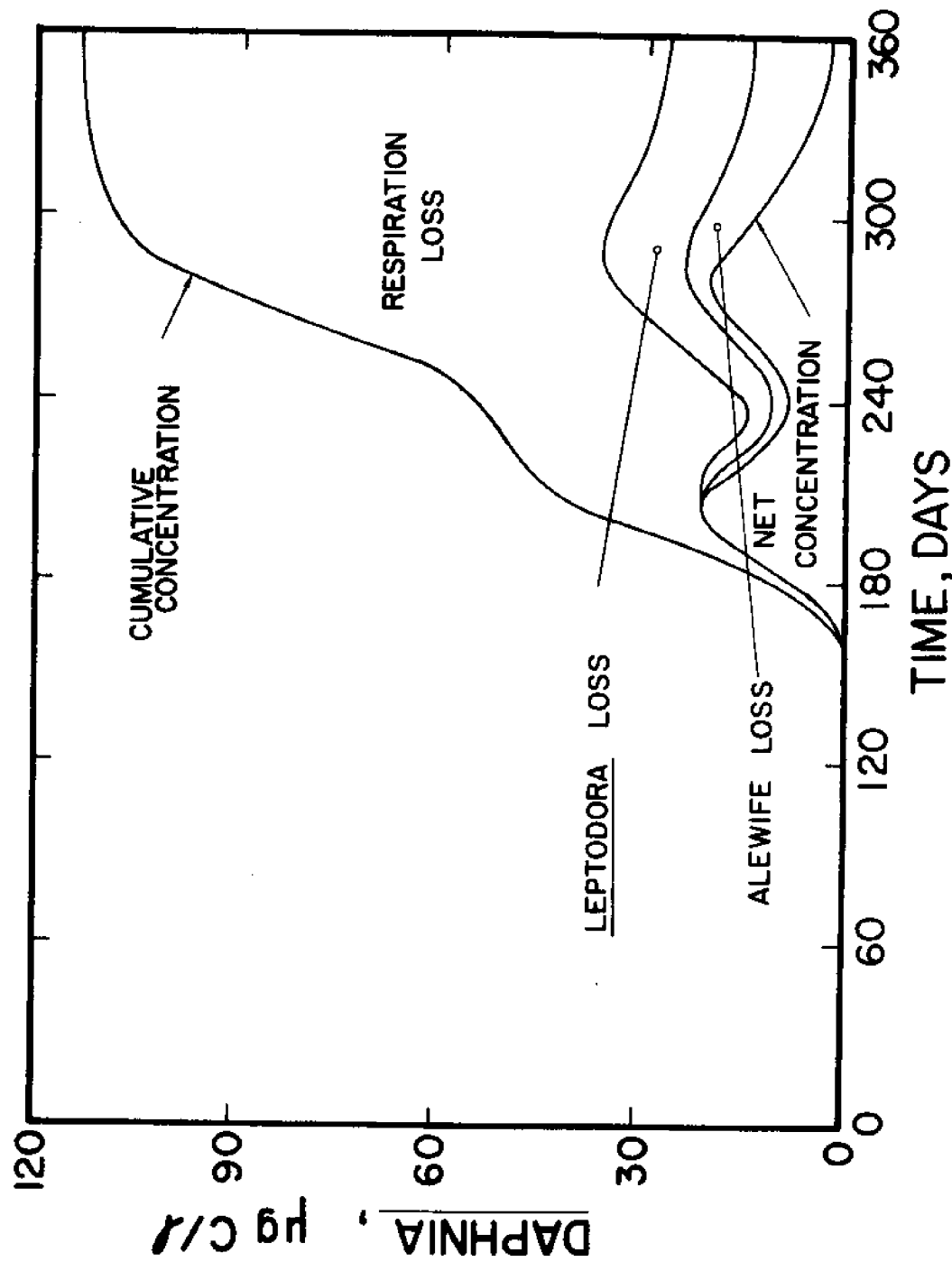


Figure 42. Calculated Energetics for Calibration Run

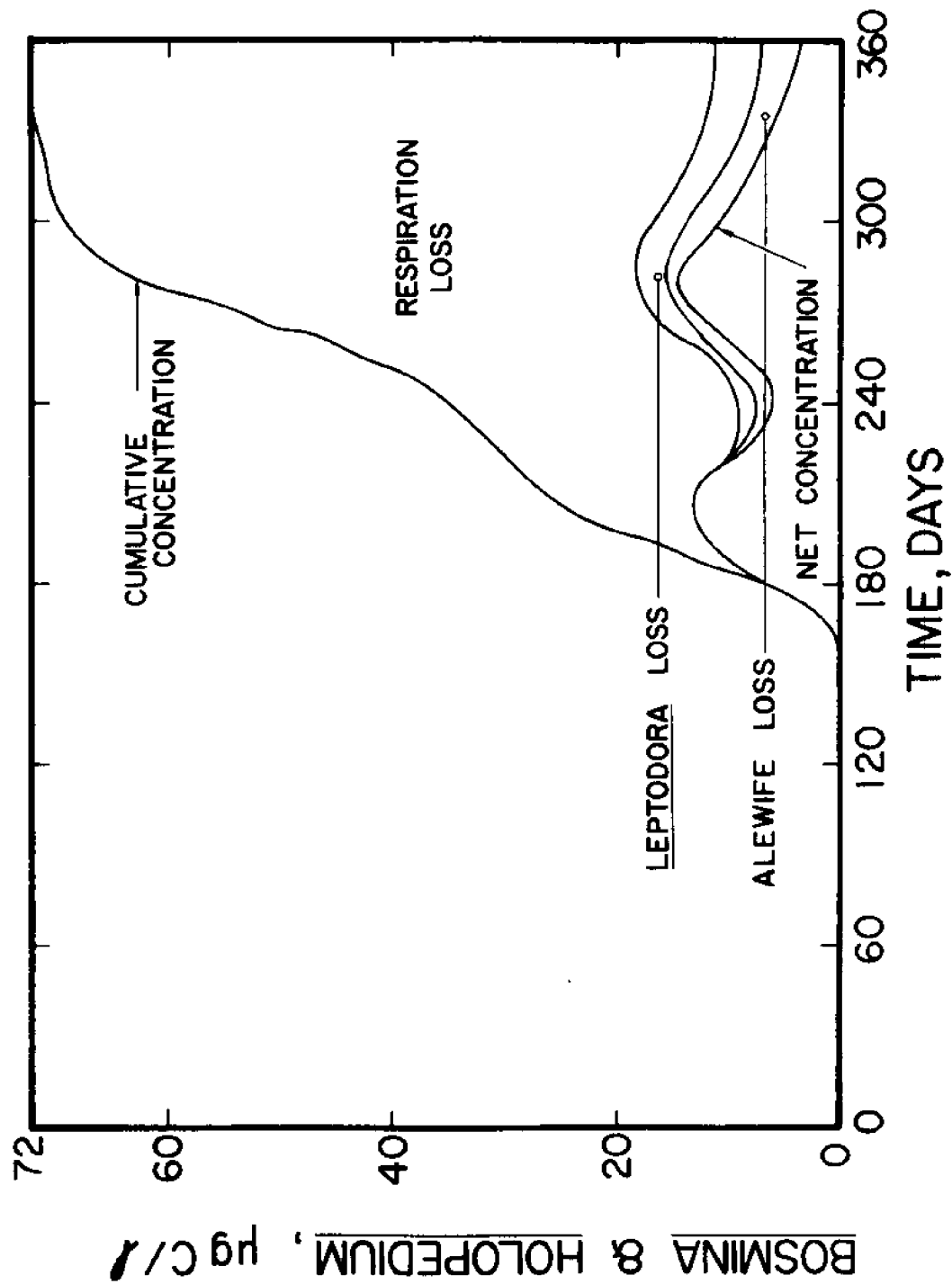


Figure 43. Calculated Energetics for Calibration Run

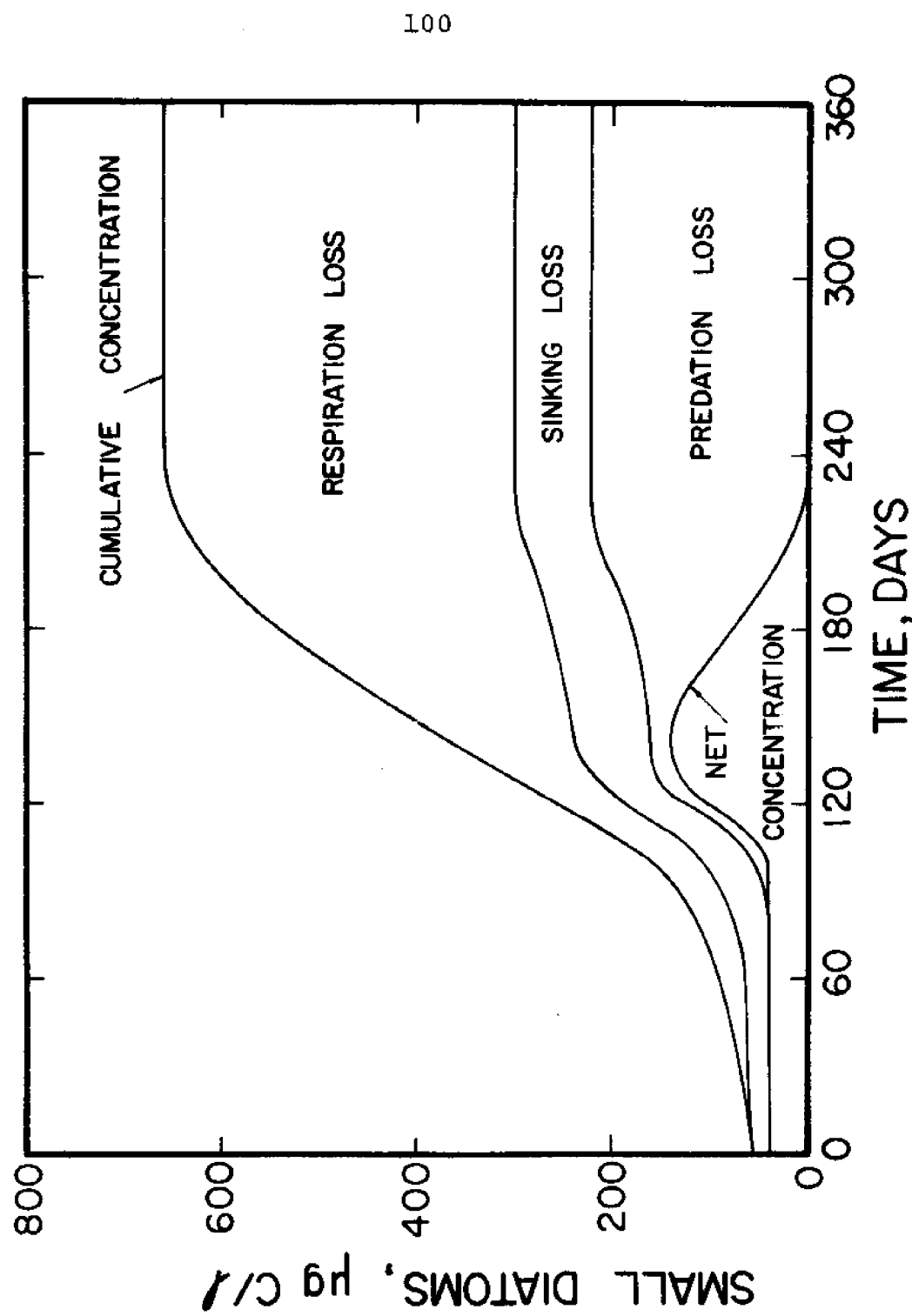


Figure 44. Calculated Energetics for Calibration Run

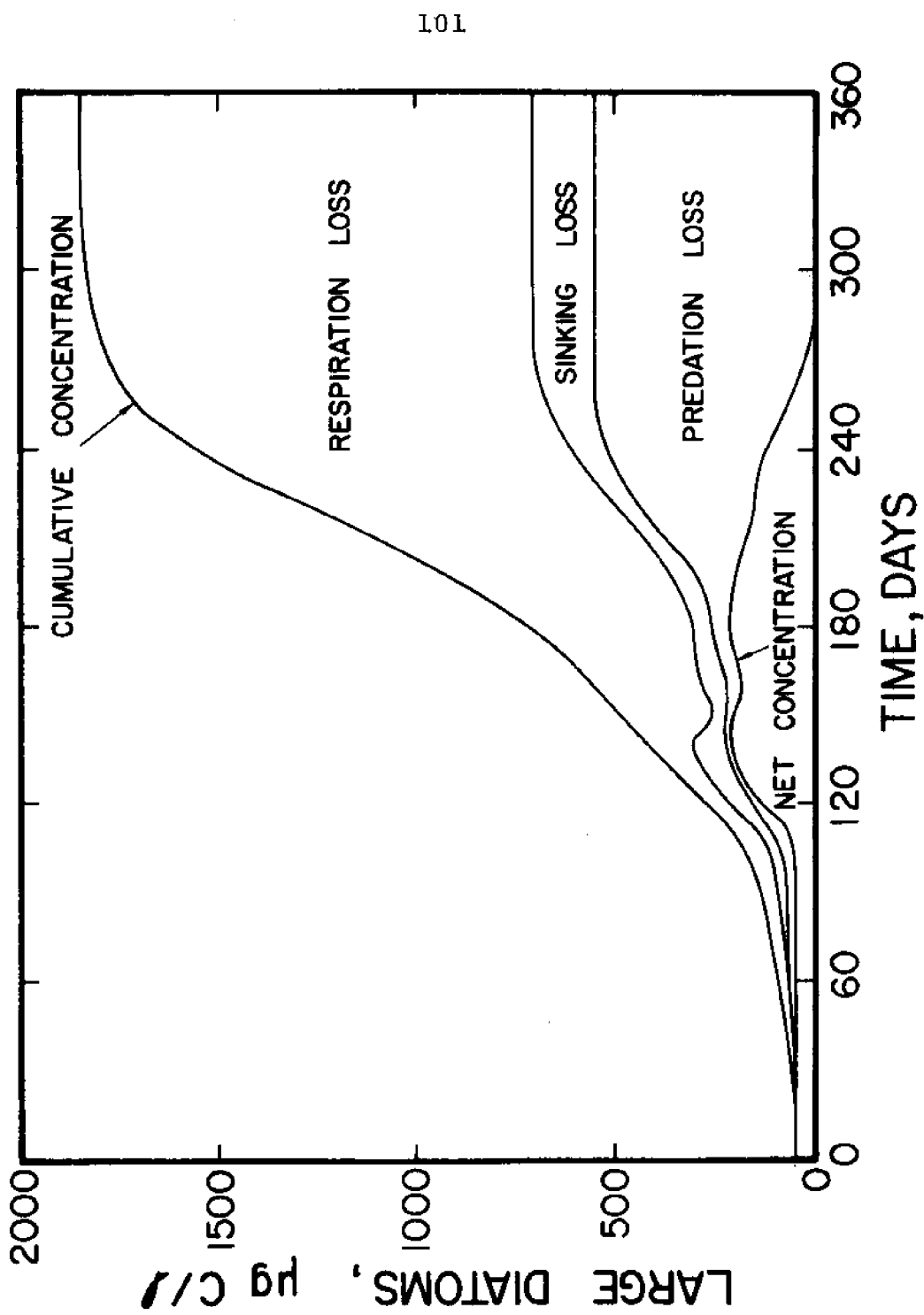


Figure 45. Calculated Energetics for Calibration Run

102

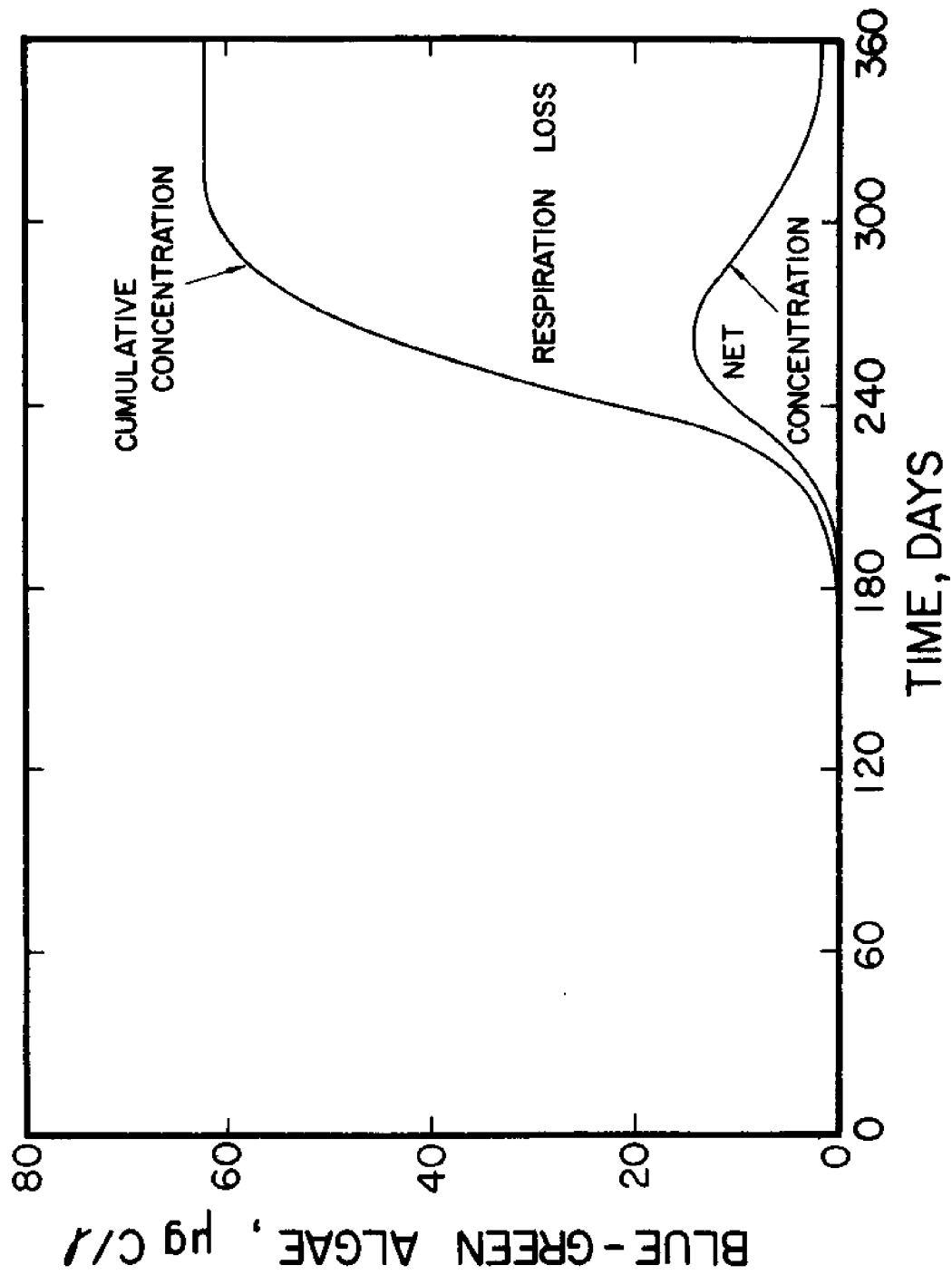


Figure 46. Calculated Energetics for Calibration Run

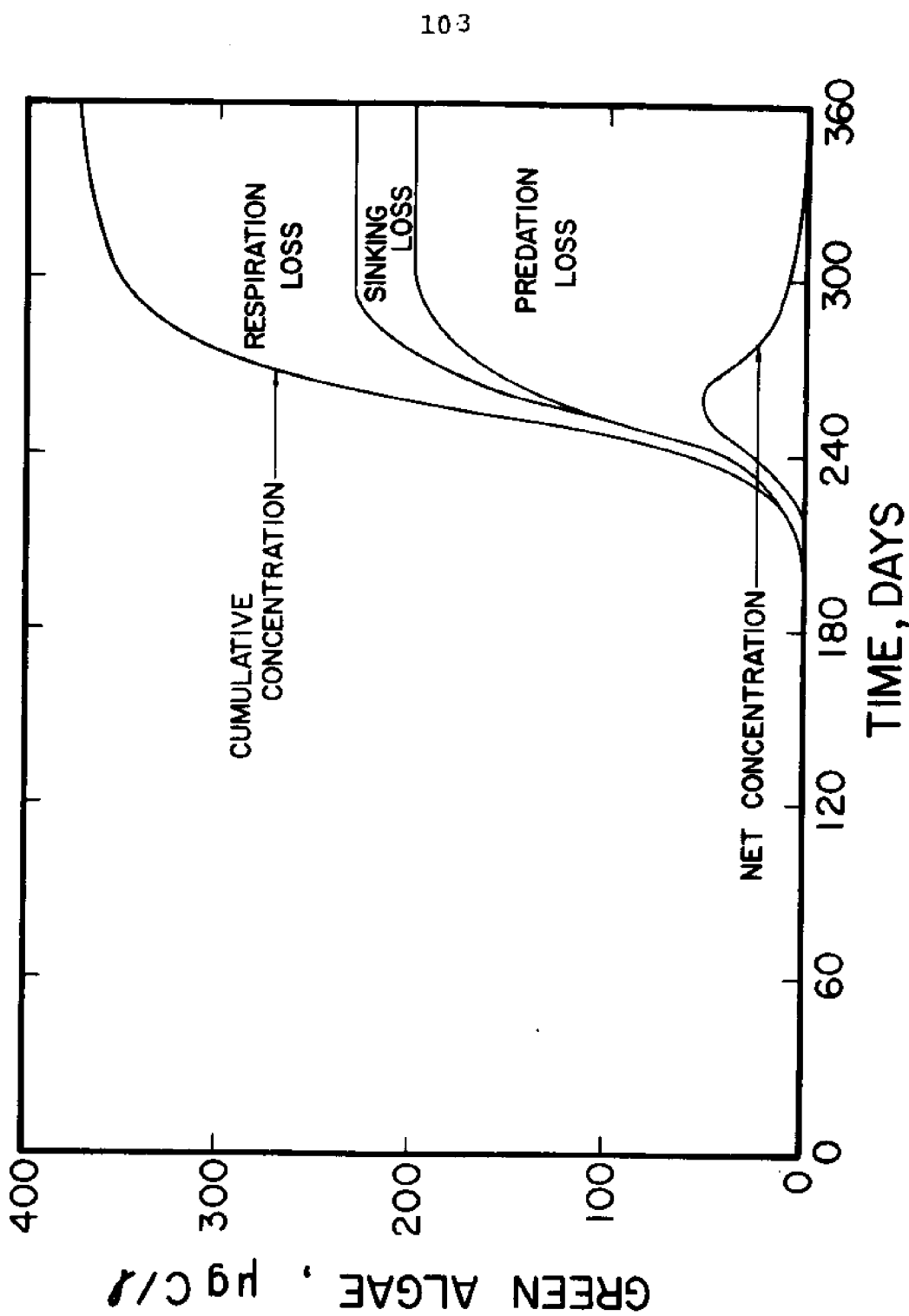


Figure 47. Calculated Energetics for Calibration Run

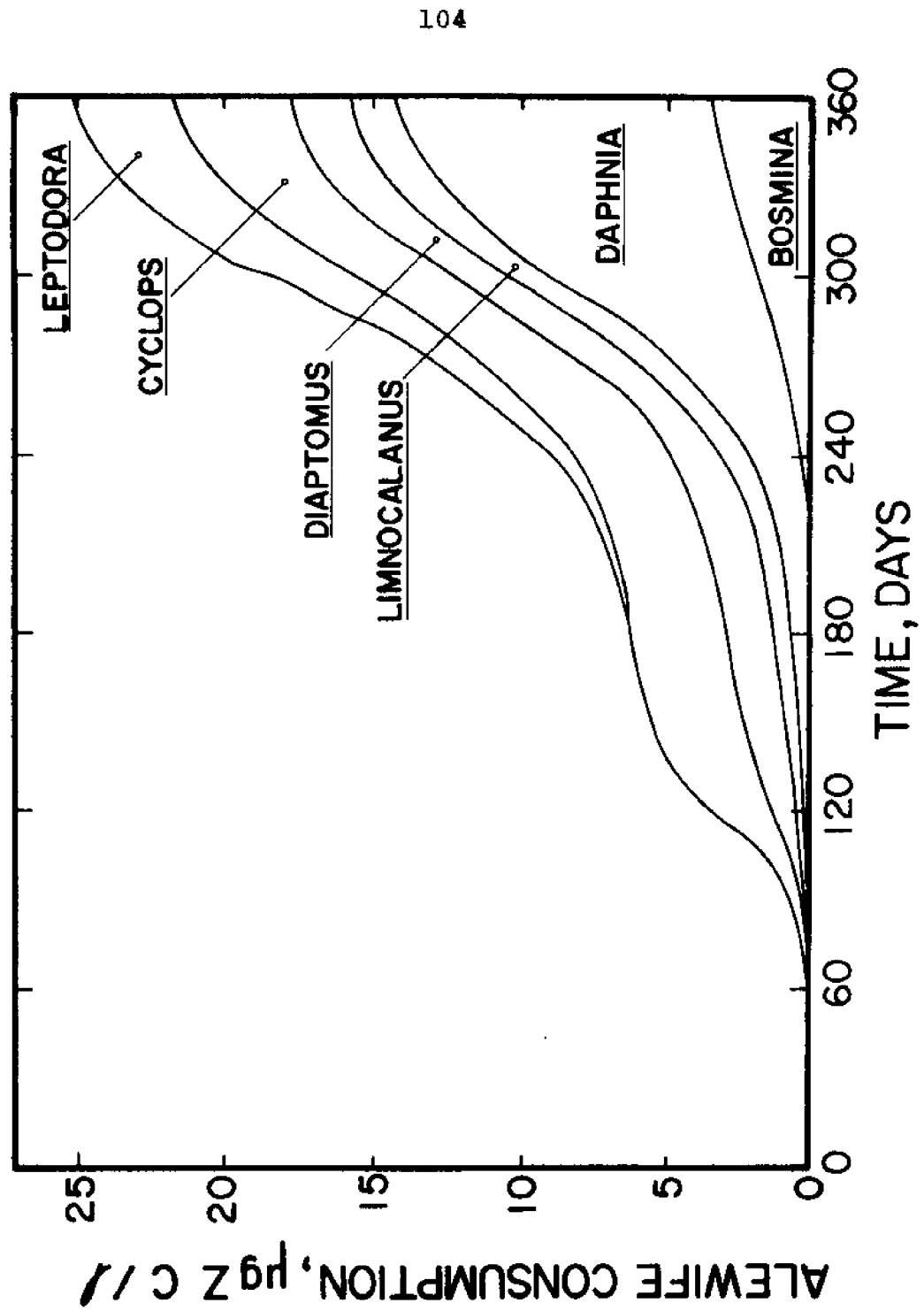


Figure 48. Calculated Energetics for Calibration Run

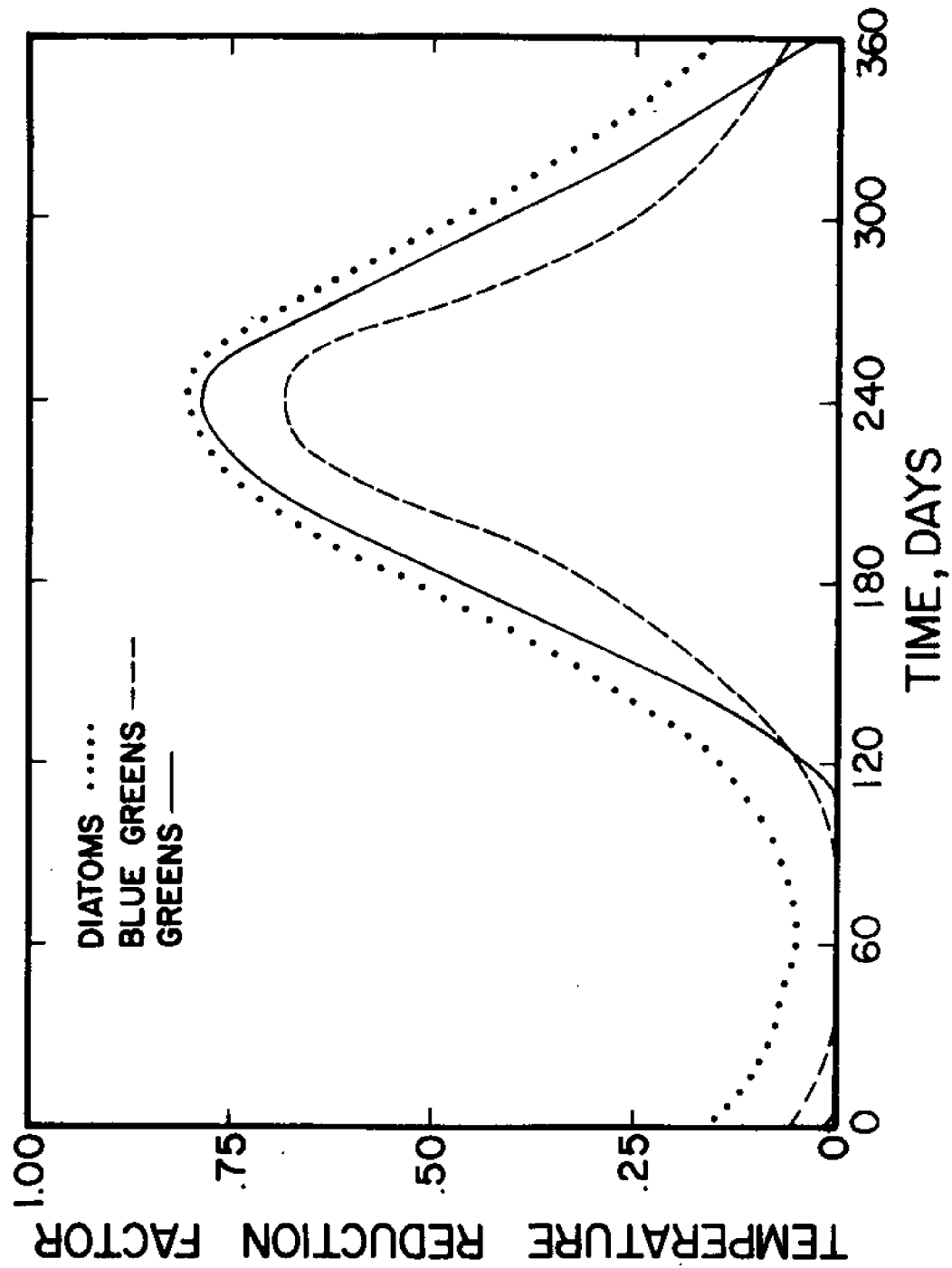


Figure 49. Resultant Temperature Reduction Factor Cycles

106

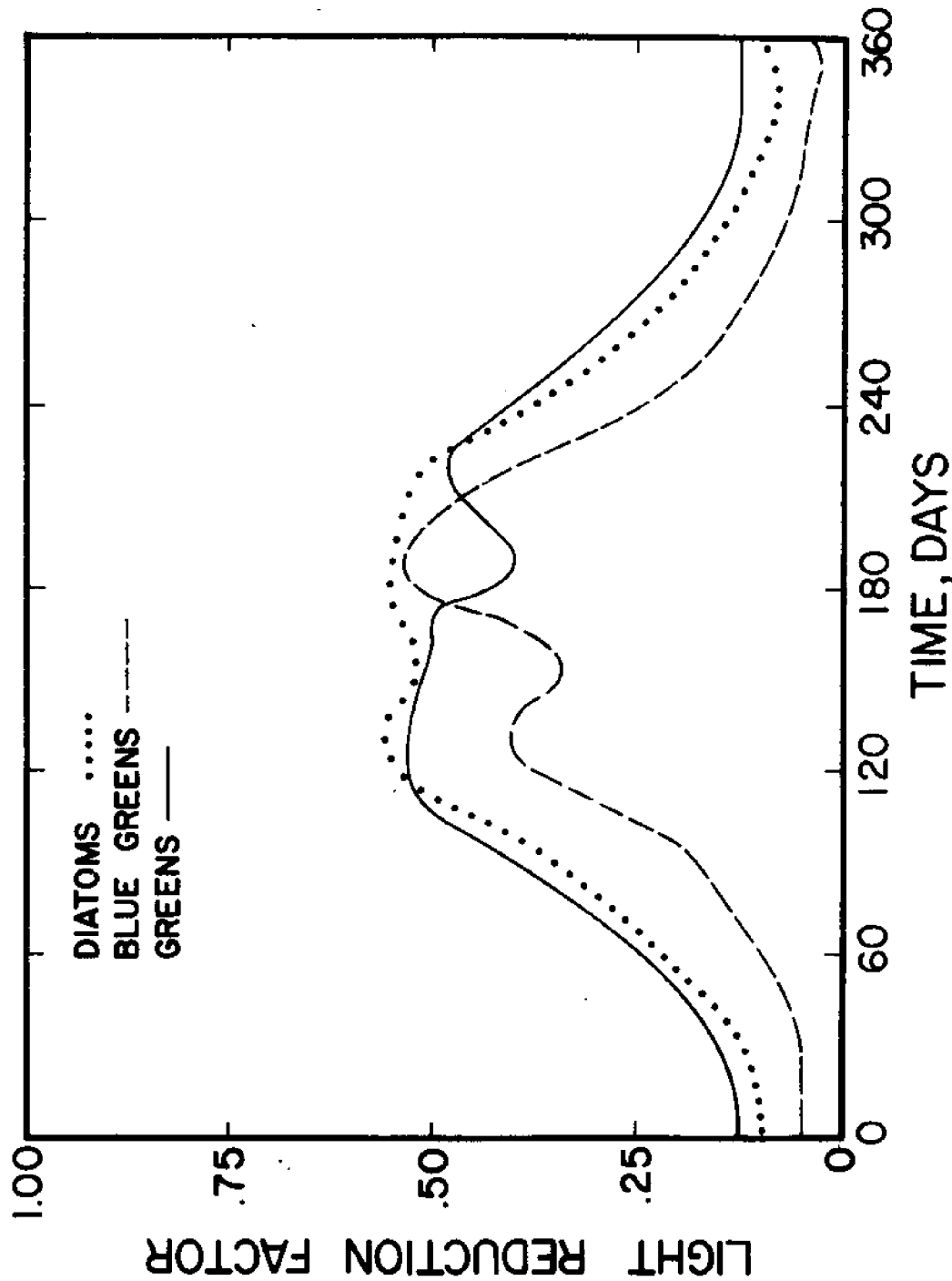


Figure 50. Resultant Light Reduction Factor Cycles

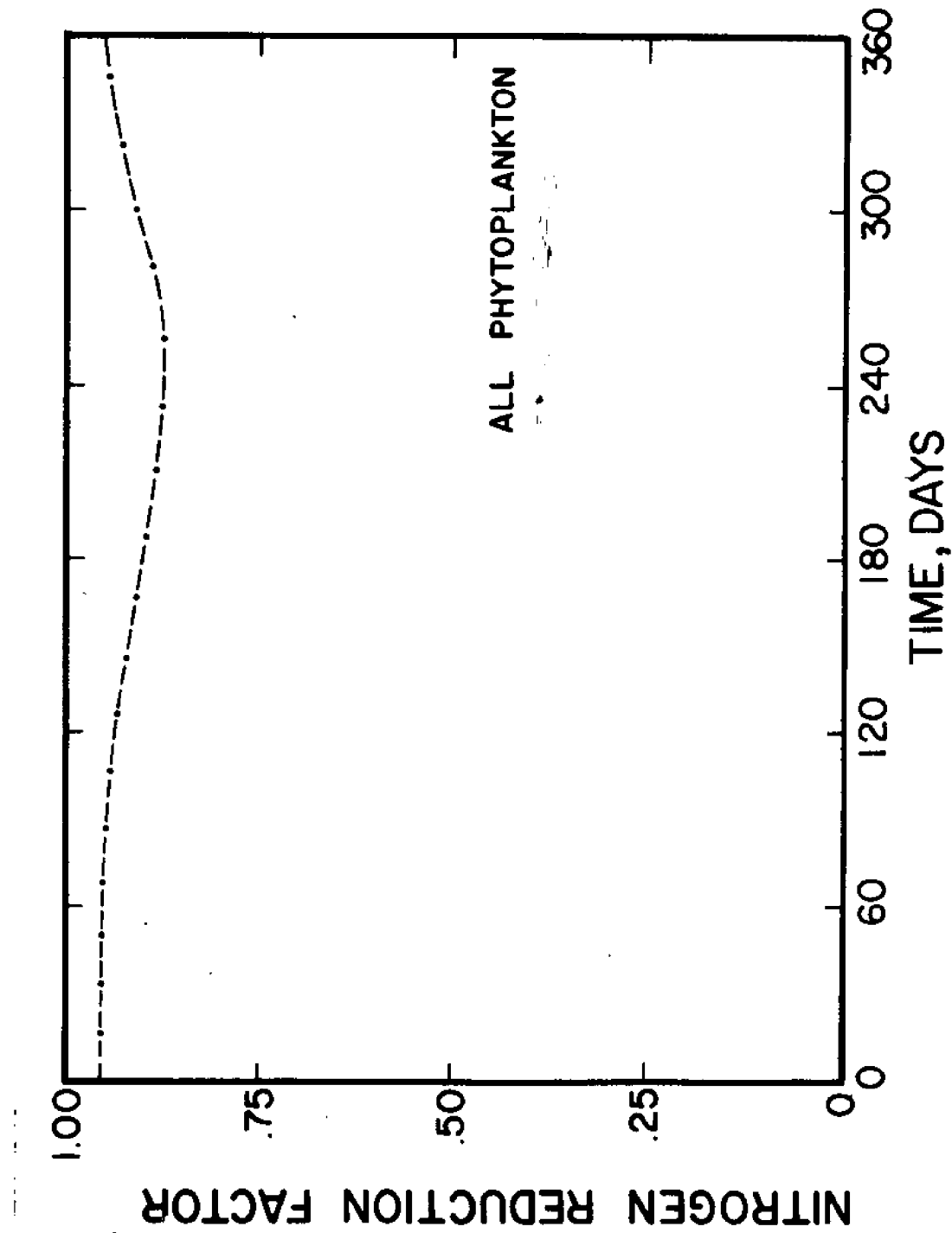


Figure 51. Resultant Nitrogen Reduction Factor Cycle  
For Calibration Run (Reduction Factor is identical  
for each phytoplankton group)

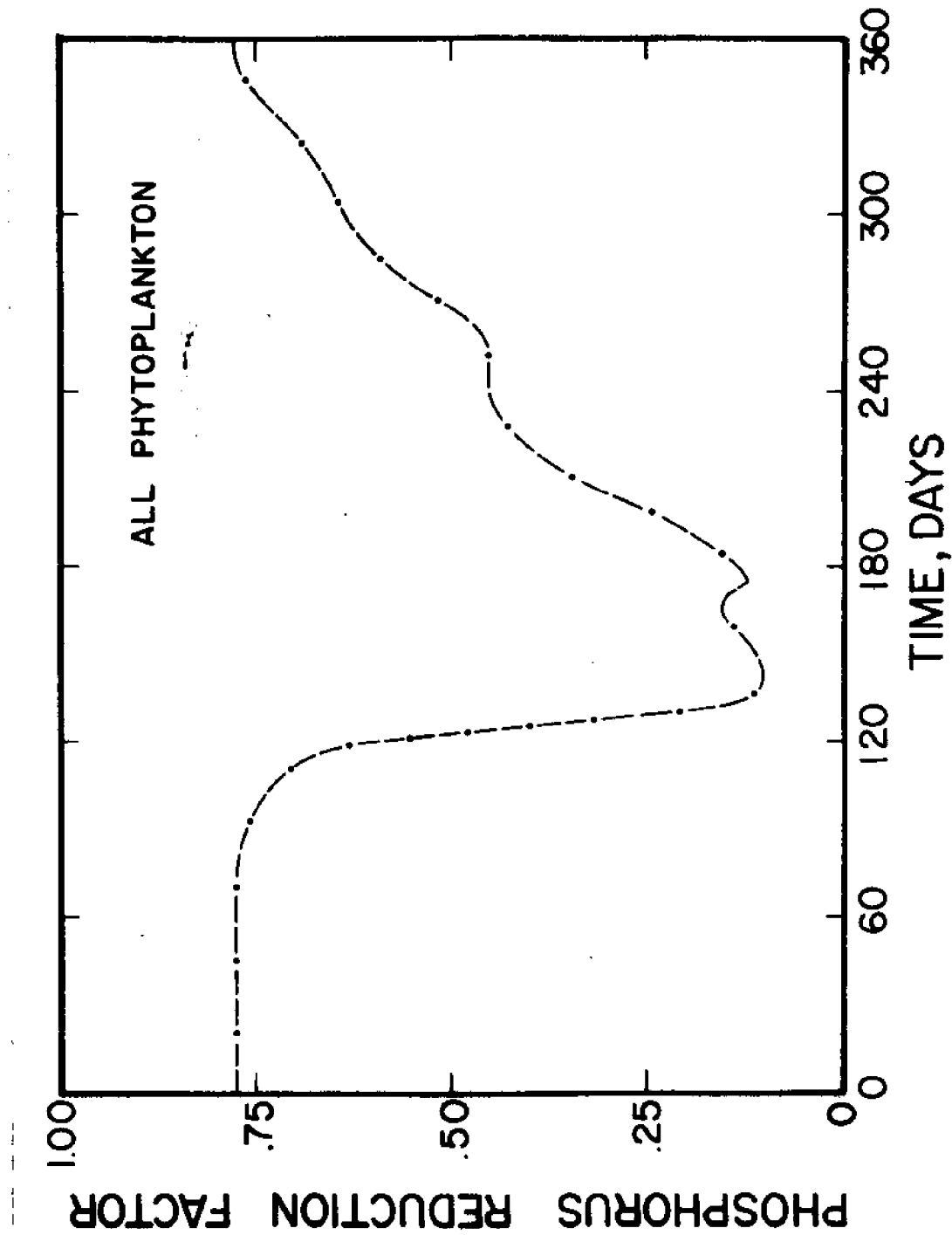


Figure 52. Resultant Phosphorus Reduction Factor Cycle  
For Calibration Run (Reduction Factor is identical for  
each phytoplankton group)

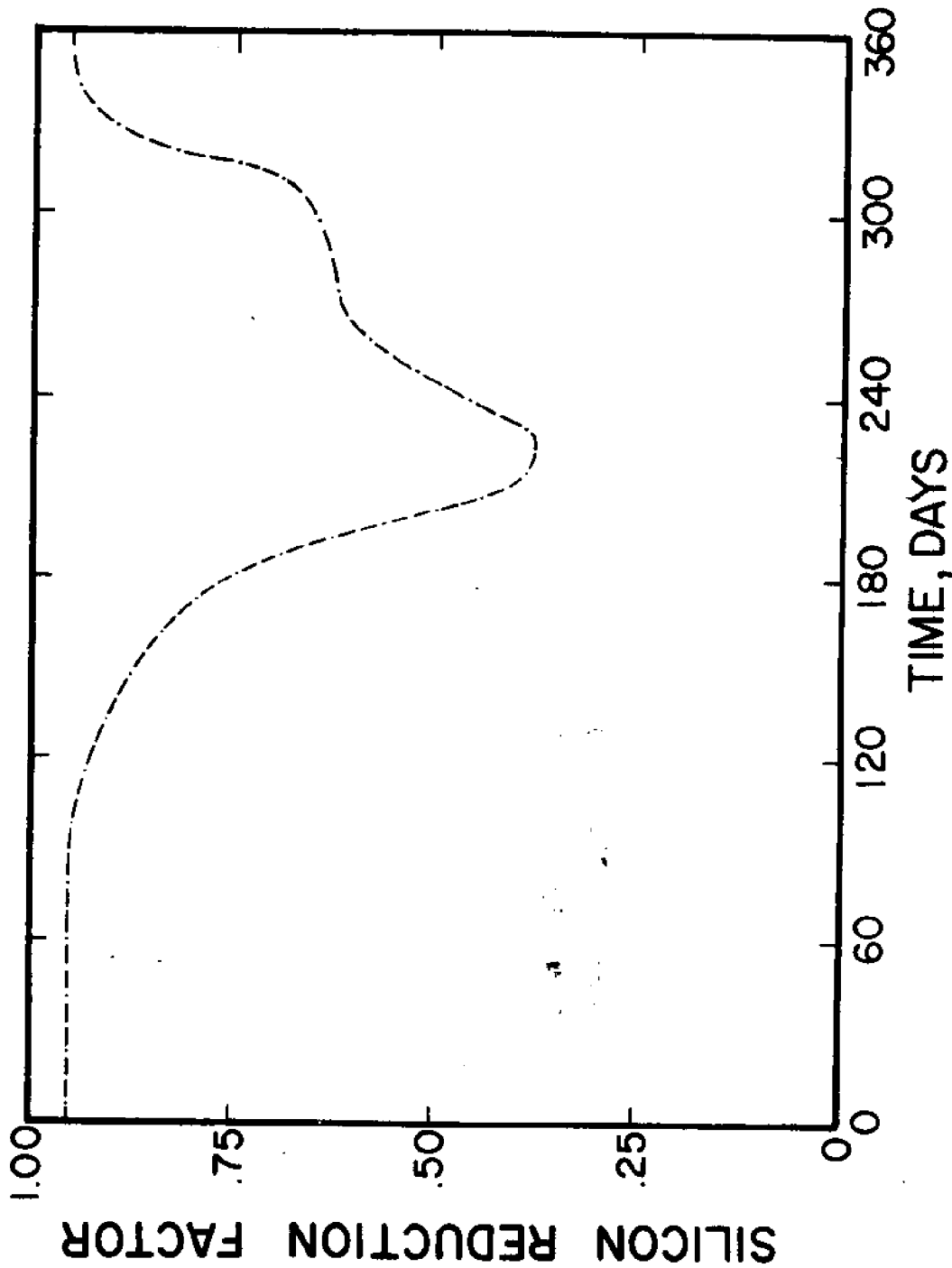


Figure 53. Resultant Silicon Reduction Factor Cycle For Calibration Run. (Reduction Factor is identical for both Diatom groups)

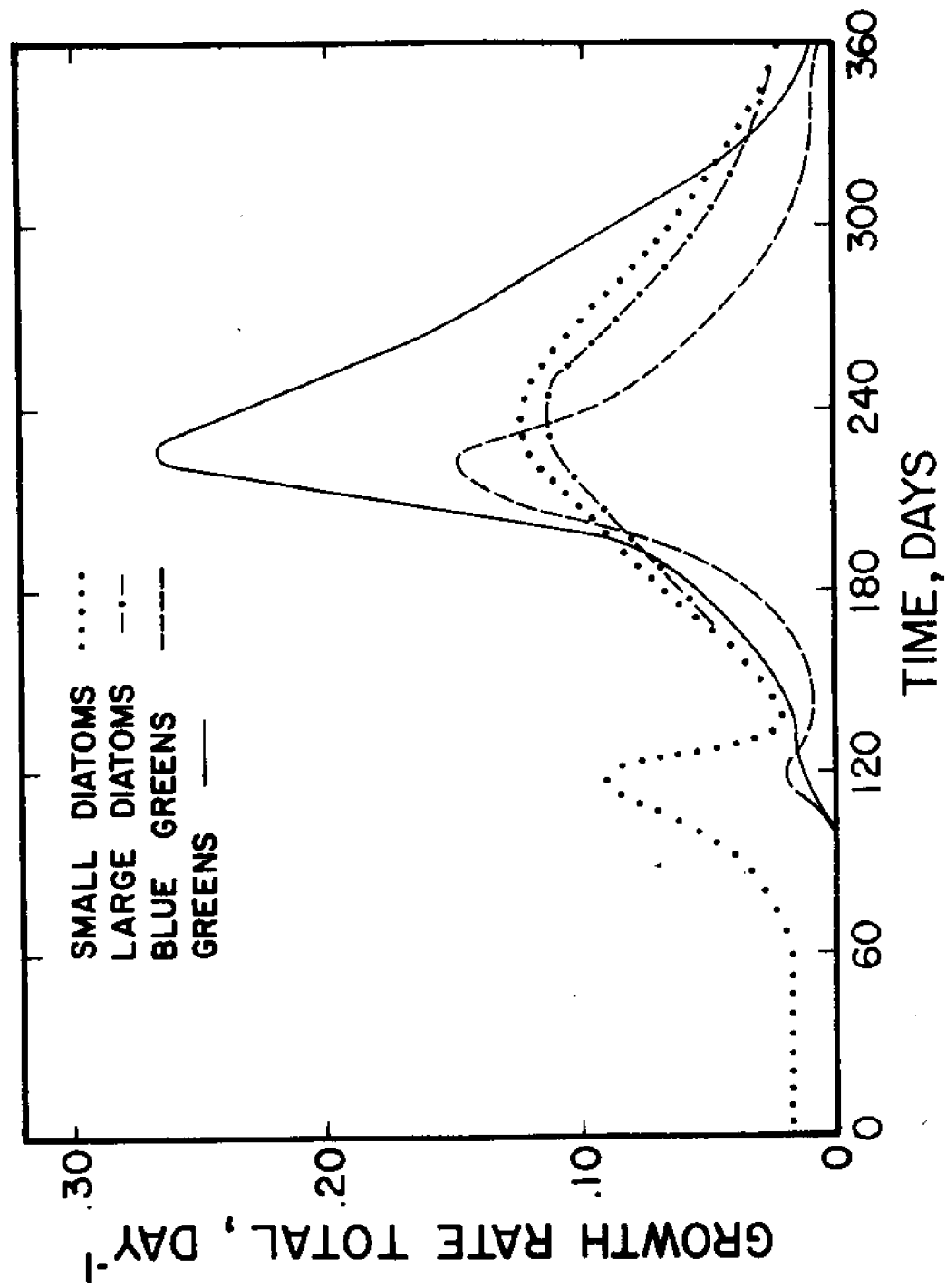


Figure 54. Resultant Total Grow Rates for Calibration Run

## ANALYSIS

The objective of this section is to analyze the model calibration results in order to test the validity of the biological assumptions of the Lake Michigan food web model. This analysis permits an evaluation of the parameter values selected for the model. The model calculations have been divided into two types: the calibration or preliminary verification which represents an attempt to replicate present conditions; and four simulations which have altered initial conditions to approximate past or potential future conditions which might arise in the lake. The simulations are not intended to be predictive, but rather are attempts to check the coupling network and parameter values of the model.

Calculated Zooplankton vs. Observations

Seasonal data on zooplankton abundance in Lake Michigan are scanty, even those from Grand Traverse Bay; thus any model calibrations must be considered tentative estimates of zooplankton interactions in a poorly sampled lake. The annual cycles of the predatory cladocerans, Leptodora and Polyphemus, as calculated in the model, appear to peak at about the same time as they do in Grand Traverse Bay (see Figure 16). However, the model taxon does not disappear as quickly as the observed population. By breaking the production and losses into components (see Figure 38) one can evaluate the validity of the model parameters for Leptodora and Polyphemus. A comparison of model results with an energetics study of Leptodora by Cummins et al. (1969) indicates that the model, at least for the predatory cladocerans, utilizes valid parameter values. For instance, the fraction of consumed food actually assimilated in the model is .47 as opposed to .40 observed by Cummins. Respiration figures are even closer (.73 in the model vs. .70 found by Cummins). These comparisons indicate that the gross energetics of the predatory cladocerans in the model approximate the real world. Furthermore, the model indicates that .18 of the annual Daphnia production is lost to Leptodora predation, whereas Hall (1964) found a value of .26.

The annual cycles of the two herbivorous cladoceran states of the model (Daphnia, and Bosmina & Holopedium) compare less favorably with the data (see Figures 23 and 24). Both model states show bimodal peaks, one in the summer and one in the fall. The bimodal shape of the herbivorous cladocerans' cycles is apparently due to the decline of their summer food, the small diatoms, and the increase of Leptodora. For both states, recovery in the fall results from an increase in green algae.

Data available for Daphnia and for Bosmina and Holopedium tend to indicate but not confirm such a bimodal peak. The magnitude of the model Bosmina peaks appears realistic; however, the Daphnia peak is too low. It may be that the general physiological rates of Daphnia are slower in the model than in Lake Michigan. This may be due to acclimation to colder waters of Lake Michigan by daphnid species not studied in the laboratory. During the last 60 days of the year, the model overestimates the observed populations. A breakdown of the energetics of Daphnia has been studied by Hall (1964). The fraction due to respiration losses in the model is .75, whereas Hall (1964) calculated .71. The fraction due to natural mortality loss in the model is .075 vs. .03, whereas predation losses are .18 vs. .26 (See Figures 42 and 43.)

The model trajectories for Cyclops follow the data approximately, although the major peak and collapse during the second half of the year appears to be somewhat more extreme than the data would suggest (see Figure 17). Perhaps the model coefficients involved overestimate the effect of Cyclops predation upon nauplii. However, only 26% of the model cyclopoid nauplii are grazed as opposed to 30% reported by McQueen (1969).

Model calculated Diaptomus peaks slightly higher than the data (see Figure 21). Apparently the model coefficients for production are accurate, although model Diaptomus respiration (Figure 40) was .83 of the assimilated material over the year while Kibby (1971) observed an average of .69. However, D. gracilis, the organism used by Kibby (1971), is a larger species than Great Lakes diaptomids.

No investigations of Limnocalanus and Epischura have been found for comparison with model energetics. However, both the data and model suggest a fall peak for this group (see Figure 22). Seasonal sampling of these species in the Great Lakes has not been satisfactory. In the model these species appear to increase and decline as a function of the amount of Diaptomus present.

Data which define the seasonal variation of nauplii in Grand Traverse Bay are not available for comparison with the model calculations. It is recommended that nauplii from Lake Michigan be collected for enumeration and process studies despite the sampling difficulties anticipated. However, the model result can be compared with observations from other lakes. Hutchinson (1967), summarizing several studies, suggests that naupliar and early copepodite stages of various diaptomids occur in lakes for a duration of 50 to 120 days.

In the model the diaptomid naupliar state lasts for about 90 days. Diaptomid eggs in Lake Erie are most abundant during April (Hutchinson, 1967, p. 656), so the maximum naupliar and early copepodite populations should occur in May. The model calculates a June peak for Lake Michigan. The model timing therefore appears appropriate since Lake Michigan is colder than Lake Erie. The model cyclopoid nauplii peak in June and are present during most of the year. This is similar to the annual cycle of Mesocyclops leuckarti in Lake Maggiore as reported by Hutchinson (1967).

#### Calculated Phytoplankton vs. Observations

The diatom patterns of bloom and collapse in the model are similar to observed cycles in Grand Traverse Bay (see Figures 25 and 26). Phosphorus controls the diatom fluctuations in the model, although slow silicon turnover keeps diatoms low during late summer and early fall. Large amounts of silicon locked in the detrital state and the presence of regenerated phosphorus enable the greens to bloom in the fall. However, in the model the green algal peak is higher than that represented in Grand Traverse Bay data (see Figure 28). Model calculations for the blue-greens follow the data closely, both showing a small mid-September bloom (See Figure 27).

Since Lake Michigan is never warm enough for the taxa to attain the maximum growth rates, nutrient-independent growth rates are dominated by the annual temperature cycle with diatoms having an advantage over greens and blue-greens. The average light intensity in the euphotic zone will inhibit the greens between days 110 and 240 and the diatoms between days 180 and 210. The blue-greens are never inhibited by light. Although the greens are more temperature-controlled than diatoms, their competitive position in the food web is critically affected by light. During high periods (day 180 to 220) greens are more inhibited than diatoms because their optimum light intensity is lower. According to the model, the greens gain a competitive advantage over diatoms during low light periods (see Figure 50). Because of high light and temperature requirements, blue-greens never dominate (see Figures 49 and 50).

Although nitrogen is not limiting in Lake Michigan (see Figure 51), phosphorus limitation reduces the growth rates significantly (see Figure 52). The diatom growth rates are further reduced by silicon limitation as depicted in Figure 53. These computed cycles can be indirectly justified by comparing model phytoplankton trajectories with the observed data (Figures 25 to 28). However, primary productivity data are not available for direct comparison.

### Calculated Nutrients vs. Observations

Ammonia, nitrate, total-dissolved silicon, and total-dissolved phosphorus have been measured routinely since 1971 in Grand Traverse Bay. The model calculated patterns are compared with available data from 1971, 1972, and 1973.

The model calculated and observed levels of ammonia in Figure 31 are in the same range although seasonal cycles do not compare well. Distinct patterns in the data are difficult to define since ammonia concentrations in the lake are near the analytical detection limit. The computed variation of nitrate agrees with data from Grand Traverse Bay (Figure 32). No data are available to validate the detrital and soluble organic nitrogen model calculations.

Silicon in the computer runs starts high and declines slowly until day 100, then rapidly declines to 60  $\mu\text{g/l}$  by day 200 (Figure 37). Recovery takes place after fall overturn (beginning day 300) and is complete by day 340. Recovery in the model is mainly due to the fall overturn; however, according to the data, there is some regeneration of silicon from diatom **decomposition** prior to overturn. Thus, between day 200 and day 330, the data are higher than the model calculates.

Dissolved-organic and dissolved-inorganic phosphorus are assigned separate states in the model. Dissolved-organic phosphorus represents all soluble forms which are unavailable to algae, whereas dissolved-inorganic phosphorus represents all forms which are available. However, only total-dissolved phosphorus data are available for Grand Traverse Bay. Thus, the overall results of this approach can be checked only by adding the two model states and comparing the results against data for total-dissolved phosphorus. Since phosphorus appears to be the limiting nutrient in Grand Traverse Bay, it is critical that the model duplicate the observed phosphorus cycles. The data, as seen in Figure 35 (although erratic because of sampling and laboratory limitations), and the computed curve for total-dissolved phosphorus agree. It is noted that the model-calculated total-dissolved phosphorus levels are higher than spring data. This suggests that some spring diatom growth may be cells that have excess phosphorus. An internal reservoir need not be large to account for the extra dissolved phosphorus in the model. For example, at day 60 the concentration of algae is about 100  $\mu\text{g c/l}$ . These algae have a requirement of about 3.6  $\mu\text{g/l}$  of phosphorus. On day 60 the excess total dissolved phosphorus is 1.6  $\mu\text{g/l}$ . The difference could be explained by phosphorus storage of about 50%. This phosphorus would be in the algae and not soluble, though usable for growth. Azad and Borchardt (1970) have

shown that 50% excess phosphorus is possible. No data are available for comparison with detrital phosphorus calculations.

### Model Simulations

Four simulations were conducted with the calibrated model for the purpose of examining the behavior of the model when phosphorus and alewife concentrations are higher than present conditions. The first simulation assumes that the initial level of phosphorus is 1.5 times present initial conditions; the second simulation assumes that alewife predation is 5 times present conditions. The third simulation combines the assumptions of the first two simulations, and the last assumes that the initial condition for phosphorus is 3 times present conditions and that alewife predation is normal. The results of these calculations are shown in Figures 55 to 76.

Figure 71 shows excess nitrate under existing phosphorus conditions. However, as phosphorus is increased, nitrate becomes more limiting and finally becomes clearly limiting when phosphorus is increased by a factor of 3. It is expected that nitrogen-fixing blue-green algae would develop under such circumstances, and indeed nitrogen limitation and large populations of blue-green algae are known to occur in other parts of the Great Lakes such as Green Bay. It is noted that nitrate, as well as the other dissolved oxidized nutrient states, is less sensitive to increases in alewife predation than corresponding detrital states. As shown in Figure 70, the ammonia concentration remains low and insensitive to the simulations. The dynamic patterns are complex because of the effects of uptake, ammonification, and nitrification.

Figure 74 shows incomplete utilization of the inorganic phosphorus when initial conditions are increased by a factor of 3 over existing levels in Lake Michigan. It is anticipated that nitrogen-fixing blue-greens would take advantage of this excess. At present the model does not consider nitrogen-fixing blue-greens, although the theoretical framework for including this effect has been considered by Bierman (1973).

Figure 76 shows that high levels of inorganic phosphorus cause complete dissolved silicon utilization (down to the unavailable level) approximately 60 days earlier than under normal circumstances. The earlier utilization also results in an earlier mid-summer regeneration of silicon. This early regeneration of silicon is the apparent cause of the small late-fall large diatom bloom observed in Figure 65.

Detrital nitrogen increases with increases in the initial level of phosphorus and decreases as a result of increased

alewife predation on zooplankton. The general trend of the detrital phosphorus is similar, but the dynamics are more complicated. The detrital silicon curve is not very sensitive to changes in the phosphorus level because practically all the dissolved silicon is processed by the diatoms at all the phosphorus levels considered. Dissolved organic nitrogen and phosphorus follow a similar pattern. This response is the result of nonlinear utilization of the additional phosphorus when silicon first and then nitrogen begin to limit production of the phytoplankton.

The above changes in nutrient patterns are filtered up the food chain causing changes in both the phytoplankton and the zooplankton. In the first simulation where the initial phosphorus was increased by a factor of 1.5, diatoms become less dominant and bloom earlier in the year (see Figures 64 and 65). The blue-green population increases by an order of magnitude, and the green pattern becomes bimodal. The grazing of the herbivorous cladocerans on the greens allows the blue-greens to become more dominant. However, because cladocerans are low during the last part of the year, the greens are able to bloom a second time thus halting the blue-greens. As discussed in an earlier section, greens will always dominate blue-greens in a predator-free environment. The first bloom of greens allows the herbivorous zooplankton, Daphnia, Bosmina, Diaptomus, and the nauplii, to peak higher. The initial Daphnia and Bosmina blooms occur later and the second peak for both is greatly depressed. The lower second peak is probably caused by the early collapse of the small diatoms. It is interesting to note that the initial Daphnia and Bosmina peaks are about double the calibration run. The Diaptomus peak is somewhat less than double, while the peak of Cyclops is only moderately increased. This results from the shorter peak of the large diatoms rather than the insufficient supplies of nauplii because the nauplii increased significantly, and suggests that the model Cyclops state is primarily herbivorous. The two predatory zooplankton states, Leptodora and Limnocalanus, demonstrate a generally greater increase than their prey. Thus new productivity resulting from increased phosphorus is transferred up the food web and accumulates in the top levels. This suggests that the increase in alewives which occurred in Lake Michigan during the 1960's was facilitated by increasing eutrophication of the lake.

The second simulation assumes that phosphorus levels are normal and that alewife predation increases by a factor of 5, which corresponds roughly to the peak abundance of this fish observed in Lake Michigan around 1966. Following the increase of alewives the abundance of Leptodora, Limnocalanus, and Daphnia is less than half that at normal alewife levels. The populations of Cyclops and Diaptomus are also smaller, but

the effect is less dramatic. Cyclops nauplii and Bosmina are enhanced slightly during certain parts of the year due to increased consumption of their predators by alewives. The green algal state is enhanced by the alewife increase which in turn causes a decrease of the blue-greens through competition.

The third simulation combines the effects of the first two simulations by assuming 1.5 times normal phosphorus and 5 times normal alewife predation. Increased alewife predation at 1.5 times normal phosphorus results in a major decline of Leptodora over the first simulation. On the other hand, a relatively minor decrease occurs in Cyclops, Diaptomus, Limnocalanus, and Daphnia. The Cyclops nauplii undergo a minor increase and Bosmina increases significantly over the first simulation with increased phosphorus only. Apparently, an implicit feature of the model is that the increased predation by alewife on Bosmina is more than offset by alewife predation upon the main zooplankton predator of Bosmina, i.e., Leptodora, and upon Daphnia and Diaptomus which are the main competitors of Bosmina. Diatoms remain practically unchanged while greens increase. Blue-greens decrease as a result of increased alewife predation. A similar effect was noted when increased alewife predation was added at normal phosphorus levels.

The fourth simulation triples the amount of phosphorus presently in the system. While the diatoms peak very high, the duration of their peak is short and blue-greens and greens correspondingly increase. Silicon limits the duration of diatom growth, so that most of the extra phosphorus goes into blue-green and green algae. The herbivorous cladocerans, Daphnia and Bosmina, are able to make use of this increased primary productivity, their populations showing great increases. The omnivorous cyclopoids show some increase, whereas the herbivorous calanoids, primarily Diaptomus, decrease slightly below the first simulation. The nauplii increase slightly. It appears that with increasing initial levels of phosphorus, the feeding mechanisms of the herbivorous zooplankton cause a shift from calanoid copepods to cladocerans. Thus, with small changes in initial phosphorus, all zooplankton states increase. However, as the maximum filtering rate of the calanoid copepods is approached, further increases in phytoplankton shift the advantage to the cladocerans. Leptodora populations are lower than for the case of only 1.5 times normal phosphorus. An explanation is offered for this seeming anomaly. Phytoplankton peak and decline earlier so the herbivorous zooplankton, Daphnia and Bosmina, peak earlier and higher. The peaks are too early to be fully exploited by Leptodora.

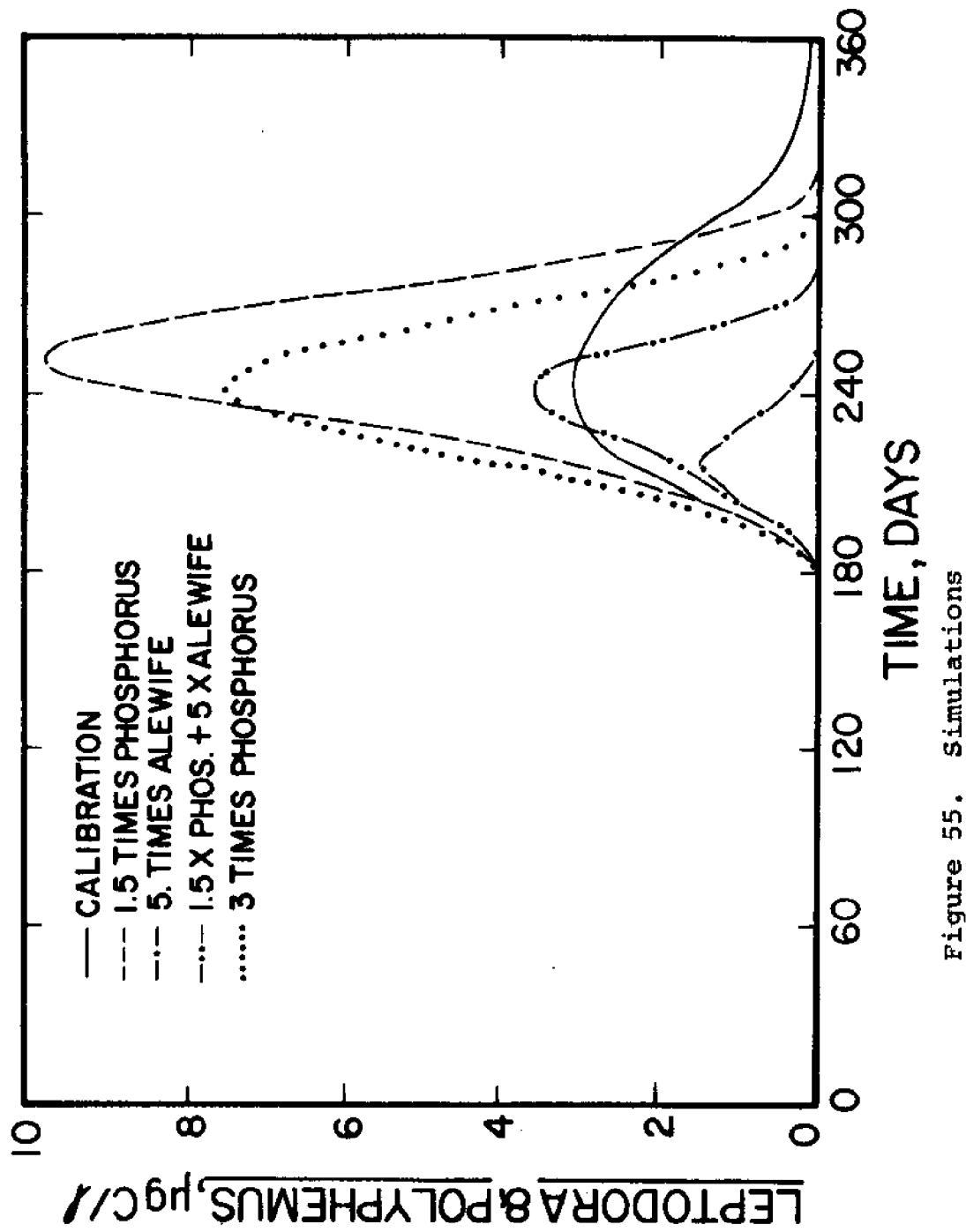


Figure 55. Simulations

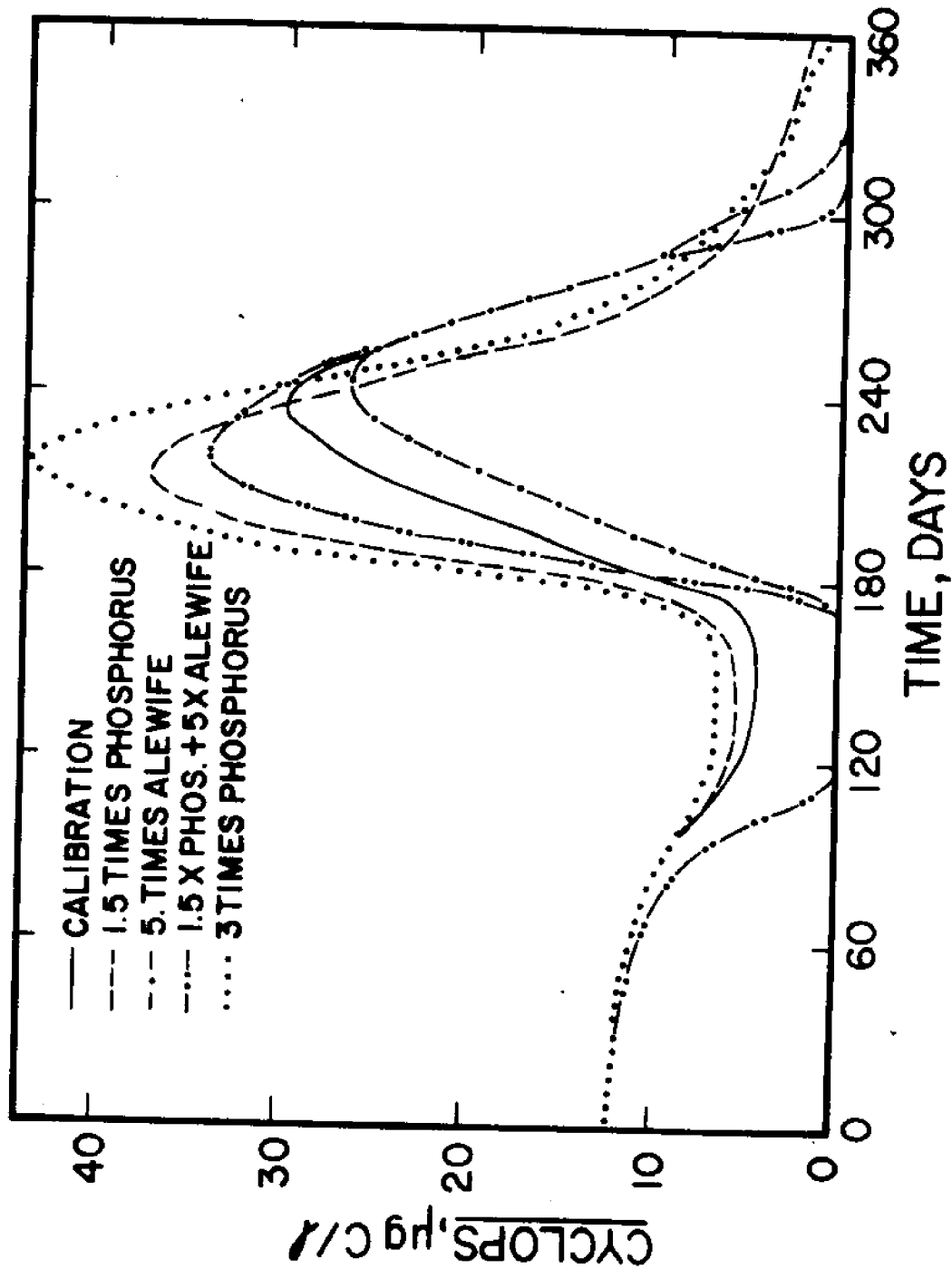


Figure 56. Simulations

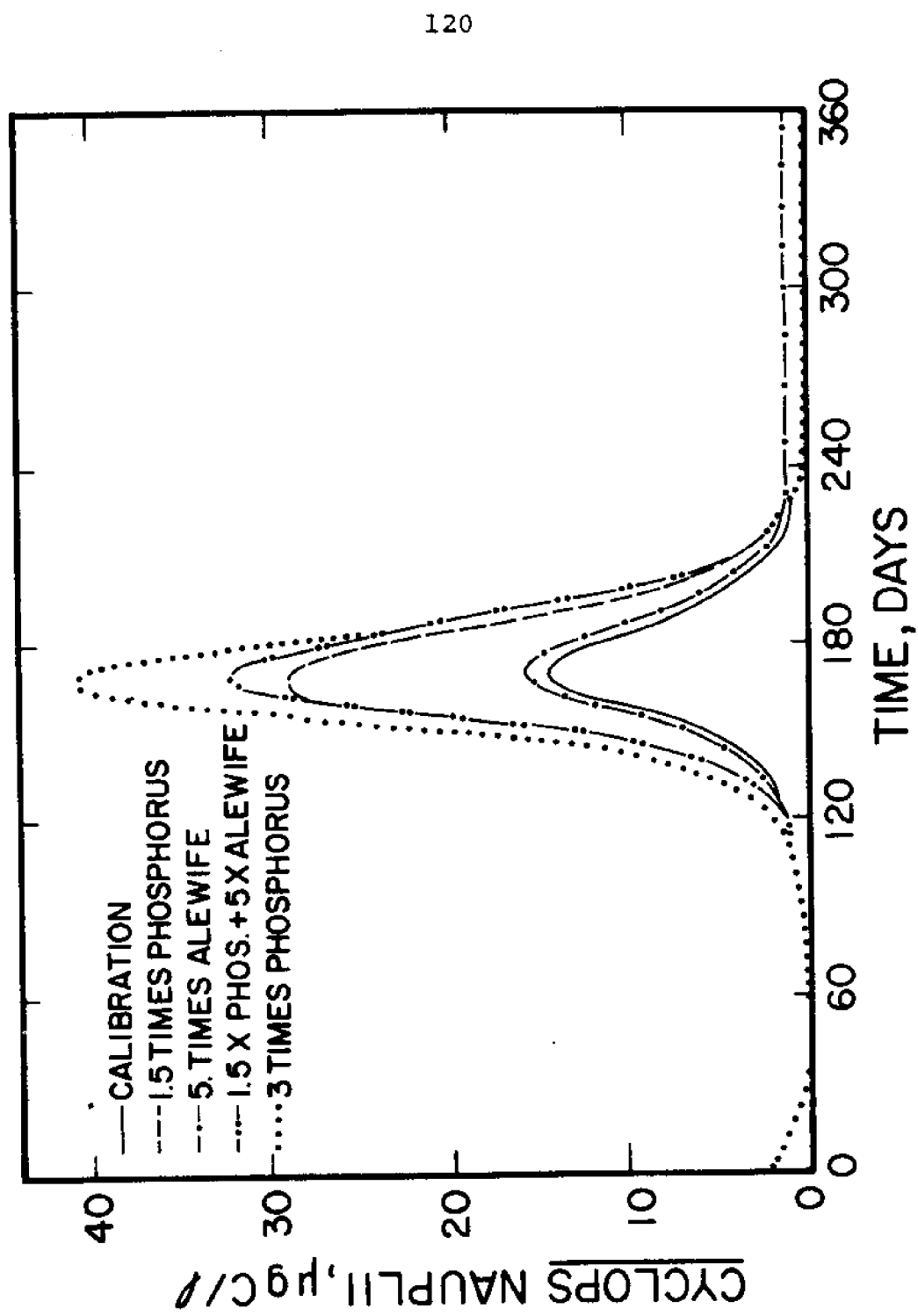


Figure 57. Simulations

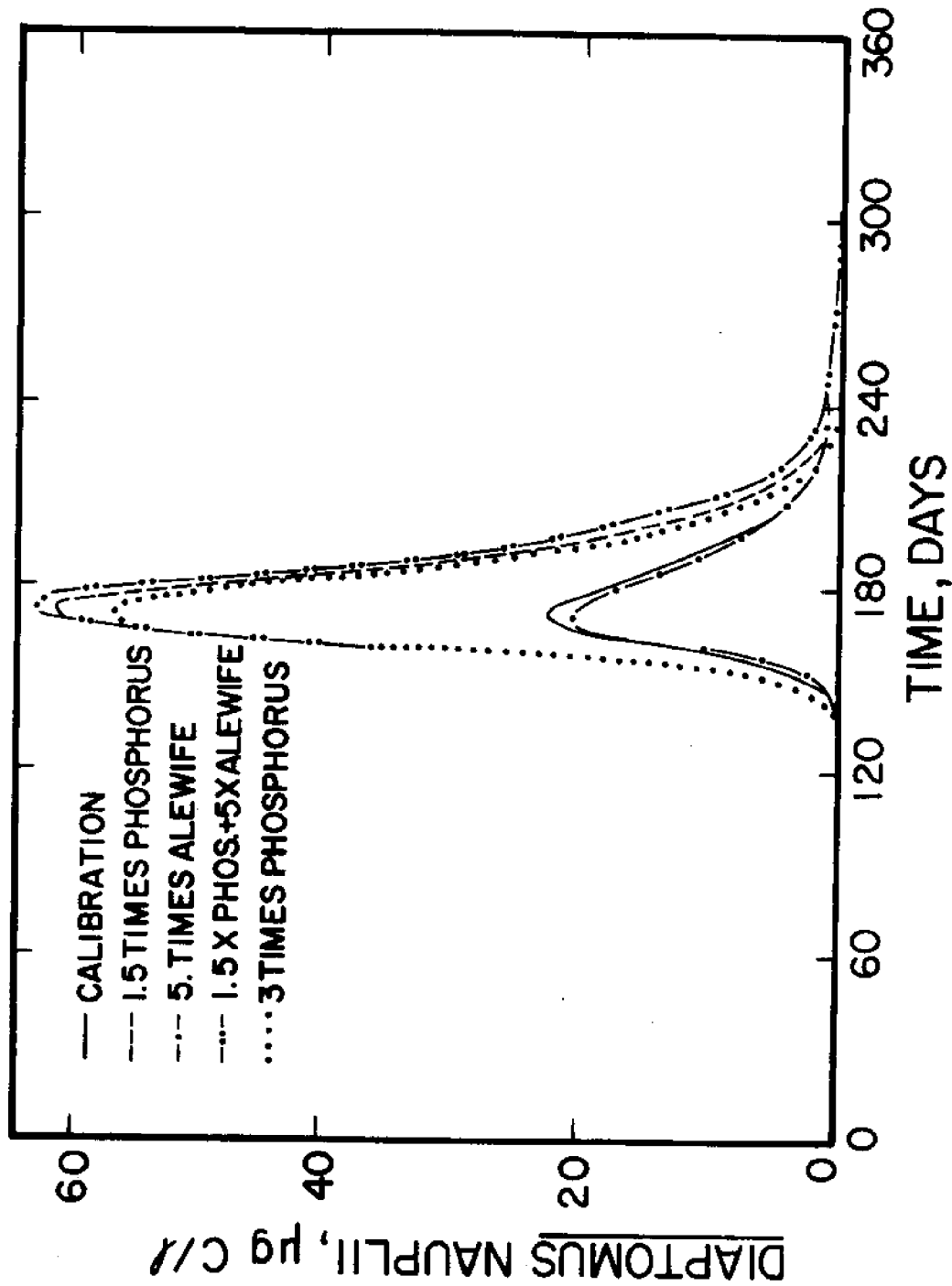


Figure 58. Simulations

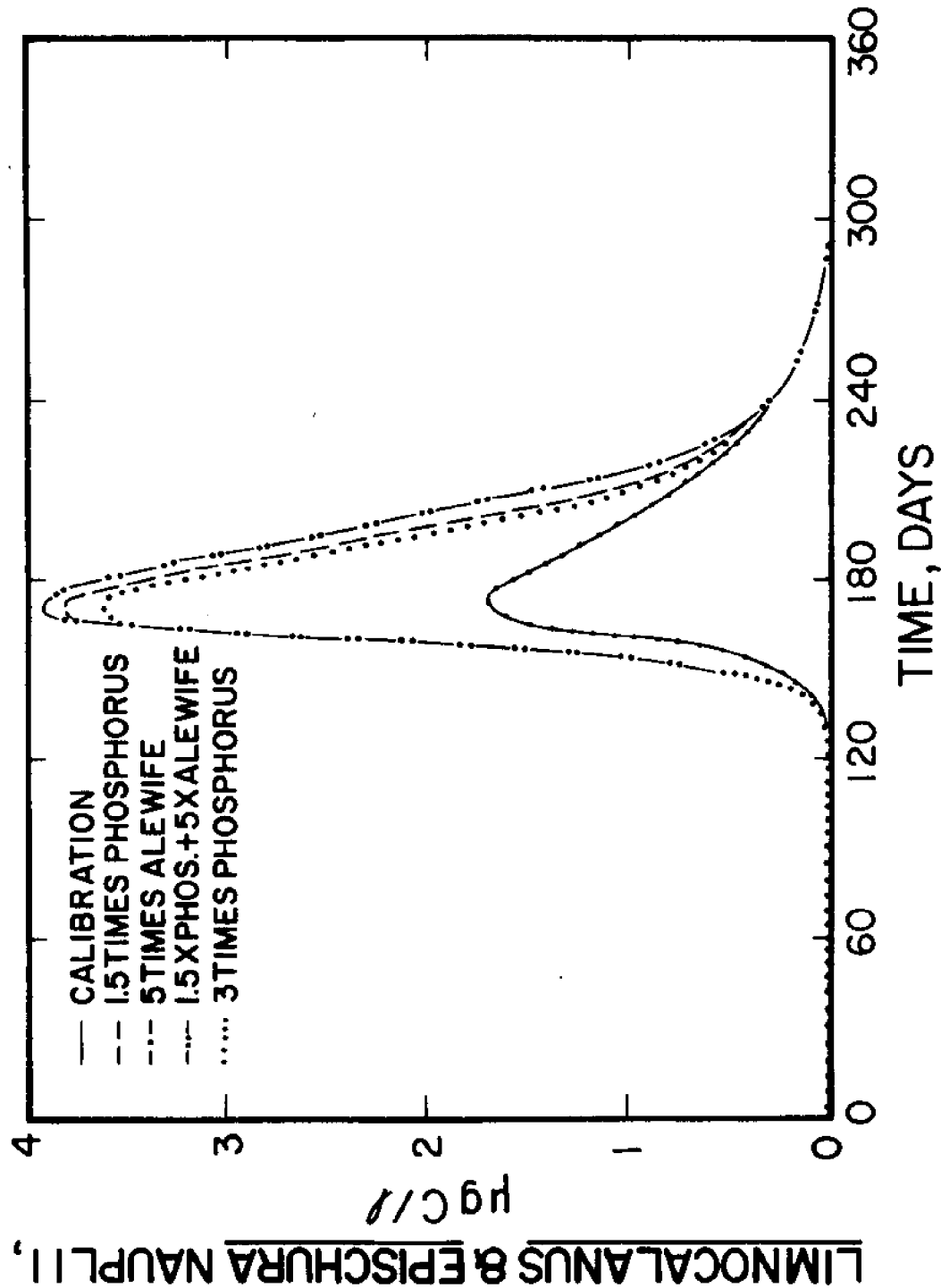


Figure 59. Simulations

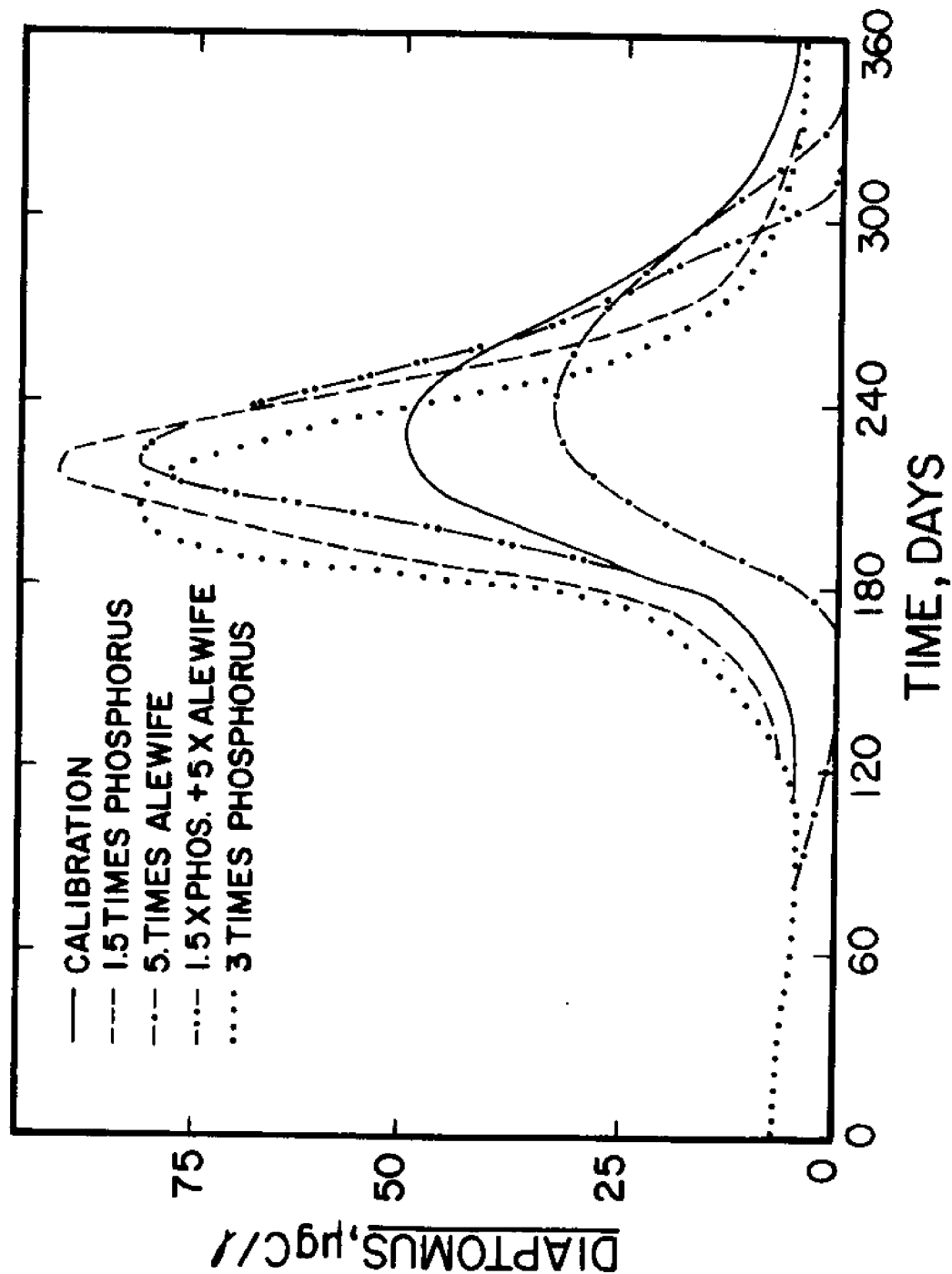


Figure 60. Simulations

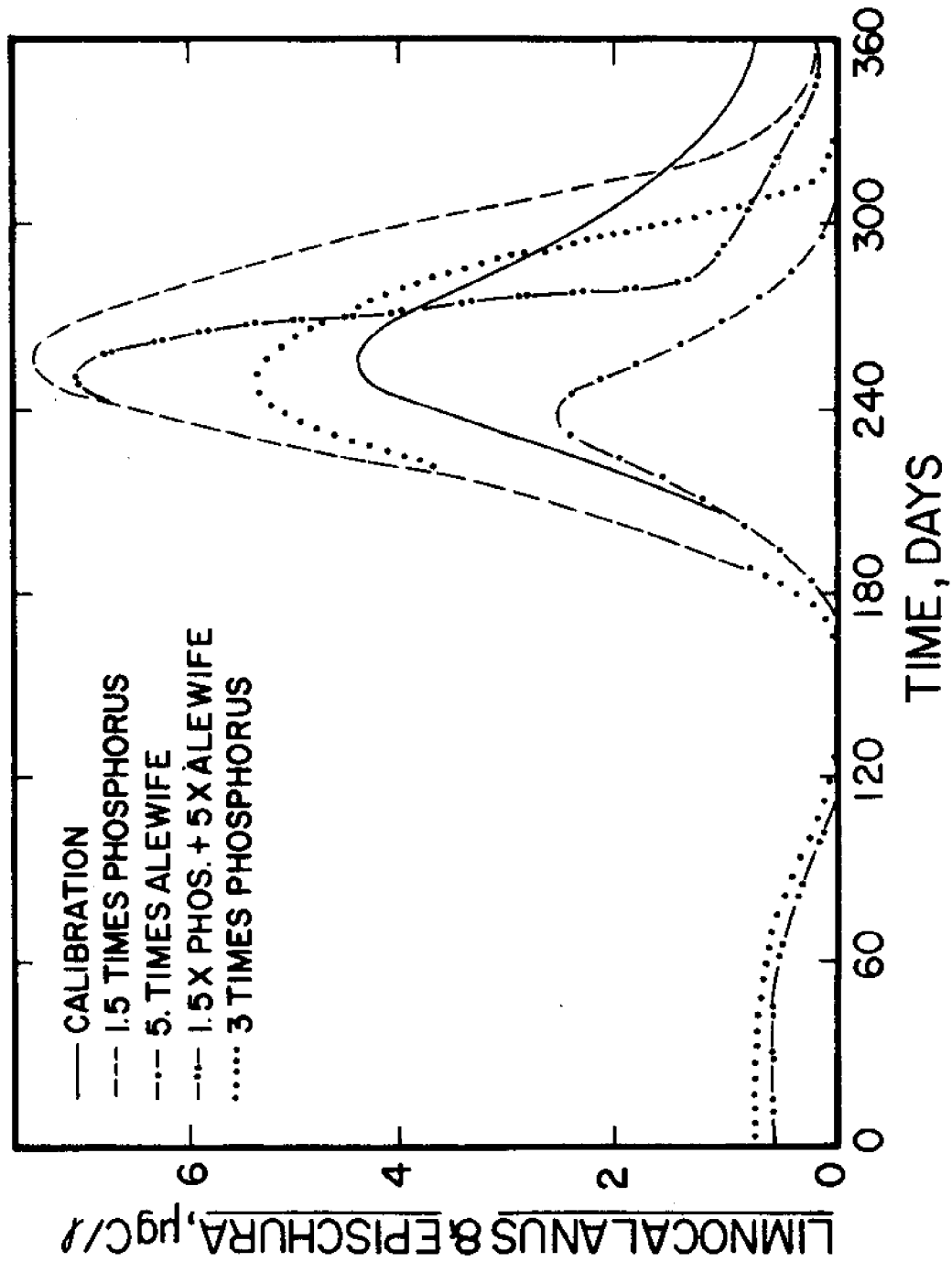


Figure 61. Simulations

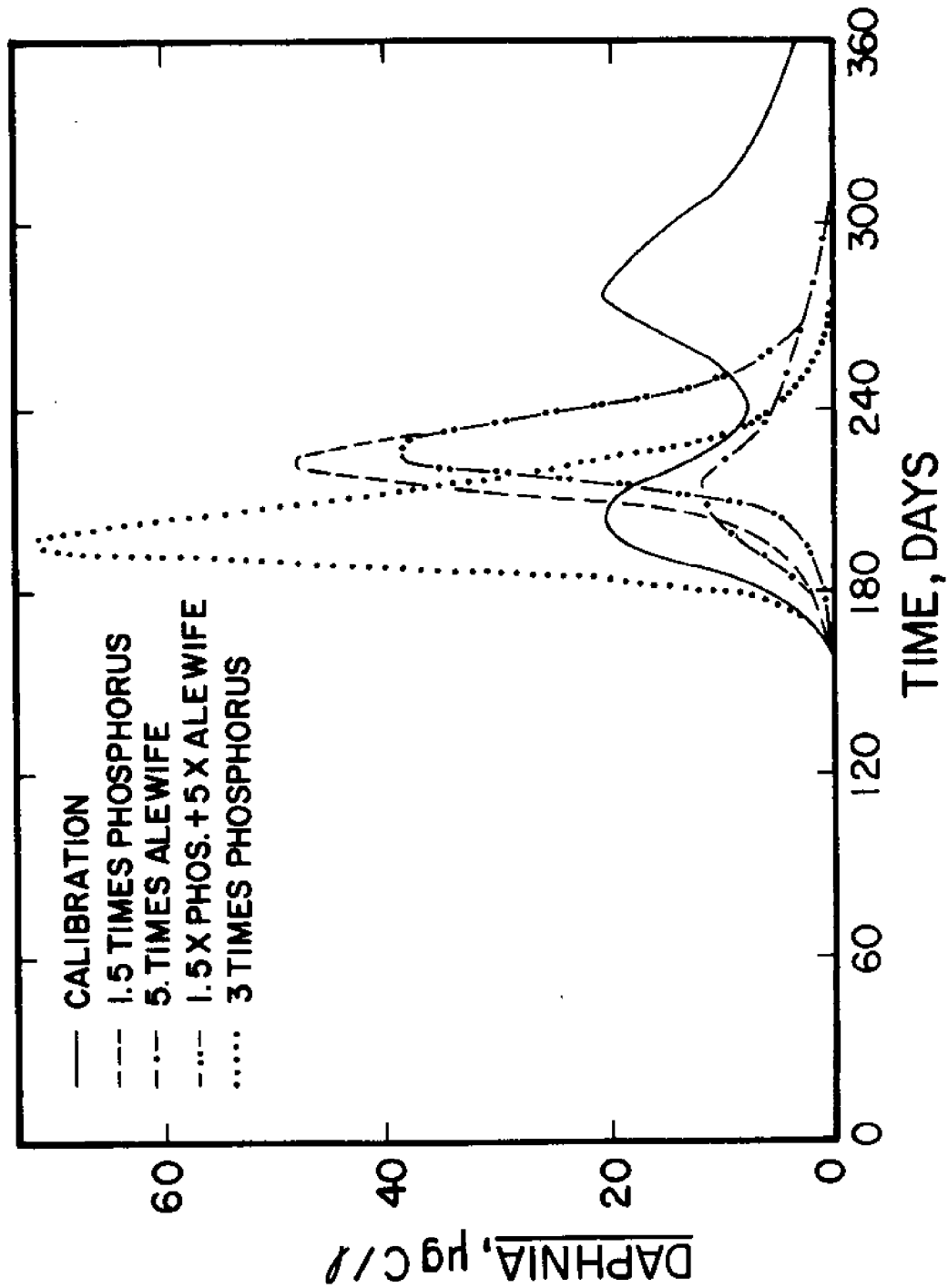


Figure 62. Simulations

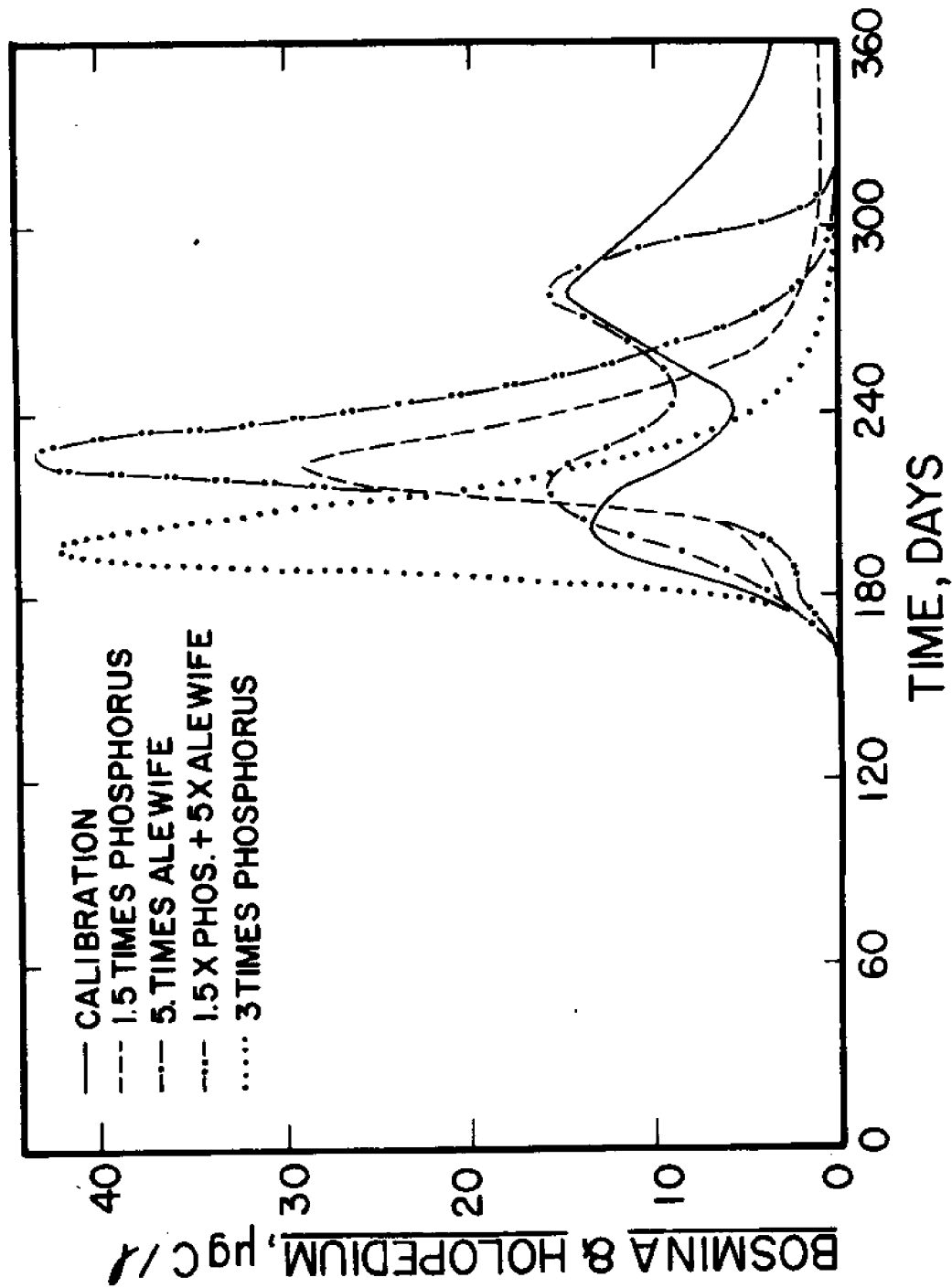


Figure 63. Simulations

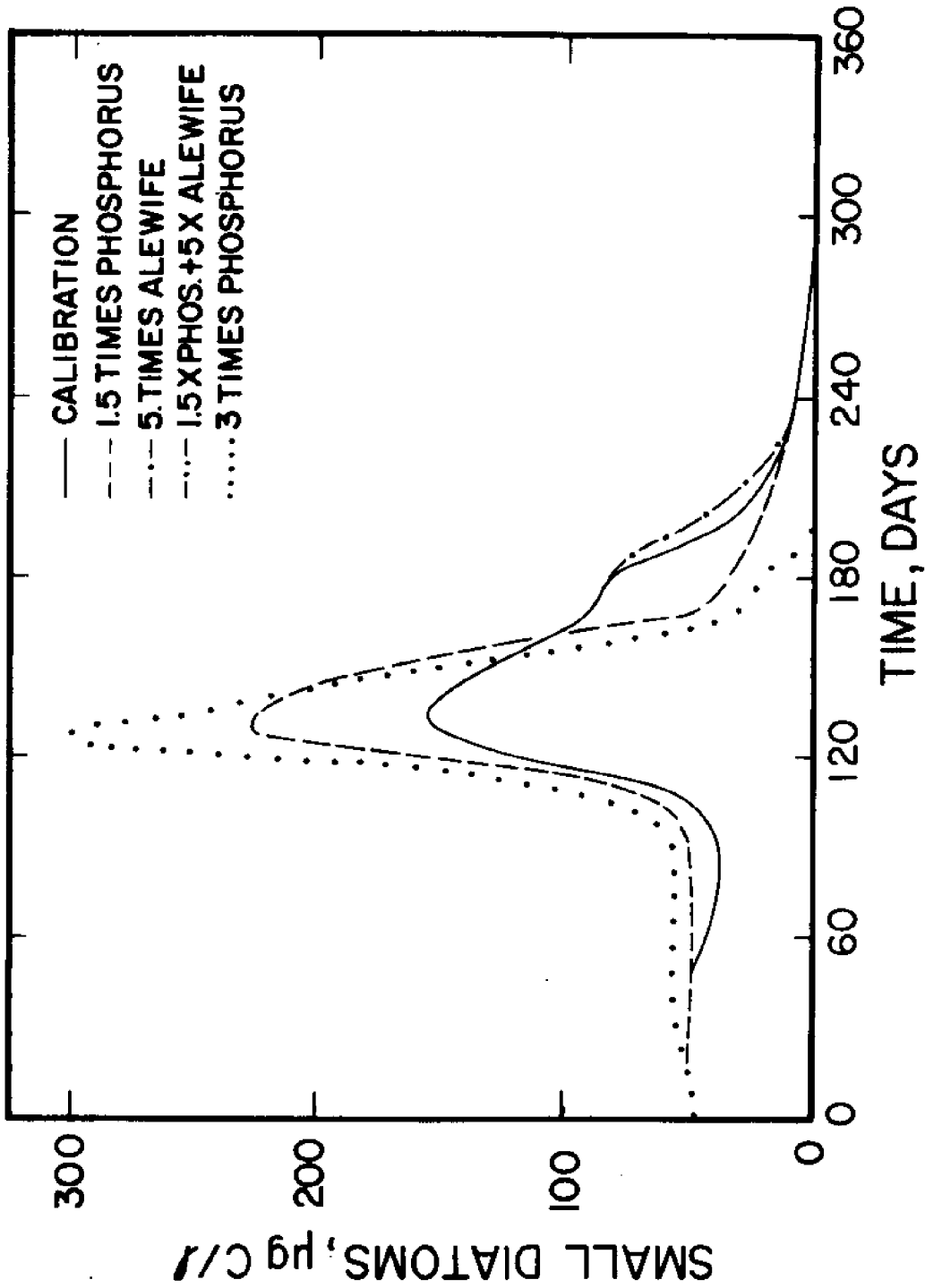


Figure 64. Simulations

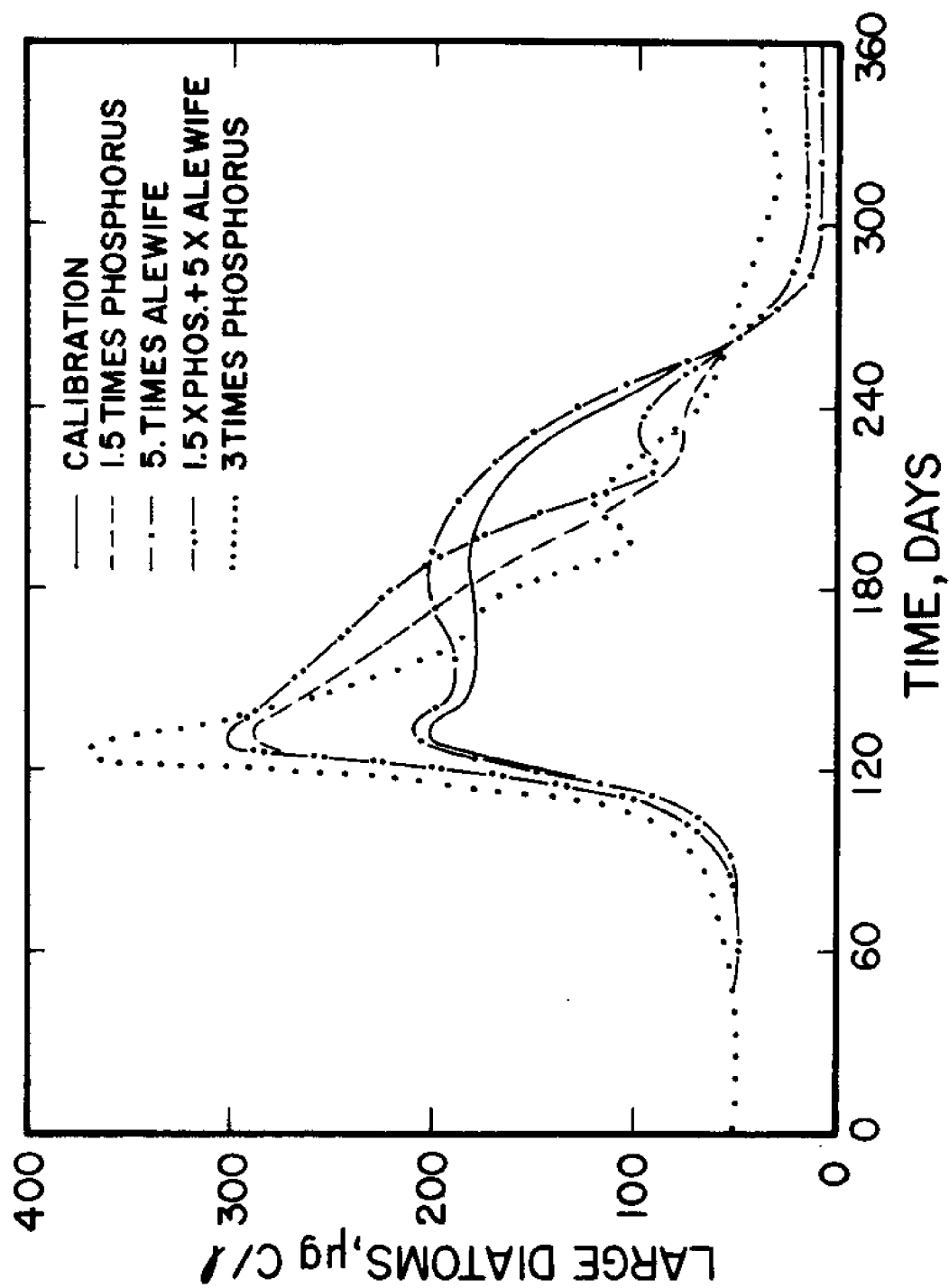


Figure 65. Simulations

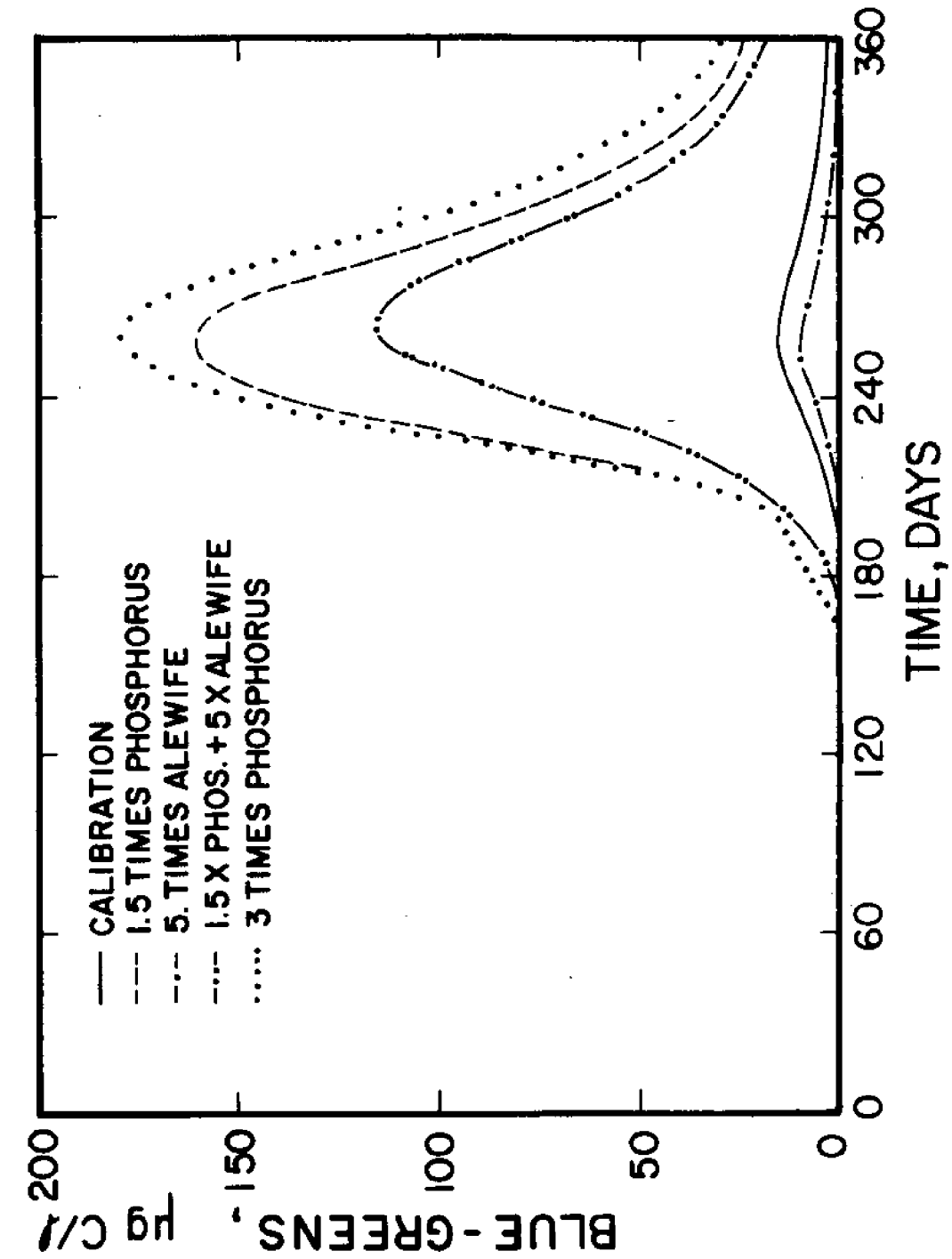


Figure 66. Simulations

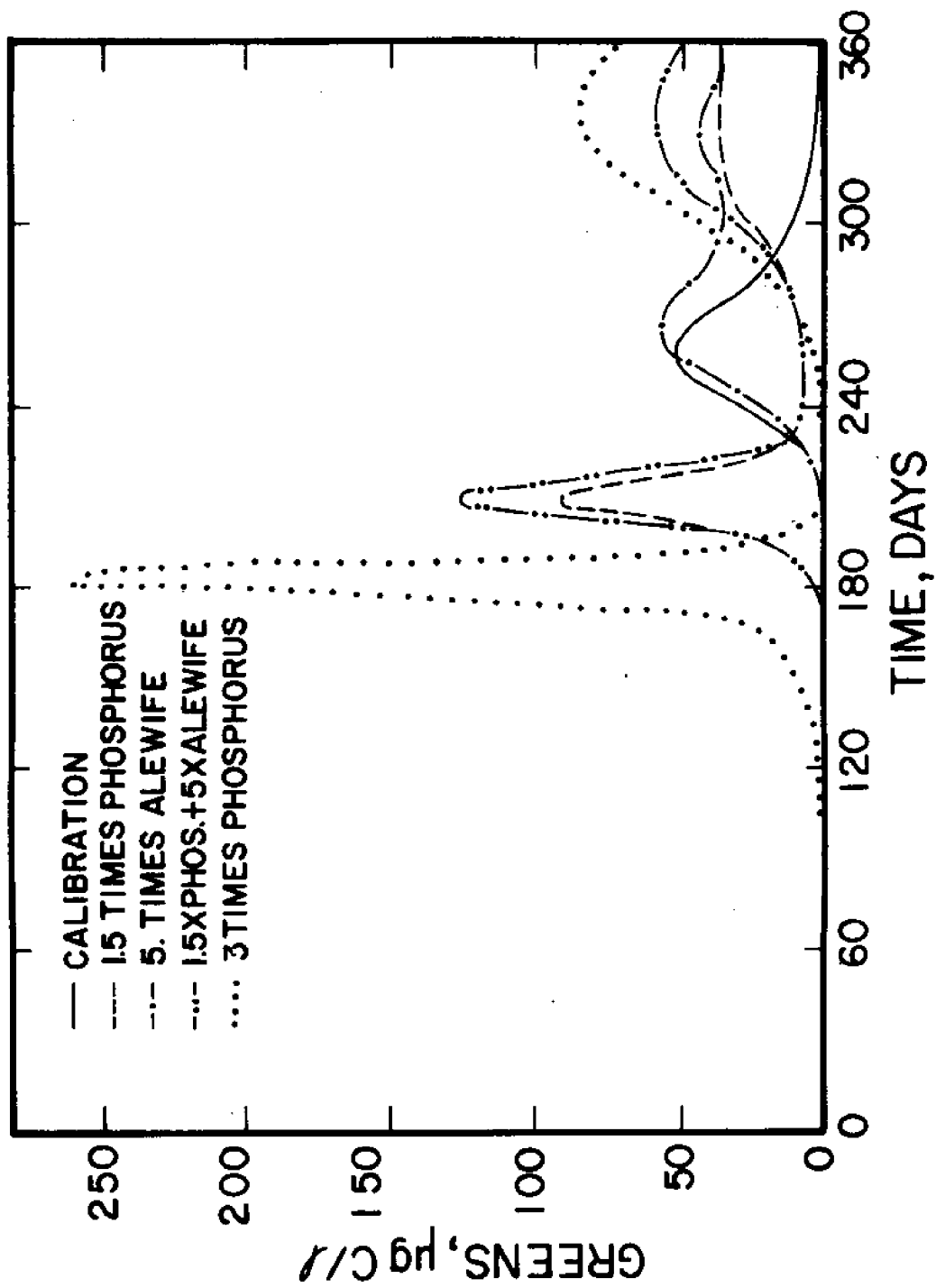


Figure 67. Simulations

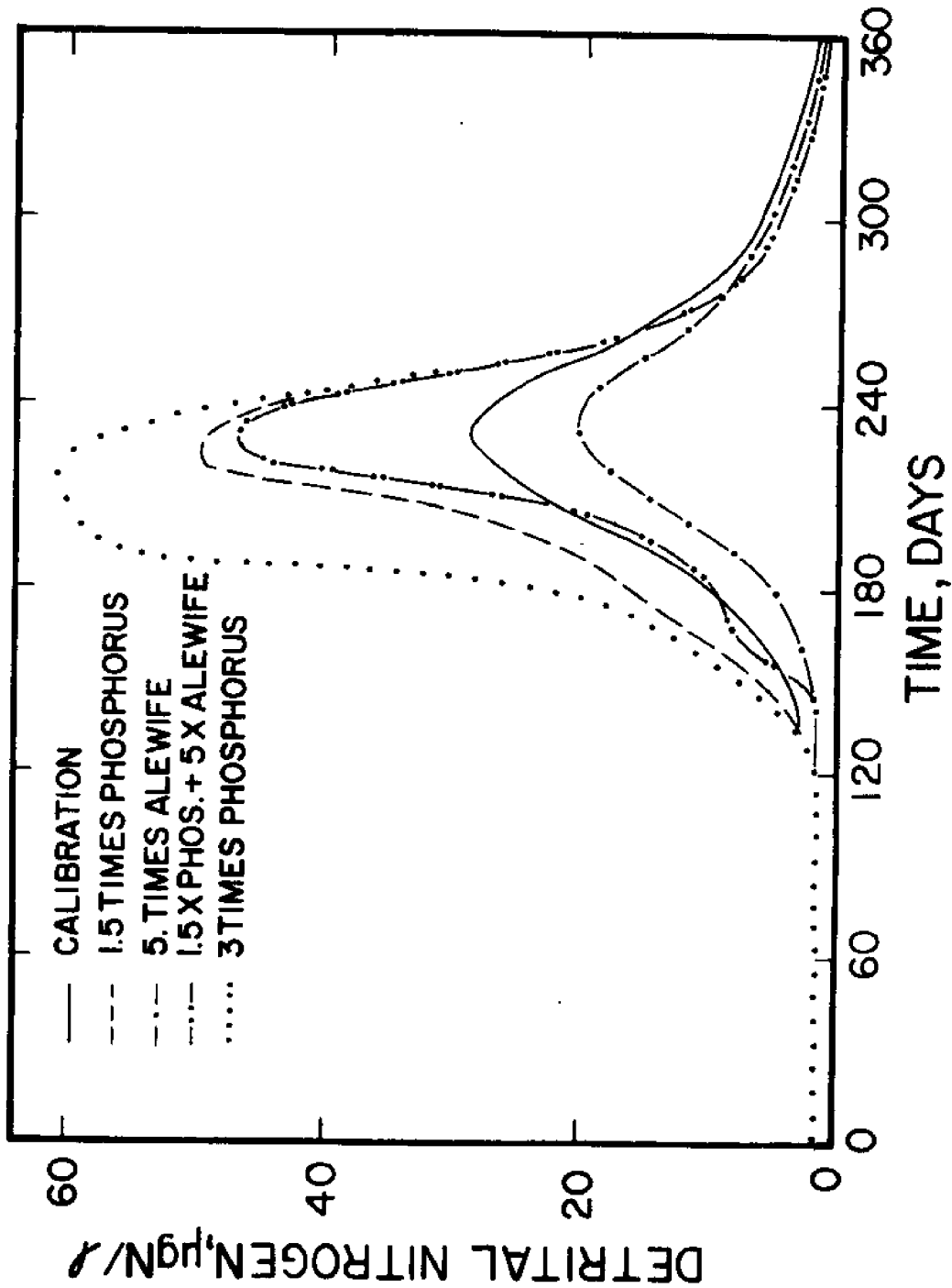


Figure 68. Simulations

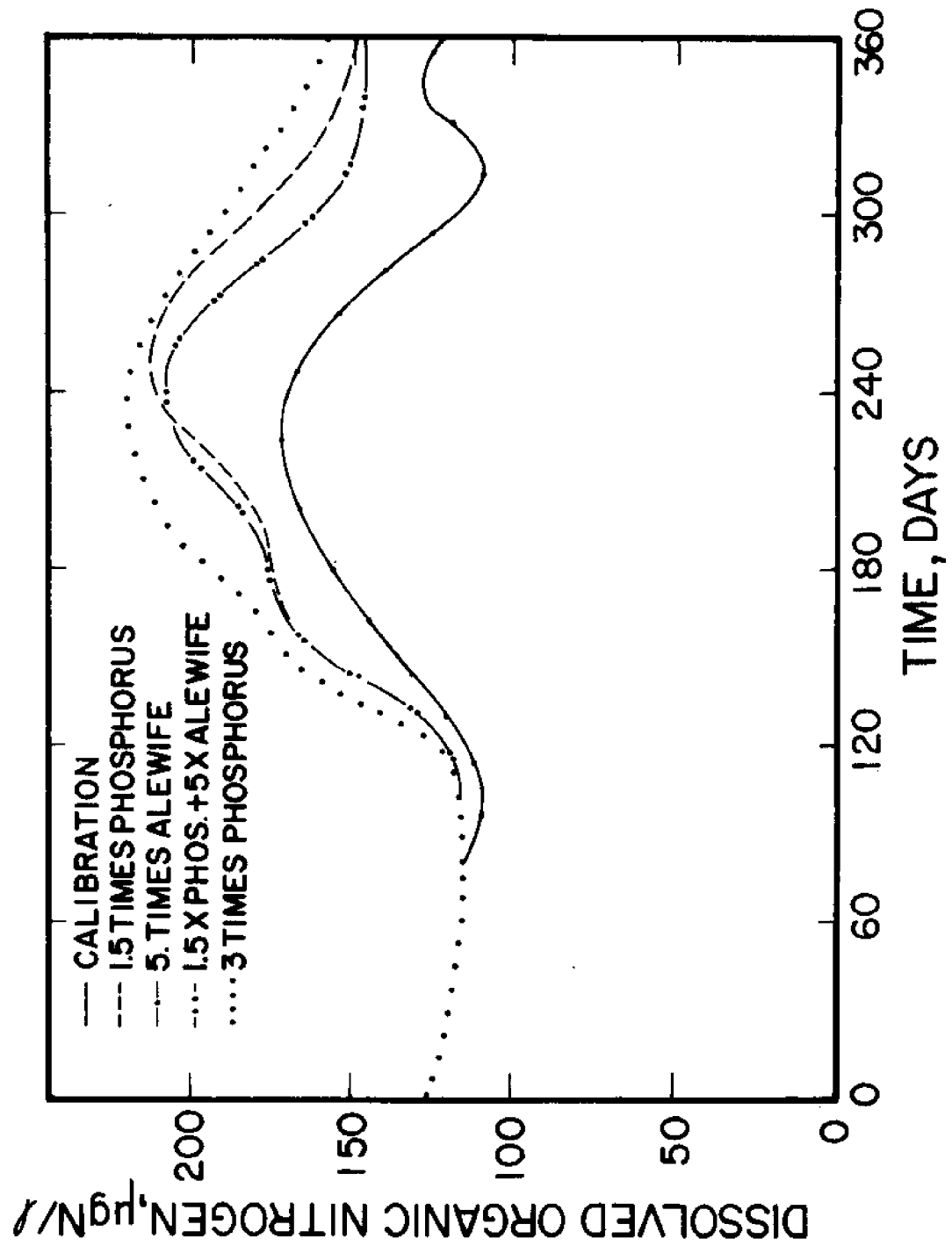


Figure 69. Simulations

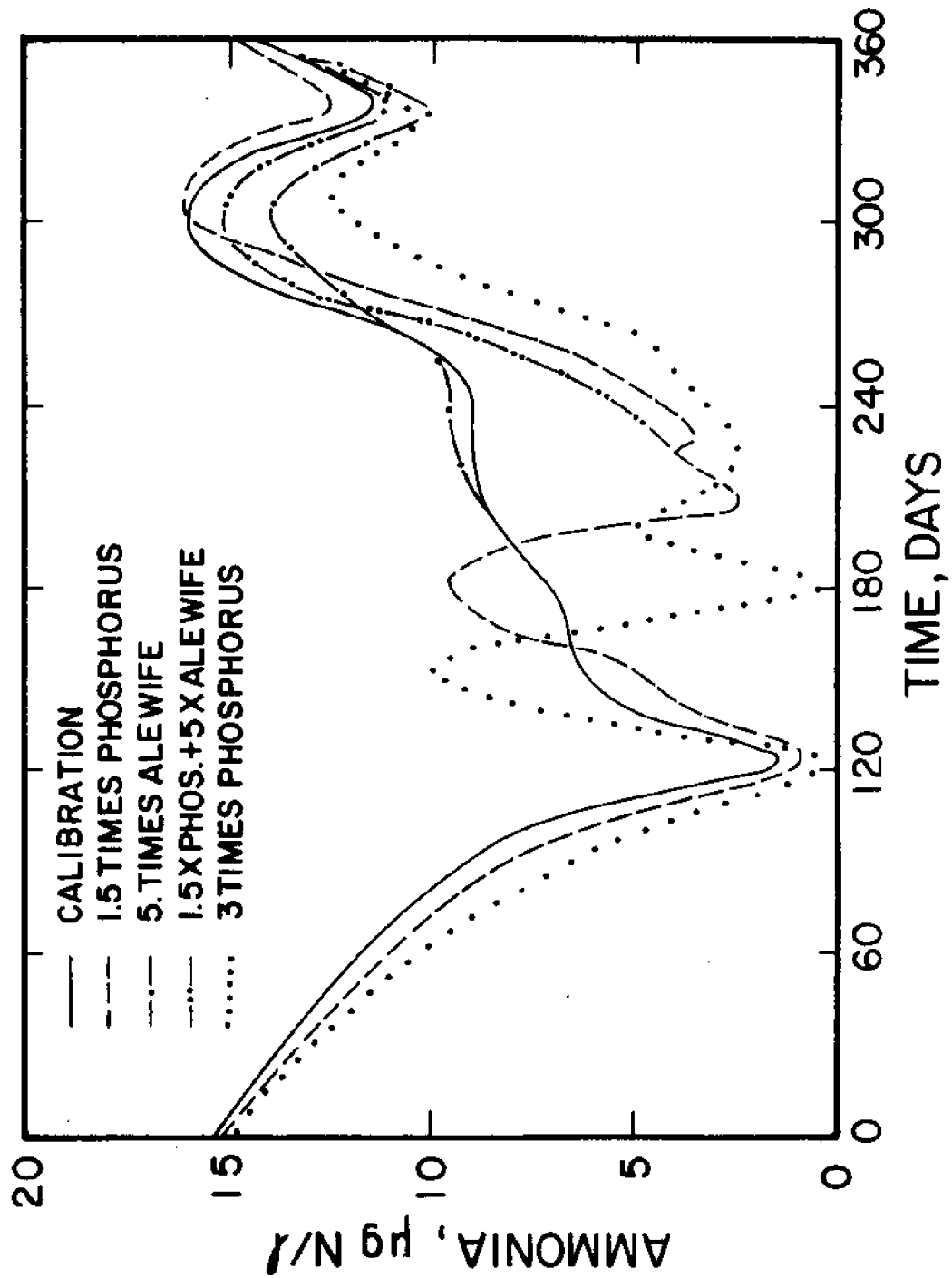


Figure 70. Simulations

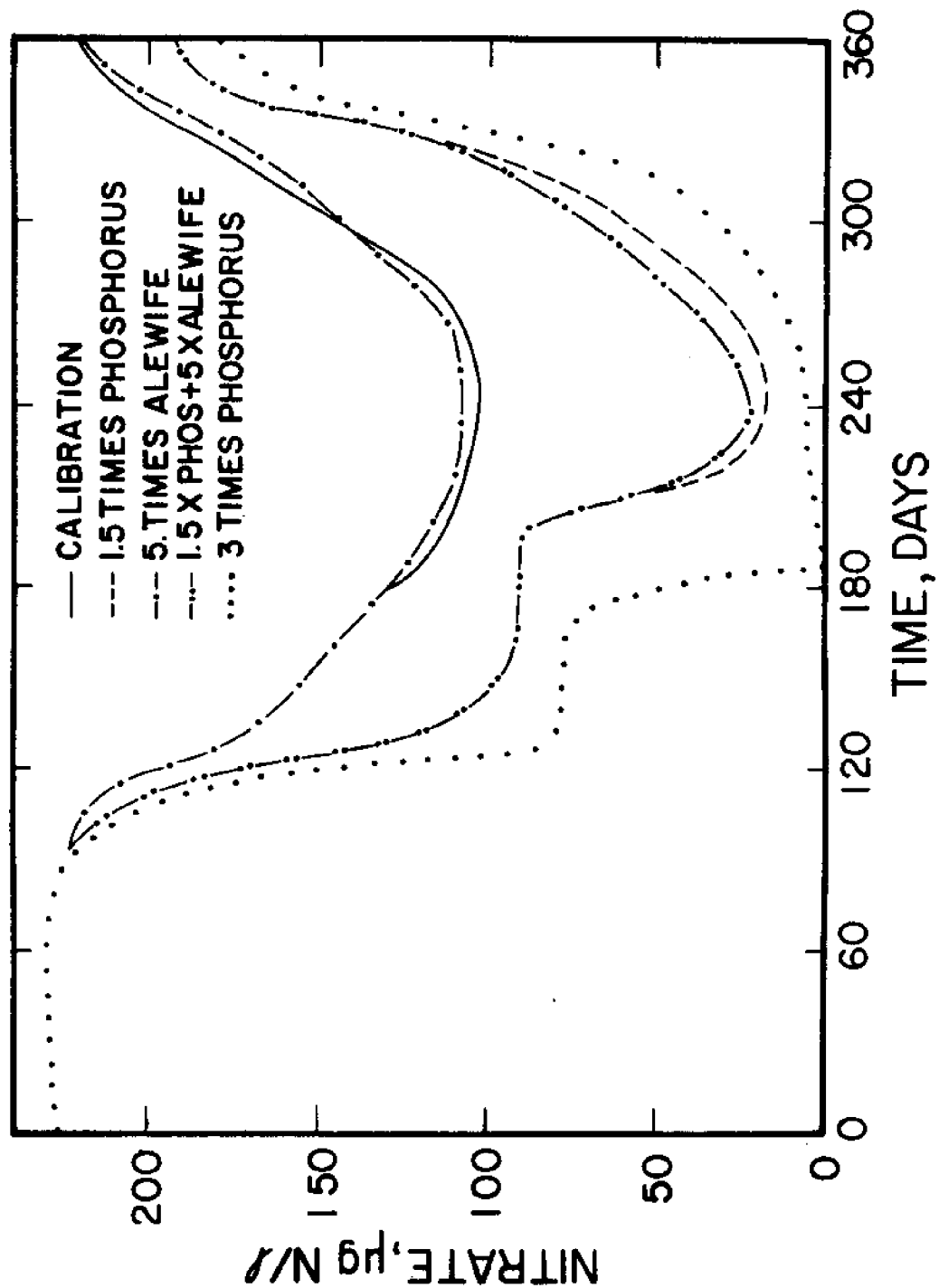


Figure 71. Simulations

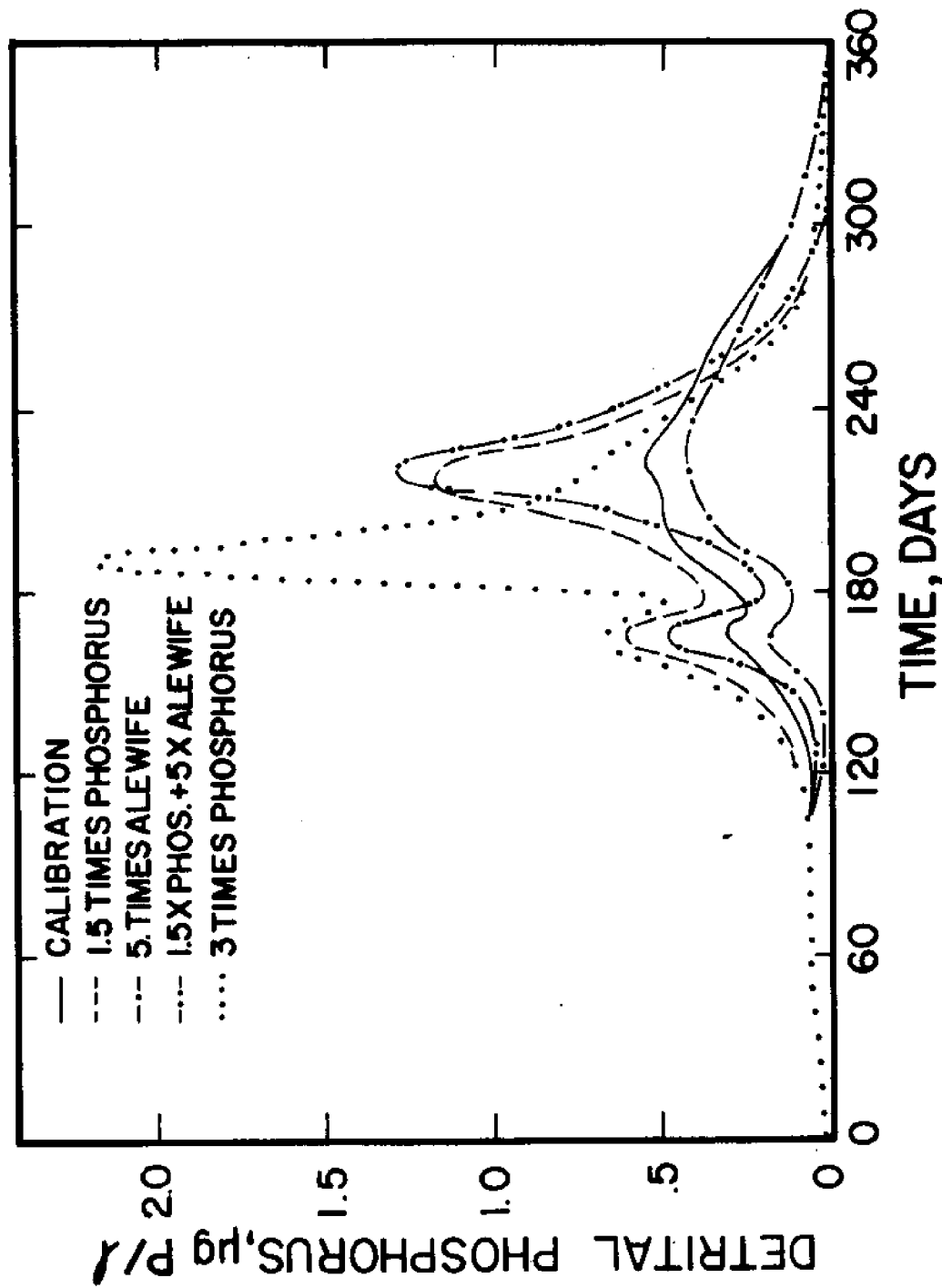


Figure 72. Simulations

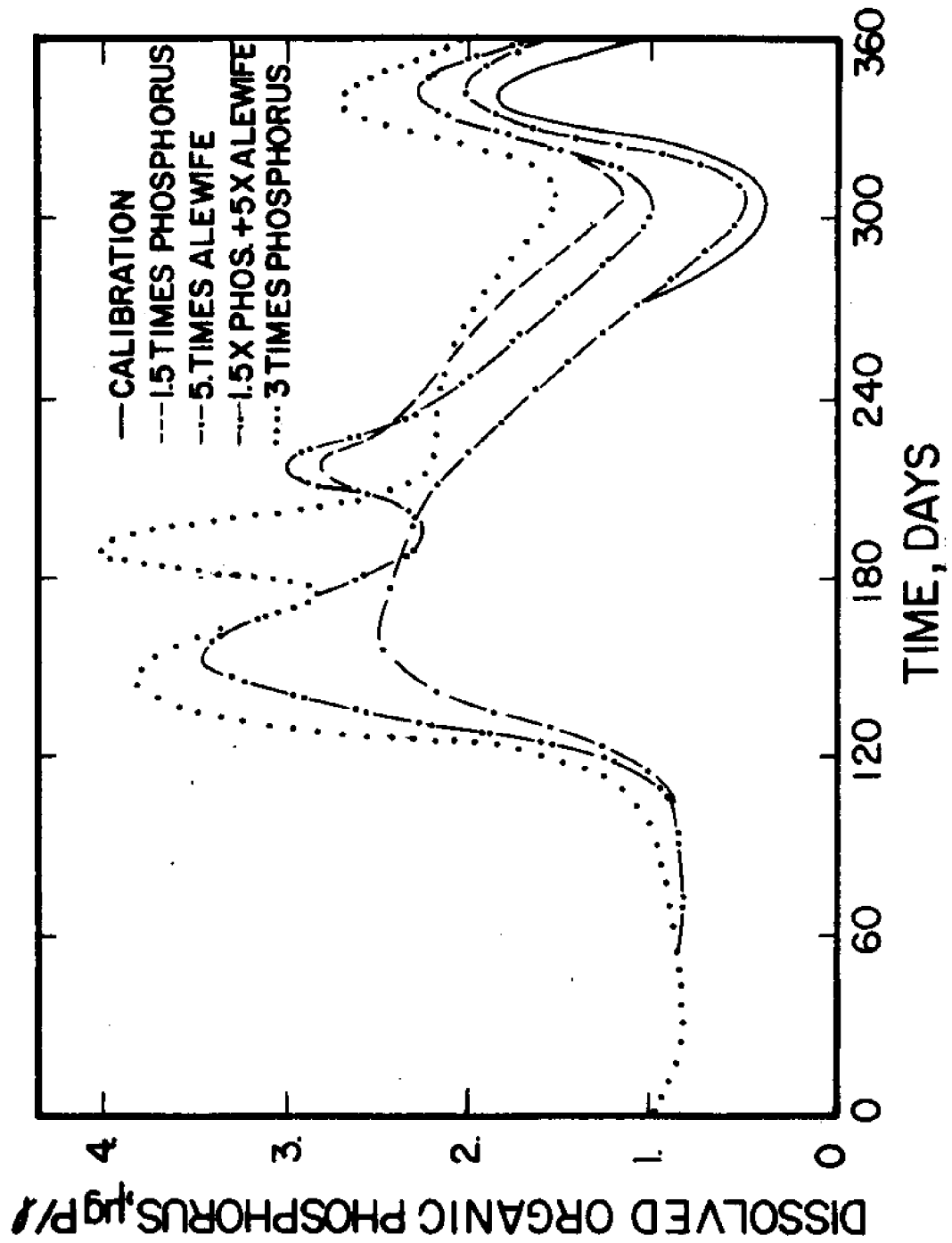


Figure 73. Simulations

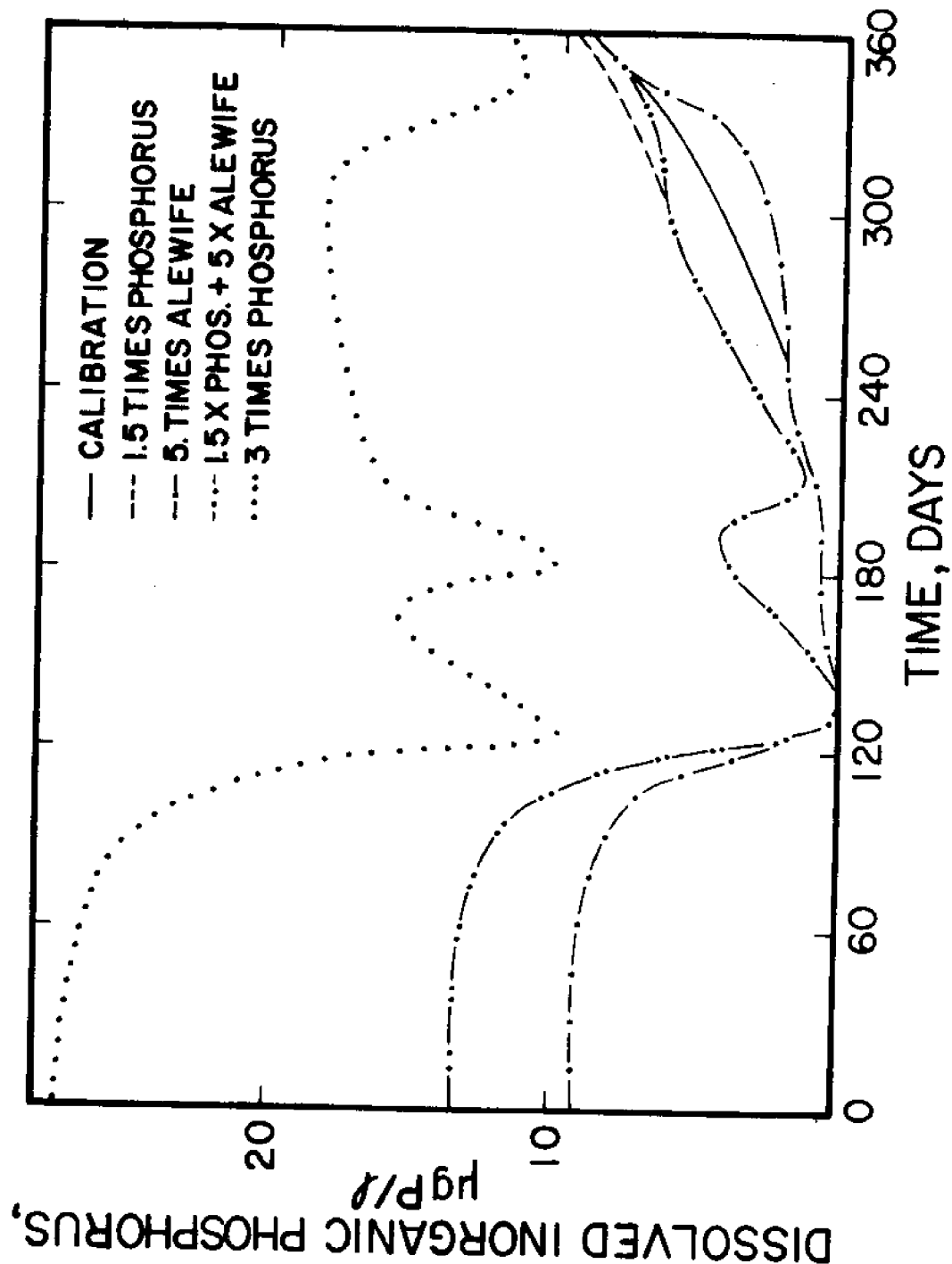


Figure 74. Simulations

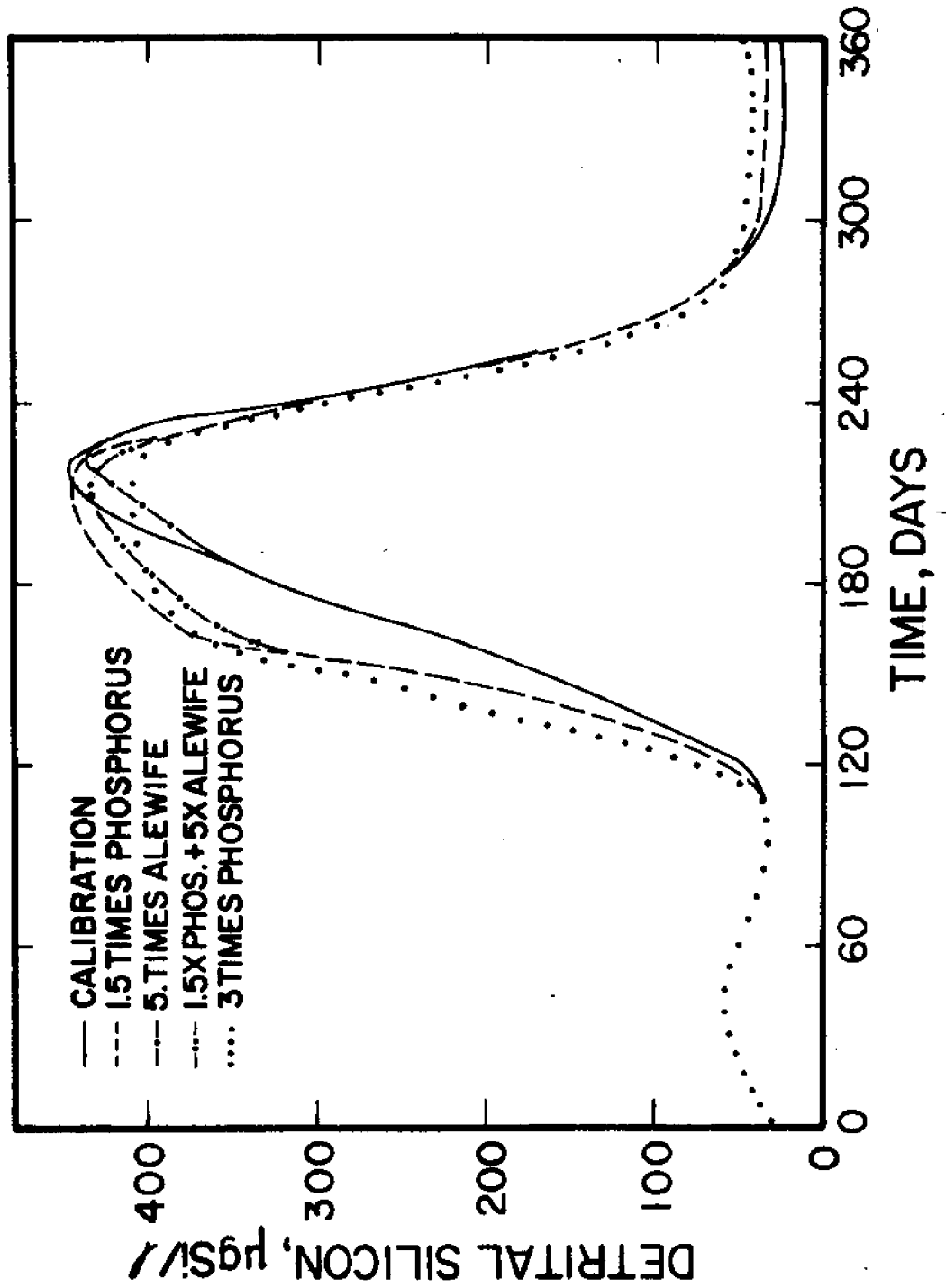


Figure 75. Simulations

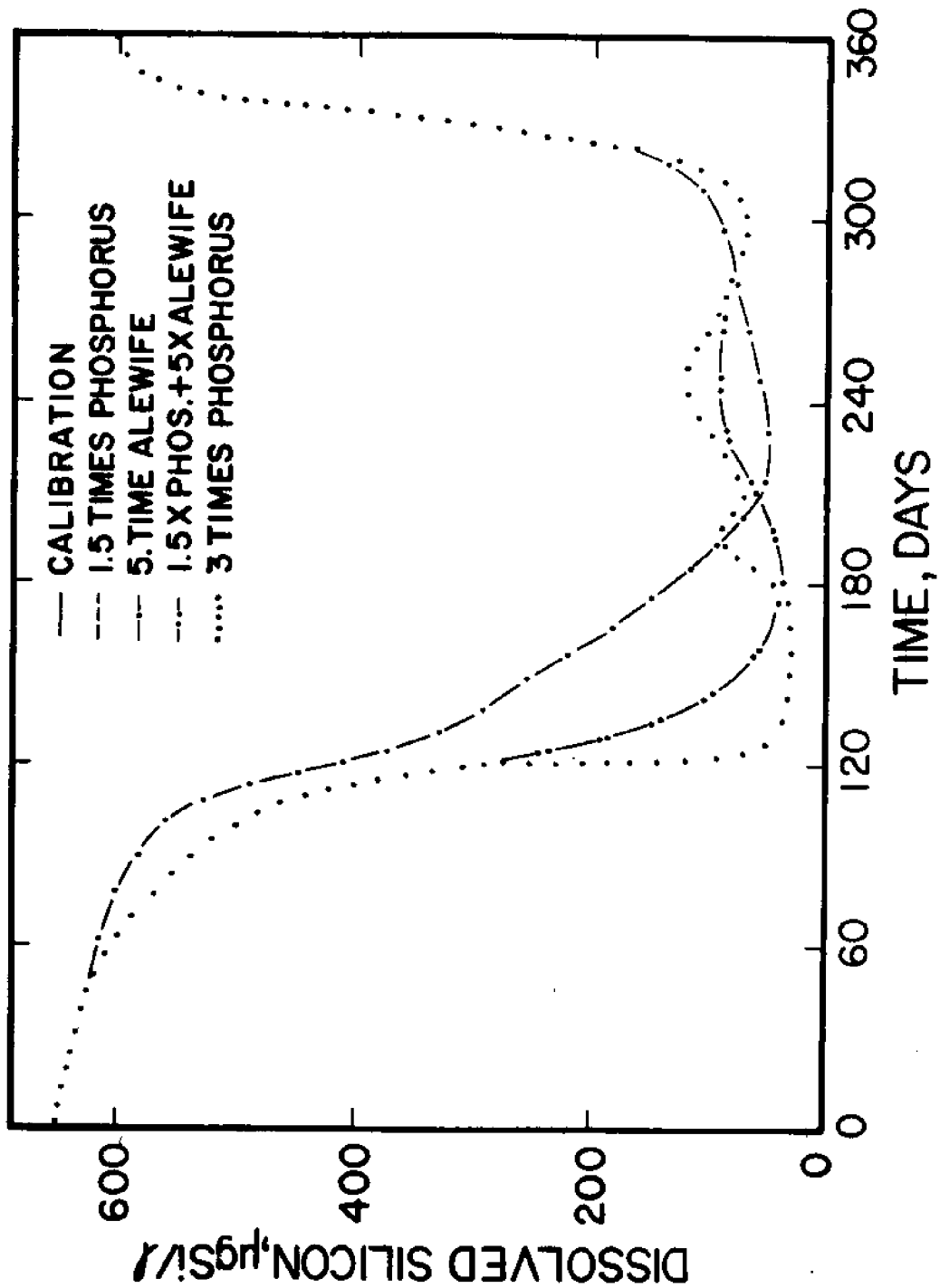


Figure 76. Simulations

Evaluation of Proposed Food Web

The purpose of this section is to re-evaluate and justify the taxonomic detail proposed in the food web model. It is appropriate to re-evaluate the model structure at this point because of the insights gained from the computational experience discussed earlier in this report. An obvious corollary to this issue concerns the success of the chosen taxa at answering the questions for which the model was created. If the goal were to model the effects of minor nutrient additions to an oligotrophic lake, then a model such as that of Canale et.al. (1974) with two plankton states--phytoplankton and zooplankton--may be adequate. However, the problems which the present model has been designed to study are more complex. The questions being addressed concern the restoration of water quality and fisheries production in Lake Michigan.

Division of phytoplankton into diatoms and non-diatoms to account for silicon requirements was discussed earlier in the report. Because green algae, in general, are grazed upon by zooplankton and blue-greens are not, separation is necessary in models of an aquatic system which is affected by a long-term increase in trophic condition. Therefore, questions concerning the effect of eutrophication may require a tripartite division of the phytoplankton. The further division of the diatoms in the present version of the model is justified only if zooplankton are divided into more than two groups.

A comprehensive model for Lake Michigan might also separate the blue-green algae into nitrogen-fixers and non-fixers since nitrogen limitation exists in some regions of the lake (Vanderhoff, et al. 1974). Flagellates are another taxon which might be added, since they appear to require high nutrient levels and may exhibit certain heterotrophic characteristics. These capabilities would be essential in certain areas of the Great Lakes such as Saginaw Bay, where flagellates become the dominant summer algae.

In summary, three of the four algal groups presently in the model appear to represent a valid use of taxonomic units in modeling biological productivity responses to eutrophication. At least two more groups would be added to the model to treat highly eutrophic environments. The separation of diatoms into two size classes is probably not justified on the basis of studying eutrophication alone. Justification for this division is based upon division of the zooplankton by taxa.

While separation of the phytoplankton by taxa is easy to

justify on the basis of estimating productivity caused by increased eutrophication, separation of the zooplankton by taxa is more difficult to justify. Indeed if the model were seeking to answer only questions concerning eutrophication, only two groups of zooplankton would be necessary, predatory and herbivorous. Division of the zooplankton into two groups in a eutrophication model is desirable because the predators reduce the grazing of herbivores upon the phytoplankton. A eutrophication model including three phytoplankton states, the herbivorous zooplankton, and the predatory zooplankton has the virtue of being easy to handle and of simulating critical plankton interactions under increased eutrophication.

However, there are two difficulties with such a model. First, omnivorous zooplankton occur in Lake Michigan. The addition of a third zooplankton state as shown in Figure 77 must therefore be recommended. The figure illustrates the interactions in such a simplified food web model. A second problem with the simplified model concerns the fact that the forage fish of Lake Michigan, particularly the alewife, graze upon the zooplankton differentially. Alewives are size-selective. Whereas all the predators are large enough to be eaten, the omnivores and herbivores are not. Thus a realistic model would have to provide for a division based on forage-fish predation.

A final complication in the food web arises because the alewife prefers cladocerans over copepods. Therefore, the small herbivores must be divided into cladocerans and copepods. The cannibalism of Cyclops, a small omnivore, requires further division of the small herbivorous copepods into Diaptomus and the nauplii. The above division of zooplankton leads to the model proposed herein with assignment of taxonomic names to the six types of zooplankton: (1) Predators = Leptodora, Polyphemus, and Mesocyclops; (2) Large Omnivores = Limnocalanus, Epischura, and Senecilla; (3) Small Omnivores = Cyclops; (4) Large Herbivorous Cladocerans = Daphnia and Diaphanosoma; (5) Small Herbivorous Copepods = Diaptomus and Eurytemora; (6) the nauplii; and (7) Small Herbivorous Cladocerans = Bosmina, Holopedium, Ceriodaphnia, and the chydorids (see Figure 78).

The zooplankton interactions in the model could be extended to include rotifers. Separation of the diatoms into large and small forms is justified by the presence of different zooplankton herbivores. As the model is presently organized, only the omnivores and herbivorous copepods can graze upon the large diatoms.

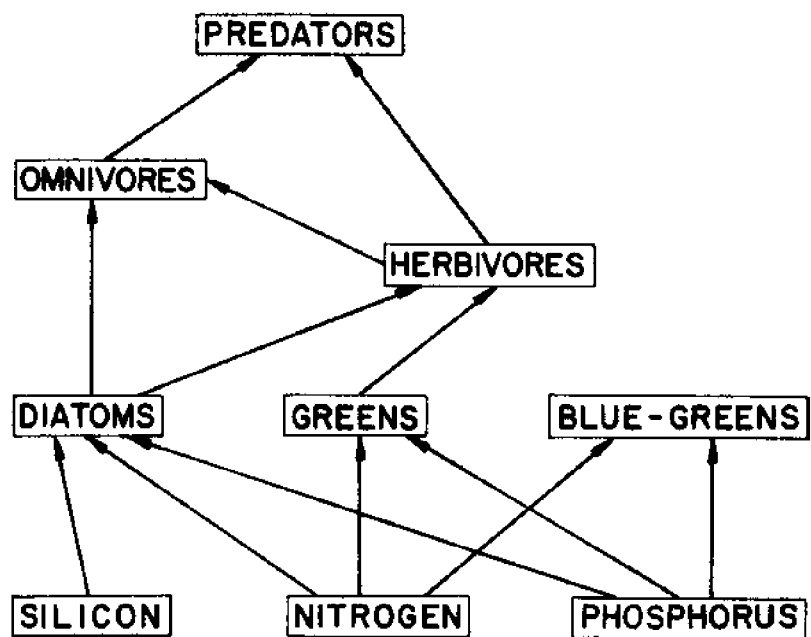


Figure 77. Simple Food Web

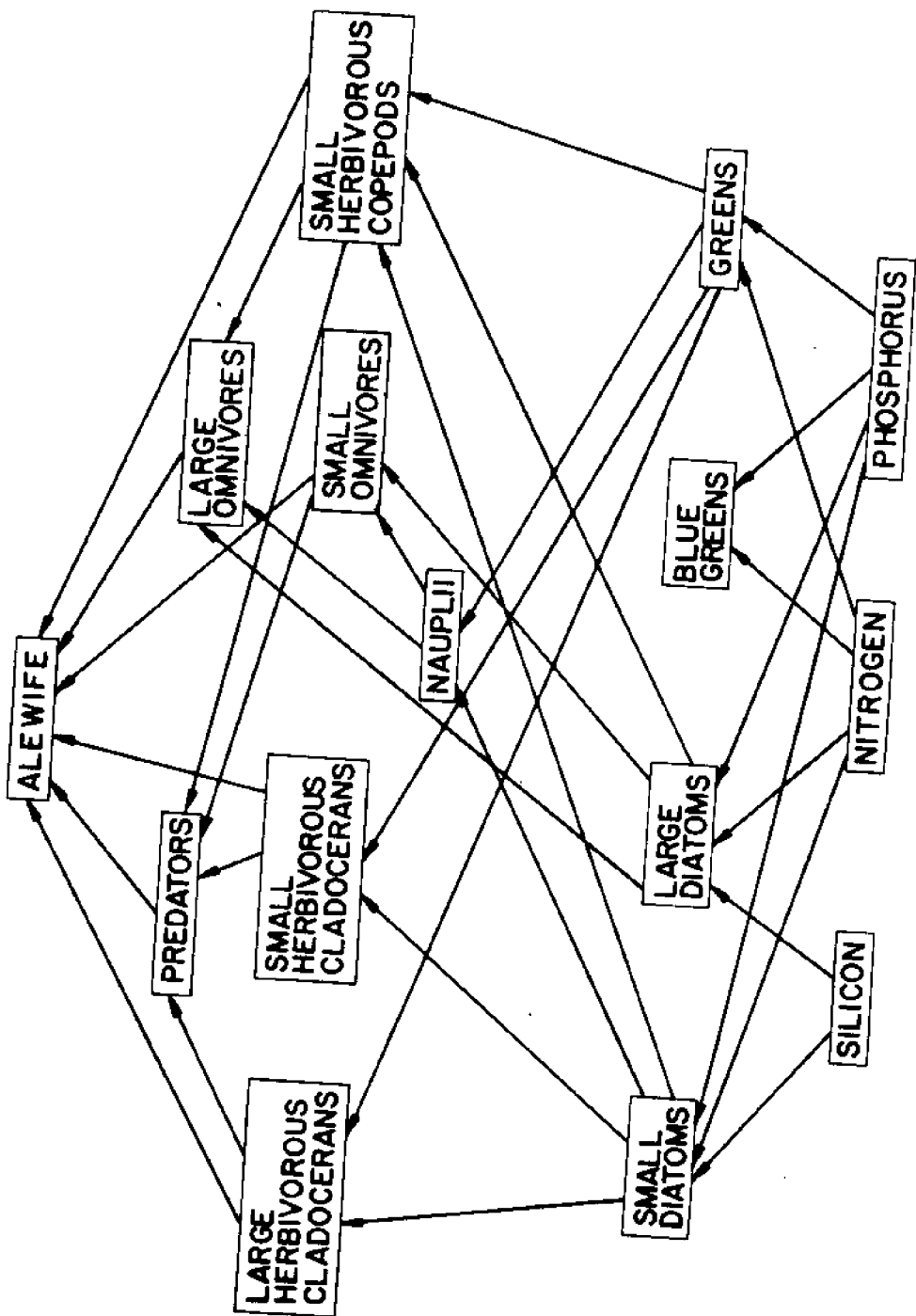


Figure 78. Complex Food Web

## REFERENCES

Anderson, R.S. 1970a. "Predator-prey relationships and predation rates for crustacean zooplankters from some lakes in western Canada." Can. J. Zool. 48:1229-1240.

Anderson, R.S. 1970b. "Effects of rotenone on zooplankton communities and a study of their recovery patterns in two mountain lakes in Alberta." J. Fish. Res. Bd. Canada. 27:1335-1356.

Armstrong, F.A.J. 1965. "Silica." in Chemical Oceanography, ed. J.P. Riley and G. Skirrow Pp. 409-432.

Arnold, D.E. 1971. "Ingestion, assimilation, survival, and reproduction by Daphnia pulex fed seven species of blue-green algae." Limnol. Oceanogr. 16:906-920.

Auer, N.A. 1974. Nitrogen Utilization by the Algae: A Review. Unpublished report to University of Michigan Sea Grant Program. 30 pages.

Ayers, J.C. 1970. Lake Michigan Environmental Survey. Great Lakes Res. Div., Spec. Rep. No. 49, The University of Michigan, Ann Arbor. 109 pages.

Azad, H.S., and J.S. Borchardt. 1970 "Variations in phosphorus uptake by algae." Environmental Science and Technology. 4:737-743.

Bierman, V.J. Jr., F.H. Verhoff, T.L. Paulson, and M.W. Tenney, 1973. "Multi-nutrient dynamics models of algal growth and species competition in eutrophic lakes." in Modeling the Eutrophication Process, ed. E. J. Middlebrooks, D. H. Falkenborg and T. E. Maloney. Pp. 89-109.

Brooks, J.L. 1969. "Eutrophication and changes in the composition of the zooplankton." In Eutrophication: Causes, Consequences, Correctives. NAS Symposium Proceedings. Pp. 236-255.

Brown, E.H., Jr. 1972. "Population biology of alewives, Alosa pseudoharengus in Lake Michigan, 1949-70," J. Fish. Res. Bd. Canada. 29: 477-500.

Burns, C.W. 1969. "Relation between filtering rate, temperature, and body size in four species of Daphnia." Limnol. Oceanogr. 14:693-700.

Burns, C.W. and F. H. Rigler. 1967. "Comparison of filtering rates of Daphnia rosea in lake water and in suspensions of yeast." Limnol. Oceanogr. 12:492-502.

Burns, N.W., and A.E. Pashley. 1974. "In-situ measurement of the settling velocity profile of particulate organic carbon in Lake Ontario." J. Fish. Res. Bd. Canada. 31:291-297.

Canale, R.P., D.J. Hineman, and S. Nachiappan. 1974. A Biological Production Model for Grand Traverse Bay. Sea Grant Technical Report No. 37, The University of Michigan, Ann Arbor. 115 pages.

Canale, R.P., and A.H. Vogel, 1974. "The effects of temperature on phytoplankton growth." ASCE. J. Environmental Eng. Div. 100 (EE1):231-241.

Colby, P.J. 1971. "Alewife dieoffs; why do they occur?" Limnos 4:18-27.

Comita, G.W. 1956. "A study of calanoid copepod population in an Arctic lake." Ecol. 37:576-591.

Confer, J.L. 1971. "Intrazooplankton predation by Mesocyclops edax at natural prey densities." Limnol. Oceanogr. 16:663-666.

Conover, R.J. 1959. "Regional and seasonal variation in the respiratory rate of marine copepods." Limnol. Oceanogr. 4:259-268.

Conover, R.J. 1966a. "Assimilation of organic matter by zooplankton." Limnol. Oceanogr. 11:338-345.

Conover, R.J. 1966b. "Factors affecting the assimilation of organic matter by zooplankton and the question of superfluous feeding." Limnol. Oceanogr. 11:346-354.

Crowley, P.H. 1973. "Filtering rate inhibition of Daphnia pulex in Wintergreen Lake water." Limnol. Oceanogr. 18:394-402.

Cummins, K.W., R.R. Costa, R.E. Rowe, G.A. Moshiri, R.M. Scanlon, and R.K. Zajdel. 1969. "Ecological energetics of a natural population of the predaceous zooplankter Leptodora kindtii Focke (Cladocera)."Oikos. 20:189-223.

DiToro, D.M., D.J. O'Connor, and R.B. Thomann. 1971. "A dynamic model of the phytoplankton population in the Sacramento-San Joaquin Delta." Advances in Chemistry Series 106: Nonequilibrium Systems in Natural Water Chemistry. Pp. 131-180.

Dugdale, R.C. 1967: "Nutrient limitation in the sea: Dynamics, identification, and significance." Limnol. Oceanogr. 12:685-695.

Edsall, T.A., E.H. Brown, Jr., T.G. Yocom, and R.S.C. Wolcott. 1972. "Utilization of alewives by coho salmon in Lake Michigan." Unpublished laboratory technical report. U.S. Bur. Sport Fish and Wild, Ann Arbor, Michigan 32 pages.

Eppeley, R.W., J.N. Rogers, and J.J. McCarthy, Jr. 1969. "Half-saturation constant for uptake of nitrate and ammonium by marine phytoplankton." Limnol. Oceanogr. 14:912-920.

Fletcher, R., and M.F.D. Powell, 1963 "A rapid descent method for minimization." Computer Journal. 6:163-168.

Frazho, D.B., W.F. Powers, and R.P. Canale. 1973. "Numerical integration aspects of a nutrient utilization ecological problem." Proc. ASS/SIAM Conf. on Numerical Integration. Pp. 167-182.

Frost, B.W. 1972. "Effects of size and concentration of food particles on the feeding behavior of the marine planktonic copepod Calanus pacificus." Limnol. Oceanogr. 17:805-815.

Fryer, G. 1957a. "The feeding mechanism of some freshwater cyclopoid copepods." Proc. Zool. Soc. Lond. 129:1-25.

Fryer, G. 1957b. "The food of some freshwater cyclopoid copepods and its ecological significance." J. Animal Ecol. 26:263-286.

Gause, G.F. 1934. The Struggle for Existence. Baltimore. Williams and Wilkins. 163 pages.

Great Lakes Institute. 1962. Great Lakes Institute data record surveys, Part I: Lake Ontario and Lake Erie. University of Toronto, Report PR16.

Great Lakes Institute. 1963. Great Lakes Institute data record surveys, Part II: Lake Ontario and Lake Erie. University of Toronto, Report PR24.

Grill, E.V. and F.A. Richards. 1964. "Nutrient regeneration from phytoplankton decomposing in sea water." J. Mar. Res. 22:51-69.

Halcrow, K. 1963. Acclimation to temperature in the marine copepod, Calanus finmarchicus (Gunner). Limnol. Oceanogr. 8:1-8.

Hall, D.J. 1964. "An experimental approach to the dynamics of a natural population of Daphnia galeata mendotae." Ecol. 45:94-112.

Harris, E. 1959. "The nitrogen cycle in Long Island Sound." Bull. Bingham Oceanogr. Coll. 17:31-65.

Herbes, S.E. 1974. Biological utilization of dissolved organic phosphorus in natural waters. Ph.D. Dissertation. The University of Michigan. Ann Arbor 236 pages.

Hineman, D.J. 1973. Estimating of reaction rates and kinetic constant for a model of primary production in Grand Traverse Bay. M.S. Thesis. The University of Michigan, Ann Arbor. 81 pages.

Hutchinson, B.P. 1971. "The effect of fish predation on the zooplankton of ten Adirondack lakes, with particular reference to the alewife, Alosa pseudoharengus." Trans. Amer. Fish. Soc. 101:325-335.

Hutchinson, G.E. 1967. A Treatise on Limnology. Vol. 2: Introduction to Lake Biology and the Limnoplankton. New York: Wiley. 115 pages.

Hydroscience Inc. 1973: Limnological Systems Analysis for Great Lakes. Phase I: Preliminary Model Design. Great Lakes Basin Commission, Ann Arbor, Michigan. DACW-35-71-30030. Pp. 473.

Johnson, D.L. 1972. Zooplankton population dynamics in Indiana waters of Lake Michigan in 1970. M.S. Thesis. Ball State University, Muncie, Indiana. 129 pages.

Kibby, H.V. 1971. "Effect of temperature on the feeding behavior of Daphnia rosea." Limnol. Oceanogr. 16:580-581.

Kitchell, J.F., J.F. Koonce, R.V. O'Neill, H.H. Shugart, Jr., J.J. Magruson, and R.S. Booth. 1972. Implementation of a Predator-Prey Biomass Model for Fishes. Eastern Deciduous Forest Biome, Memo Report #72-118. The University of Wisconsin. Madison 57 pages.

Krogh, F. T., 1969. "VODQ/SVDQ, DVDQ-variable order integrators for the numerical solution of ordinary differential equations." TV Document No. CP-2308, NOP-11643 JPL, Pasadena, California.

Lane, P.A., and D.C. McNaught. 1970. "A Mathematical analysis of the niches of Lake Michigan zooplankton." Proc. 13th Conf. Great Lakes Res. Pp. 47-57.

Main, R.A. 1962. The life history and food relations of Epischura lacustris Forbes (Copepoda: Calanoida). Ph.D. Thesis. The University of Michigan, Ann Arbor. 135 pages.

Marshall, S.M., and A.P. Orr. 1961. "Studies on the biology of Calanus finmarchicus XII." J. Mar. Biol. Ass. U.K. 41:463-488.

McMahon, J.W., and F.H. Rigler. 1965. "Feeding rate of Daphnia magna Straus in different foods labeled with radioactive phosphorus." Limnol. Oceanogr. 19:105-113.

McQueen, D.J. 1969. "Reduction of zooplankton standing stocks by predaceous Cyclops bicuspidatus thomasi in Marion Lake, British Columbia." J. Fish. Res. Bd. Canada. 26:1605-1618.

Morsell, J.W., and C.R. Norden. 1968. "Food habits of the alewife, Alosa pseudoharengus (Wilson), in Lake Michigan." Proc. 11th Conf. Great Lakes Res. Pp. 96-102.

Mullin, M.M. 1963. "Some factors affecting the feeding of marine copepods of the genus Calanus." Limnol. Oceanogr. 8:239-250.

Norden, C.R. 1968. "Morphology and food habits of the larval alewife, Alosa pseudoharengus (Wilson), in Lake Michigan." Proc. 11th Conf. Great Lakes Res. Pp. 103-110.

O'Connor, J.D., and J.A. Mueller. "A water quality model of chlorides in Great Lakes" Jour. San. Eng. Div. Proc. Amer. Soc. Civil Engr. 96:955-975.

Odum, E.P. 1971. Fundamentals of Ecology, 3rd Ed. Philadelphia: Saunders. 576 pages.

O'Neill, R.V. 1969. "Indirect estimation of energy fluxes in animal food web." J. Theoret. Biol. 22:284-290.

Paasche, E. 1973a. "Silicon and the ecology of marine plankton diatoms. I. Thalassiosira pseudonana grown in a chemostat with silicate as limiting nutrient" Marine Biology 19: 117-126.

Paasche, E. 1973b. "Silicon and the ecology of marine plankton diatoms. II. Silicate-uptake kinetics in five diatom species." Marine Biology 19:262-269.

Porter, K.G. 1973. "Selective grazing and differential digestion of algae by zooplankton." Nature. 244:179-180.

Raymont, J.E.G. 1959. "The respiration of some planktonic copepods III. The oxygen requirements of some American species." Limnol. Oceanogr. 4:479-491.

Raymont, J.E.G. 1963. Plankton and Productivity in the Oceans. Oxford: Pergamon. 660 pages.

Riley, G.A. 1956. "Oceanography of Long Island Sound 1952-1954. II. Physical oceanography." Bull. Bingham Oceanogr. Coll. 15:15-46.

Riley, G.A. 1965. "A mathematical model of regional variations in plankton." Limnol. Oceanogr. 10 (Suppl.) 202-215.

Ryther, J.H. 1956. "Photosynthesis in the ocean as a function of light intensity." Limnol. Oceanogr. 1:61-70.

Smith, S.H. 1968. "The alewife." Limnos. 1:12-20.

Steele, J.H. 1965. "Notes on some theoretical problems in production ecology." In Primary Production in Aquatic Environments, ed. C.R. Goldman. Mem. Inst. Idrobiol. 18 Suppl., University of California, Berkley, Pp. 383-398.

Stoermer, E.F., and J.J. Yang. 1969. Plankton Diatom Assemblages in Lake Michigan. Great Lakes Res. Div., Spec. Rep. No. 47, The University of Michigan, Ann Arbor. 268 pages

Stoermer, E.F., and J.J. Yang. 1970. Distribution and Relative Abundance of Dominant Plankton Diatoms in Lake Michigan. Great Lakes Res. Div., Publ. No. I6, The University of Michigan, Ann Arbor. 64 pages

Strickland, J.D.H., 1965. "Production of organic matter in the primary stages of the marine food chain." In Chemical Oceanography, ed. J.P. Riley and G. Skirrow New York: Academic Press. Pp. 478-610.

Vanderhoef, L.N., C.-Y. Huang, R. Musil, and J. Williams. 1974. "Nitrogen fixation (acetylene reduction) by phytoplankton in Green Bay, Lake Michigan, in relation to nutrient concentrations." Limnol. Oceanogr. 19:126-132.

Vogel, A.H., and R.P. Canale. 1974. A Food Web Model for Lake Michigan: Part I - Justification and Development of the Model. Sea Grant Technical Report No. 40., the University of Michigan, Ann Arbor. 59 pages.

Warren, C.E. 1971. Biology and Water Pollution Control. Philadelphia: Saunders. 434 pages.

Warshaw, S.J. 1972. "Effects of alewives (Alosa pseudoharengus) on the zooplankton of Lake Wononskipomuc, Connecticut." Limnol. Oceanogr. 17:816-825.

Waterman, T. H., ed. 1960. The Physiology of Crustacea, New York: Academic Press. 670 pages.

Wells, L. 1970. "Effects of alewife predation on zooplankton populations in Lake Michigan." Limnol. Oceanogr. 15:556-565.

Wright, J.C. 1965. "The population dynamics and production of Daphnia in Canyon Ferry Reservoir, Montana." Limnol. Oceanogr. 19:583-590.